

# **Molecular Cross-talk between Sa3int Phages and their *Staphylococcus aureus* Host**

## **Dissertation**

der Mathematisch-Naturwissenschaftlichen Fakultät  
der Eberhard Karls Universität Tübingen  
zur Erlangung des Grades eines  
Doktors der Naturwissenschaften  
(Dr. rer. nat.)

vorgelegt von  
Ronja Dobritz  
aus Filderstadt

Tübingen  
2025

Gedruckt mit Genehmigung der Mathematisch-Naturwissenschaftlichen Fakultät der  
Eberhard Karls Universität Tübingen.

Tag der mündlichen Qualifikation:

13.02.2026

Dekan:

Prof. Dr. Thilo Stehle

1. Berichterstatter/-in:

Apl. Prof. Dr. Christiane Wolz

2. Berichterstatter/-in:

Prof. Dr. Andreas Peschel



## Table of Contents

Summary .....	1
Zusammenfassung .....	2
List of publications and personal contributions .....	4
Introduction .....	6
<i>S. aureus</i> .....	6
Virulence Factors of <i>S. aureus</i> .....	7
Regulation of Virulence in <i>S. aureus</i> .....	7
Wall teichoic acids .....	10
Bacteriophage Replication and Regulation .....	11
Temperate Phages of <i>S. aureus</i> .....	13
Sa3int Phages .....	14
Aim of this thesis .....	17
Results .....	18
Part I: Influence of <i>Staphylococcus aureus</i> strain background on Sa3int phage life cycle switches .....	18
Part II: The phage $\Phi$ 13-encoded transcriptional regulator Ltr controls phage assembly in <i>Staphylococcus aureus</i> .....	46
Part III: Multiple effects of the bacterial DNA-binding protein SarA on the life cycle of <i>Staphylococcus aureus</i> phages .....	78
General Discussion .....	110
Phage Replication as Driver of Strain-Specific Sa3int Transfer Frequencies .....	110
Ltr Mediates the Activation of Late Gene Expression in $\Phi$ 13 .....	111
Host Factors Influence Phage Dynamics .....	113

## Summary

*Staphylococcus aureus* is a major opportunistic pathogen that asymptotically colonizes the human nasal cavity but also causes severe infections. Temperate phages play a central role in *S. aureus* genetic diversity and pathogenicity. Among them, Sa3int phages are the most prevalent in human nasal isolates and contribute to virulence by encoding highly human-specific immune evasion factors. Their dynamic regulatory switch, controlling expression of both the *hly* integration locus and the phage-encoded virulence genes, plays a crucial role during infection. While the genomic organization and the lysogenic-lytic transition are well characterized in Sa3int phages, the regulatory mechanisms during the lytic life cycle and their interplay with host factors remain poorly understood.

In this work, the dynamics of the Sa3int phage and its transcriptional patterns across diverse *S. aureus* strain backgrounds were investigated. Distinct strain-specific differences in phage transfer frequencies were observed, enabling classification of the strains into high- and low-transfer groups. Phage replication during the lytic cycle was identified as the key driver of host-dependent variations, while differences in adsorption, prophage integration, and prophage excision were ruled out. Furthermore, substantial variations in the expression of late genes associated with phage assembly, DNA packaging, and host cell lysis were detected.

The essential promoter region P<sub>23</sub>, located upstream of the late gene cluster, was identified and its regulatory characteristics were elucidated. Through this analysis, SAOUHSC\_02200 was discovered and characterized as the late transcriptional regulator (Ltr) of lytic late genes. Both P<sub>23</sub> activity and *ltr* expression were found to vary in a host-dependent manner and to be modulated by the alternative sigma factor SigB and its downstream effector SpoVG.

Further, the influence of the global regulator and DNA-binding protein SarA on the phage life cycle was examined. Phage production of the Sa3int phage Φ13 and the Sa5int phage Φ11 was shown to be promoted by SarA. Analyses of distinct stages of the phage life cycle revealed that SarA alters the glycosylation pattern of wall teichoic acid (WTA), thereby enhancing adsorption of Φ11. Additionally, a DNA-protective effect of SarA was observed, reflected by reduced activation of the SOS response. Finally, phage genome replication of Φ13 was shown to be promoted by SarA, likely through its function as a DNA-structure protein.

Together, a complex regulatory network was revealed in which phage-encoded factors and host global regulators interact to coordinate phage gene expression, replication, and subsequent bacterial virulence.

## Zusammenfassung

*Staphylococcus aureus* ist ein bedeutendes opportunistisches Pathogen, das den menschlichen Nasenraum asymptomatisch besiedeln kann, aber auch schwere Infektionen verursacht. Temperente Phagen spielen eine zentrale Rolle für die genetische Diversität und Pathogenität von *S. aureus*. Sa3int-Phagen sind die häufigsten temperenten Phagen in humanen Nasenisolaten und tragen zur Virulenz bei, indem sie human-spezifische Virulenzfaktoren kodieren. Ihre dynamische Regulation, die sowohl die Expression des *hly* Locus als auch der phagen-kodierten Virulenzgene steuert, ist entscheidend für die Pathogenität während Infektionen. Obwohl die genomische Organisation und der Übergang vom lysogenen zum lytischen Lebenszyklus gut erforscht sind, bleiben die regulatorischen Mechanismen sowie deren Zusammenspiel mit Wirtsfaktoren weitgehend ungeklärt.

In der vorliegenden Arbeit wurden die Dynamik der Sa3int-Phagen sowie dessen transkriptionellen Profile in unterschiedlichen *S. aureus*-Stammhintergründen untersucht. Dabei traten ausgeprägte stammspezifische Unterschiede in den Transferraten der Phagen auf, anhand derer die untersuchten Stämme in Gruppen mit hoher bzw. niedriger Transferfrequenz klassifiziert wurden. Als zentraler Faktor der wirtsabhängigen Variationen wurde die Phagenreplikation während des lytischen Zyklus identifiziert, wohingegen Unterschiede in Adsorption, Prophagenintegration und -exzision ausgeschlossen werden konnten. Zudem zeigten sich signifikante Differenzen in der Expression später Gene, die für den Zusammenbau der Phagenpartikel, die DNA-Verpackung sowie die Wirtslise erforderlich sind.

Die essenzielle Promotorregion P<sub>23</sub>, die unmittelbar upstream dieser späten Gene lokalisiert ist, wurde identifiziert und ihre Regulation wurde analysiert. Auf diese Weise konnte SAOUHSC\_02200 als transkriptioneller Regulator (Ltr) der späten lytischen Gene charakterisiert werden. Sowohl die Aktivität des P<sub>23</sub>-Promotors als auch die *ltr*-Expression zeigten eine Wirtsabhängigkeit, und eine Modulation durch den alternativen Sigmafaktor SigB sowie dessen downstream Effektor SpoVG konnte nachgewiesen werden.

Des Weiteren wurde der Einfluss des globalen Regulators und DNA-bindenden Proteins SarA auf die Regulation des Phagenlebenszyklus untersucht. Dabei wurde festgestellt, dass SarA die Produktion des Sa3int-Phagen  $\Phi$ 13 sowie des Sa5int-Phagen  $\Phi$ 11 fördert. Analysen der unterschiedlichen Schritte des Phagenlebenszyklus zeigten, dass SarA das Glykosylierungsmuster der Wandteichonsäure (WTA) beeinflusst und dadurch die Adsorption von  $\Phi$ 11 begünstigt. Darüber hinaus wurde ein protektiver DNA-Effekt von SarA beobachtet, der sich in einer reduzierten Aktivierung der SOS-Antwort manifestierte. Schließlich konnte gezeigt werden, dass SarA die Genomreplikation von  $\Phi$ 13 unterstützt, wahrscheinlich vermittelt über seine Funktion als DNA-Struktur Protein.

Insgesamt wurde ein komplexes regulatorisches Netzwerk aufgezeigt, in dem phagenkodierte Faktoren und globale Wirtsregulatoren miteinander interagieren und gemeinsam die Phagengenexpression, die Replikation sowie die bakterielle Virulenz steuern.

## List of publications and personal contributions

### Accepted publications

**1. Influence of *Staphylococcus aureus* strain background on Sa3int phage life cycle switches**

Carina Rohmer<sup>†</sup>, Ronja Dobritz<sup>†</sup>, Dilek Tuncbilek-Dere, Esther Lehmann, David Gerlach, Shilpa Elizabeth George, Taeok Bae, Kay Nieselt, Christiane Wolz

<sup>†</sup> These authors contributed equally to this work.

**Viruses.** 2022 Nov 8;14(11):2471. doi: 10.3390/v14112471.

For this research article, I performed parts of the biological experiments and was involved in data analysis and interpretation. I designed all figures and was involved in editing of the manuscript to its final version.

**2. (p)ppGpp-mediated GTP homeostasis ensures survival and antibiotic tolerance of *Staphylococcus aureus***

Andrea Salzer, Sophia Ingrassia, Parvati Iyer, Lisa Sauer, Johanna Rapp, Ronja Dobritz, Jennifer Müller, Hannes Link, Christiane Wolz

**Commun Biol.** 2025 Mar 28;8(1):508. doi: 10.1038/s42003-025-07910-6.

For this research article, I contributed by generation of the phage-cured mutant strain and subsequent experiments. I was also involved in editing of the figures and the manuscript during revision.

**3. Multiple effects of the bacterial DNA-binding protein SarA on the life cycle of *Staphylococcus aureus* phages**

Ronja Dobritz, Carina Rohmer, Elena Niepoth, Valentin Egle, Natalya Korn, Vittoria Bisanzio, Martin Saxtorph Bojer, Hanne Ingmer, Christiane Wolz

**J Bacteriol.** 2025 Oct 16:e0027925. doi: 10.1128/jb.00279-25.

For this research article, I made major contributions to the conception and design of the study. All experiments were performed or supervised and subsequently analysed by me. I designed all figures for the manuscript and contributed to writing the manuscript under the supervision of Christiane Wolz.

## Submitted manuscripts

### 1. The phage $\Phi$ 13-encoded transcriptional regulator Ltr controls phage assembly in *Staphylococcus aureus*

Ronja Dobritz, Marcel Bäcker, Carina Rohmer, Natalya Korn, Vittoria Bisanzio, Christiane Wolz

Preprint on biorxiv.org, <https://doi.org/10.1101/2025.11.28.691083>, (submitted Virology Journal)

For this research article, I made major contributions to the conception and design of the study. All experiments were performed or supervised and subsequently analyzed by me. I designed all figures and wrote the manuscript under the supervision of Christiane Wolz.

## Introduction

Parts of this introduction have been published in the following articles. The submitted manuscript has been uploaded to the preprint server bioRxiv and might differ from the final published article. Publications can be accessed under the following links:

**'Influence of *Staphylococcus aureus* strain background on Sa3int phage life cycle switches'**, research article, <https://doi.org/10.3390/v14112471>

**'The phage  $\Phi$ 13-encoded transcriptional regulator Ltr controls phage assembly in *Staphylococcus aureus*'**, submitted manuscript, <https://doi.org/10.1101/2025.11.28.691083>

**'Multiple effects of the bacterial DNA-binding protein SarA on the life cycle of *Staphylococcus aureus* phages'**, research article, <https://doi.org/10.1128/jb.00279-25>

### ***S. aureus***

*Staphylococcus aureus* is a Gram-positive bacterium that asymptotically colonizes the skin and mucosal surfaces of approximately 30% of the adult human population [1]. Despite its frequent commensal presence, *S. aureus* is also an opportunistic pathogen and a leading cause of severe, life-threatening infections such as atopic dermatitis, endocarditis, osteomyelitis, pneumonia, and sepsis [2].

Genetic classification of *S. aureus* isolates using multi-locus sequence typing (MLST) on the core genome, grouped isolates into eight major clonal complexes (CC) based on their sequence types (STs) [3]. As *S. aureus* is not naturally competent, horizontal gene transfer (HGT) depends on mobile genetic elements (MGEs) transferred via bacteriophage transduction to contribute to genetic diversity between *S. aureus* strains. The presence of restriction modification systems (R-M) that regulate recognition and uptake of foreign DNA influences the distribution of prophages in clonal lineages [4-6]. Hence, exchange of MGE, encoding virulence factors and antibiotic resistances is facilitated within clonal complexes.

Infections caused by methicillin-resistant *S. aureus* (MRSA) represent a major clinical and public health challenge. In hospital settings, antibiotic treatment is complicated, due to the acquisition of the staphylococcal cassette chromosome mec (SCCmec), encoding a penicillin-binding protein that confers  $\beta$ -lactam resistance [7]. Many MRSA strains have also developed resistance to several additional antibiotic classes, and the increasing incidence of vancomycin-intermediate *S. aureus* (VISA), which are less susceptible to the last line of antibiotic, further complicates treatment of *S. aureus* infections [8].

The emergence of community-associated MRSA (CA-MRSA) strains, capable of causing severe infections in otherwise healthy individuals, has intensified additional public health concerns [9]. The most prevalent CA-MRSA strain USA300, which is associated with outbreaks in the USA and Europe, has been extensively studied. Its success has been attributed to altered regulation of virulence factors, acquisition of additional virulence genes, and protein sequence variations [10]. These observations highlight the pivotal role of *S. aureus* virulence factors in determining pathogenicity, host colonization, and infection potential.

### **Virulence Factors of *S. aureus***

*S. aureus* possesses an extensive repertoire of virulence factors that contribute to its pathogenicity during human and animal infection. Many of these factors are secreted as toxins that directly interact with the host, disrupting cellular integrity or immune function [11].

Membrane-damaging toxins such as  $\beta$ -barrel-forming toxins like  $\alpha$ -toxin and Panton-Valentine leucocidin (PVL), as well as peptides like phenol-soluble modulins (PSMs) and  $\delta$ -hemolysin, cause lysis of erythrocytes and leukocytes, thereby facilitating immune evasion and tissue damage [12-15]. Other virulence factors, including superantigens like toxic shock syndrome toxin (TSST), trigger T-cell activation and cytokine release, leading to systemic inflammation [16]. Secreted enzymes, including  $\beta$ -hemolysin, a sphingomyelinase that degrades sphingomyelin in host cell membranes and promotes red blood cell lysis, also contribute to pathogenicity. Other enzymatic virulence factors include proteases that degrade host proteins, and coagulases that promote fibrin clot formation, which contributes to bacterial protection [17].

Many *S. aureus* virulence factors are encoded on mobile genetic elements, which play a crucial role in horizontal gene transfer and bacterial evolution. For instance, plasmids frequently carry antibiotic resistance genes and staphylococcal pathogenicity islands (SaPIs) were described to serve as reservoir for superantigen genes [18].

Bacteriophages integrated as prophages within the bacterial genome, also represent important MGEs influencing virulence. Phage-encoded virulence factors include PVL, the staphylococcal inhibitor of complement (*scn*), staphylokinase (*sak*), the chemotaxis inhibitory protein (*chp*) and various enterotoxins. The role of prophages and their contribution to virulence, particularly in relation to Sa3int phages, are described in detail in the sections 'Temperate phages of *S. aureus*' and 'Sa3int phages'.

### **Regulation of Virulence in *S. aureus***

The high abundance of virulence factors encoded by *S. aureus* and their distinct roles during colonization and infection highlight the need for tight regulatory control. To ensure survival, adaptation, and evasion of host immune responses, *S. aureus* must adjust gene expression in response to environmental changes and signals. A network of regulatory systems, including

two-component systems, transcriptional regulators, and alternative sigma factors, controls the regulation of virulence in *S. aureus*.

### **Two Component Systems – The Agr Quorum-Sensing System**

Two-component systems (TCSs) enable the transformation of extracellular signals into intracellular transcriptional changes. Upon extracellular signal detection, the membrane-bound histidine kinase undergoes autophosphorylation and subsequently transmits the phosphorylation to a transcriptional regulator, which activates or represses expression of target genes. The *S. aureus* genome encodes 16 TCSs [19]. Among these, the Agr (accessory gene regulator) quorum-sensing system is best characterized and functions as a master regulator of virulence during transition from exponential to stationary growth [20].

In the Agr system, the sensor histidine kinase AgrC detects critical levels of the auto inducing peptide (AIP) and transmits the density-dependent signal to the transcriptional regulator AgrA. Activated AgrA promotes transcription from the P2 and P3 promoters within the *agr* locus, leading to expression of *agrBDCA* (RNAII) and RNAIII, the primary effector molecule of the system. RNAIII regulates the expression of virulence genes during late-exponential and early stationary growth by upregulating secreted exoproteins and toxins while repressing cell wall-associated proteins [20, 21]. Mutations in *agr* lead to reduced virulence in various infection models, underscoring its importance in pathogenesis [22].

### **Transcriptional Regulators – The SarA Protein Family**

Additionally, cytoplasmic transcription factors (TFs) including the SarA protein family, provide signal-dependent regulation of virulence gene expression. Ibarra et al. classified 135 TFs and sigma factors into 36 families and four main groups. Group 4 encompasses regulators specific to Staphylococcaceae, such as MgrA, Rot, and SarA, which are associated with virulence regulation and environmental adaptation [23].

SarA (staphylococcal accessory regulator A) is a global transcriptional regulator, encoded on the *sarA* locus, which contains three distinct promoters (P2, P3, P1) producing three overlapping transcripts [24]. SarA is a 14.7 kDa winged-helix DNA-binding protein that recognizes and binds to AT-rich promoter motifs [25, 26]. Changes in phosphorylation modulate its DNA-binding affinity [27]. Additionally, SarA does not only bind to DNA but also to RNA to control mRNA turnover [28]. With 50000 copies per cell, SarA abundance is exceeding the presence of classical regulatory proteins, suggesting a role beyond transcriptional regulation as a histone-like protein altering DNA topology to control gene expression [29, 30]. SarA expression remains constant during different growth phases [29].

SarA plays a crucial role in regulation of *S. aureus*, by controlling about 120 target genes involved in virulence and metabolism. Regulation occurs directly, via promoter binding and

indirectly through activation of the *agr* promoters P2 and P3 resulting in transcription of RNAII and RNAIII [31]. Directly regulated targets include *fnb* (fibronectin-binding protein), *spa* (protein A), *hla* (alpha-hemolysin), and protease genes such as *aur* and *ssp* [21]. Interestingly, only a small number of the SarA-regulated promoters contain the Sar-box motif, suggesting binding of SarA is less specific than suspected [32]. RNA-seq studies have further identified at least 50 small RNAs (sRNAs) as targets of SarA [33].

### **Alternative sigma factors - SigB**

Further, regulation of virulence in *S. aureus* is mediated by the alternative sigma factor SigB ( $\sigma$ B), which directs the RNA-polymerase complex to specific promoters to initiate expression of target genes. The SigB regulatory system was first characterized in *B. subtilis* and later identified in *S. aureus* with about 70% sequence similarity. While the genes upstream of *sigB* *rsbU*, *rsbV* and *rsbW*, encoding SigB regulators are conserved in *S. aureus*, it lacks the genes for the 'stressosome' complex (*rsbR*, *rsbS*, *rsbT* and *rsbX*), which is required for stress-dependent activation of SigB in *B. subtilis* [34, 35].

In *S. aureus*, the anti-sigma factor RsbW binds SigB, thereby preventing SigB-dependent promoter recognition and association with the RNA-polymerase. SigB activation depends on RsbU (PP2C-phosphatase) that dephosphorylates RsbV (anti-anti sigma factor), allowing RsbV to bind to RsbW and release SigB for transcription initiation [36]. Consistently with the absence of the 'stressosome' genes, SigB activation in *S. aureus* is not induced by energy stress. Instead, alkaline- and heat shock lead to increased SigB activity and upregulation of SigB-dependent genes [37]. Moreover, SigB activity increases during late-exponential and early-stationary growth [37, 38].

Several studies, including microarray-based analyses, have shown that the SigB regulon includes genes involved in basic cellular processes, such as metabolism, transport, cell envelope biosynthesis, and signaling transduction [37]. SigB also influences virulence by repressing exoproteins and toxins, while positively regulating cell-wall anchored adhesins [39]. Further, SigB regulates expression of other global regulators of virulence, including the upregulation of *sarA* and the inhibition of RNAIII, antagonizing Agr-dependent virulence activation [40].

A conserved SigB-binding consensus sequence (GTTTAA-12-15-GGGTAT) has been identified in several SigB-dependent promoters [41]. However, many genes seem to be regulated indirectly through SigB downstream effectors. SpoVG is one of the SigB-dependent downstream effectors and a transcriptional regulator that is suspected to activate SigB-dependent genes lacking a consensus sequence [39, 42, 43].

Overall, the regulation of virulence in *S. aureus* is controlled through an overlapping multilayered, regulatory network enabling *S. aureus* to adapt its pathogenic potential in response to environmental signals (Figure 1).

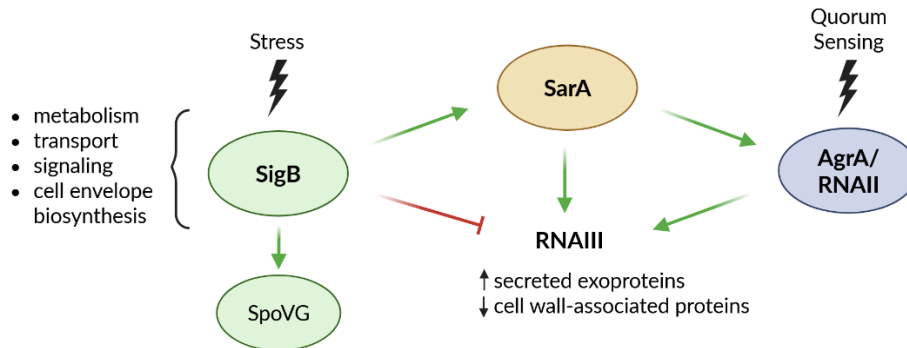


**Figure 1. Regulatory network of *S. aureus* virulence.** The schematic depicts major regulatory pathways governing virulence gene expression in *S. aureus*. Stress signals activate the alternative sigma factor SigB, which in turn upregulates its downstream effector SpoVG. SigB positively influences SarA, while also exerting inhibitory effects on Agr activity. SarA controls the Agr quorum-sensing system and Agr-dependent genes both directly via activation of RNAPII and indirectly via activation of RNAPIII. Activation of the quorum-sensing Agr system results in transcription of RNAPIII and subsequent in the regulation of downstream target genes. These interactions collectively modulate the transition between surface-associated factors and secreted virulence factors (e.g., proteases, toxins), balancing adhesion, and immune evasion in response to changing environmental conditions. Arrows indicate positive regulation and blunt-ended lines indicate repression. Created with BioRender.com.

### Wall teichoic acids

In addition to the virulence factors described above, *S. aureus* cell-wall glycopolymers, particularly wall teichoic acids (WTAs), play essential roles in pathogenesis, host cell adhesion, and immune evasion [44, 45]. Beyond their roles in cell physiology and virulence, WTAs serve as the major receptors for bacteriophage adsorption, thereby facilitating HGT through phage transduction [46]. Such phage-mediated HGT is beneficial for the transfer of new mobile genetic elements contributing to evolutionary adaptation and pathogenic potential of *S. aureus*.

Most *S. aureus* strains produce a peptidoglycan-attached WTA composed of a ribitol-phosphate (RboP) backbone, which is decorated with D-alanine and N-acetylglucosamine (GlcNAc). GlcNAc residues are attached at specific positions by glycosyltransferases TarS ( $\beta$ -1,4-GlcNAc), TarM ( $\alpha$ -1,4-GlcNAc) and TarP ( $\beta$ -1,3-GlcNAc). The WTA glycosylation patterns determine phage binding specificity and susceptibility [47-49].

## **Bacteriophage Replication and Regulation**

The following introduction focuses on the replication and regulatory mechanisms of double-stranded DNA (dsDNA) bacteriophages infecting Gram-positive bacteria, with reference to model *Escherichia coli* phage  $\lambda$ .

### **Bacteriophage Life Cycles**

Bacteriophages are viruses that specifically infect bacteria, using their host's biosynthetic machinery for their own replication. Upon infection, strictly lytic phages propagate by replicating their genomes, assembling new phage particles, and lysing the bacterial host cell to release mature phage particles. In contrast, temperate phages possess a dual life cycle. In addition to lytic propagation, temperate phages can integrate their genome into the bacterial chromosome and reside as a prophage. This process generates a bacterial lysogen, in which the prophage is replicated passively along with the host chromosome. Lysogenic conversion, the process whereby the prophage provides new genes and traits to the bacterial host, can confer benefits to both the phage and the bacterium [50]. Reactivation of the lytic life cycle can occur subsequent to the SOS-response activation in the bacterial host.

### **The SOS Response and Phage Induction – Activation of Early Lytic Genes**

The bacterial SOS response is a conserved pathway responsive to DNA-damage that enables the bacteria to repair damaged DNA prior to cell division [51]. Two key proteins, RecA and LexA, control its regulation and activation. Under normal conditions, LexA acts as a transcriptional repressor by binding to promoters of SOS genes, thereby maintaining the system in an inactive state [52]. Binding of RecA to single-stranded DNA, generated through DNA damage, activates the protein and induces the activation of the SOS response. Activated RecA promotes autocleavage of LexA, releasing the repressor and activating the transcription of DNA repair and cell division genes [53].

Many temperate phages encode LexA-like repressors within their genetic switch region, which controls the transition from lysogenic to lytic life cycle. Upon activation of the bacterial SOS response, RecA also induces the autocleavage of the phage repressors, allowing escape from damaged host cells. In model *E. coli* phage  $\lambda$ , the genetic switch and the involved regulatory proteins were extensively studied. In this model, the CI-repressor, a LexA-homolog, maintains lysogeny by binding to operator sequences within the promoter region of *cro* to block the transcription. During the activation of the SOS response, RecA-mediated autocleavage of CI prevents its binding to the promoter, initiating expression of *cro* and early lytic genes [54].

Phage gene expression during the lytic cycle is under temporal control, to allow efficient replication and assembly of mature phage particles. Early lytic genes are involved in regulatory processes and phage genome replication, while late genes encode for DNA processing,

packaging, structural, and lysis proteins that are required for phage assembly and release (Figure 2).

### **DNA Replication Mechanisms of dsDNA Phages**

During replication of double-stranded circular DNA genomes, genetic information is faithfully conserved through semi-conservative synthesis. Several replication strategies have been described, in the following the theta ( $\theta$ )-type replication, performed by *S. aureus* phage  $\Phi$ 11 and  $\Phi$ 13 is described in more detail. In this process, an initiator, also termed replication factor, binds to the AT-rich origin of replication, inducing DNA unwinding. The exposed single-stranded region allows entry and recruitment of the primosome (helicase loader and helicase) and the replisome (DNA polymerase and accessory proteins) to the replication site. Subsequent, DNA synthesis proceeds bidirectional on both the leading- and the lagging-strand [55]. Helicase, polymerase and single-stranded DNA binding proteins are phage-encoded [56].

### **Regulation of Late Gene Expression**

During early stages of the lytic cycle and phage genome replication, regulators controlling late gene expression are expressed and synthesized. In model phage  $\lambda$ , the antitermination protein Q converts the RNA-polymerase into a termination-resistant form, enabling transcription of late genes [57]. *E. coli* phage T7 encodes a specific RNA-polymerase for the initiation of late gene transcription [58]. In phages infecting Gram-positive bacteria, RinA-homologs have been identified as activators of late transcription [59]. Later, four additional families of late transcriptional regulators (Ltrs) were characterized lacking sequence homology to RinA [60]. The late gene modules activated by these regulators include genes involved in DNA processing and packaging, capsid and tail assembly, host cell lysis and phage-encoded immune evasion.

### **DNA Packaging and Phage Assembly**

Following genome replication, concatemeric phage DNA must be processed and packaged into newly assembled phage capsids. The terminase complex, composed of the small terminase subunit (TerS) that recognizes the viral DNA, and the large terminase subunit (TerL) with endonuclease and ATPase activity, mediates this process. The terminase-DNA complex assembles at the portal protein on the phage capsid, initiating DNA translocation. DNA cleavage at a specific cohesive end site (cos-site phages) or at a random sequence when the capsid is full (pac-site phages) terminates the packaging process. Subsequently, the terminase complex bound to concatemeric phage DNA is transferred to the next capsid [61].

### **Host Cell Lysis and Phage Release**

Lastly, the produced mature phage particles are released for reinfection of new host bacteria. Bacterial lysis is mediated by two proteins: a pore forming holin that forms pores in the bacterial membrane, and the endolysin that degrades the peptidoglycan layer [62, 63]. Lysins cleave

one of the four major bonds within the peptidoglycan, resulting in cell lysis and the release of phage progeny.

Despite extensive studies, characterizations of phage genomes and identification of many genes, a large number of phage genes remain of unknown function and their roles are yet to be discovered.

### **Temperate Phages of *S. aureus***

In *S. aureus*, bacteriophages are key vectors of HGT and play crucial roles in pathogenicity by encoding accessory genes that enhance virulence, immune evasion and bacterial adaptation to changing environmental conditions during infection [5, 64]. Moreover, the integration of prophages into the bacterial chromosome can increase the genome plasticity by disrupting bacterial host genes at the integration site, thereby influencing bacterial fitness and evolution.

All known staphylococcal phages belong to the order *Caudovirales*, characterized by dsDNA genomes and a head-tail morphology [65]. Exclusively lytic phages infecting *S. aureus* are classified into the families *Myoviridae*, *Podoviridae*, and *Siphoviridae*, whereas all known temperate phages of *S. aureus* belong to the *Siphoviridae* family [66]. Members of this family possess dsDNA encapsidated within an icosahedral head and a long, non-contractile tail. Moreover the genomes of *Siphoviridae* phages are organized into six functional modules: lysogeny, DNA replication, packaging, head, tail, and lysis [67]. Notably, the same functional module of one phage fulfilling the same functions can replace the functional modules within other phages. This modular replacement leads to the formation of chimeric and mosaic phage genomes [68]. Most *S. aureus* isolates harbor at least one prophage [4].

Temperate *S. aureus Siphoviridae* are further classified according to the integrase gene (*int*) they encode, which defines the chromosomal integration site. Based on sequence similarity, *S. aureus* phage are divided into eight major integrase groups (Sa-int type). Recombination events of functional modules occur more frequently among phages within the same Sa-int group. Furthermore, the presence of certain accessory genes is often associated with specific integrase types, providing information about the pathogenic potential of bacteria carrying a certain prophage [4].

For instance, Sa1int phages carry the *eta* gene, encoding the exfoliative toxin A (ETA), which causes skin lesions described for staphylococcal scalded skin syndrome [4, 69]. PVL encoded from lukSF is predominantly present in Sa2int phages [4, 70]. The presence of those phages were associated with necrotizing pneumonia and skin and soft tissue infections [71]. Sa3int phages encode an extensive set of virulence factors located within the immune evasion cluster (IEC), which contributes to escape from the human immune response. These phages are described in more detail in the following section.

Overall, temperate phages of *S. aureus* convey bacterial genetic variability that allows adaptation of the bacteria to different conditions, through lysogenic conversion. The acquisition of phage-encoded virulence factors has been linked to the emergence of highly pathogenic strains and to diseases caused by *S. aureus* infections.

### **Sa3int Phages**

The most prevalent prophages in *S. aureus* colonizing humans belong to the Sa3int group, detected in up to 96% of human nasal isolates [64]. Phages of this group integrate their genomes into the *hly* gene locus, which encodes  $\beta$ -hemolysin (Hly), a sphingomyelinase that catalyzes the hydrolysis of sphingomyelin into phosphocholine and ceramide [72]. Prophage integration disrupts the *hly* gene, resulting in the loss of  $\beta$ -hemolysin as a virulence factor.

During transmission from humans to livestock, *S. aureus* strains frequently lose Sa3int prophages, indicating their crucial role in human host adaptation. Compelling evidence for the importance in human colonization is the presence of the immune evasion cluster (IEC) on Sa3int phages, which comprises a set of human-specific virulence genes that mediate immune escape. Several IEC variants have been described, containing different combinations of the core genes *sak*, *chp*, *scn*, *sea*, and *sprG1/sprF1* [73].

### **Components of the Immune Evasion Cluster**

Staphylokinase (Sak) converts plasminogen to active plasmin, a protease that degrades extracellular matrix components. Plasmin also cleaves surface-bound proteins like complement factors, allowing *S. aureus* to evade opsonization [74].

The secretion of CHIPS (chemotaxis inhibitory protein of *Staphylococcus aureus*) inhibits the chemotactic response and neutrophil recruitment, through binding of CHIPS to the formylated peptide receptor (FPR) and C5a, which inhibits chemotactic signaling [75, 76].

Another factor that aids *S. aureus* to escape the human immune response is the staphylococcal complement inhibitor (SCIN). SCIN, as a secreted protein, interacts directly with the C3 convertase complex (C3bBb), preventing the activation of the complement system specifically in humans [77, 78].

Staphylococcal Enterotoxin A (SEA), encoded by *sea*, functions as a superantigen, stimulating production of pro-inflammatory cytokines [79]. Interestingly, Sea induces interleukin-8 (IL-8) and thereby an inflammation in nasal epithelial cells at the site of *S. aureus* colonization [80].

A non-coding RNA, transcribed by *sprF1*, regulates the toxin-antitoxin system SprG1/SprF1 that contributes to interbacterial competition. The toxin SprG1, a pore-forming toxin, shows lytic activity against other bacterial species and human erythrocytes [81].

### **Sa3int Phage Dynamics**

Integration of Sa3int prophages into *hly* disrupts  $\beta$ -hemolysin production, while excision completely restores Hly activity [82]. This reversible process acts as a regulatory switch between expression of immune evasion factors from the prophage and of the virulence factor Hly. During infection, Hly functions as an important virulence factor due to the hemolytic activity against erythrocytes and the described damaging effect on keratinocytes [83]. Moreover, sphingomyelinase activity can modulate immune cell signaling and induce apoptosis [84]. Hence, Sa3int prophage integration and excision allow *S. aureus* to control virulence factors dependent on environmental conditions.

Clinical studies, including cystic fibrosis (CF) and furunculosis isolates, demonstrated that Sa3int phage excision is favored during infection, producing a heterogeneous population with Hly-positive and Hly-negative subpopulations [85, 86]. Indeed, a comparative analysis of nasal colonizing isolates and CF infection isolates revealed a higher prevalence of Sa3int phages among nose isolates, suggesting excision might be associated with infectious diseases rather than colonization [85].

Besides classical lysogenic and lytic life cycle, Sa3int phages can exist in an active lysogenic state, where the phage genome excises and resides as circular phage genome without producing phage particles, thereby allowing *hly* transcription without the loss of the phage. A study analyzing clinical isolates found that 63% of *S. aureus* isolates carrying Sa3int phages were unable to generate infectious phage particles [87]. The active lysogeny of phage  $\Phi$ Sa3mw can be triggered by oxidative stress during infection [88], with reintegration potentially occurring at later infection stages.

Excision and induction of the lytic cycle of phages, can be stimulated by selective pressure, oxidative stress or antibiotic treatment, and is associated with increased pathogenicity. As phage-encoded virulence factors are co-transcribed with late phage genes, phage replication amplifies their expression via the multi copy effect, following lytic cycle induction [85]. For instance, restored *hly* expression and Sa3int excision were shown to increase production of cytokine IL-6 in a human monocyte (THP-1) infection model [89]. Conversely, stable Sa3int prophage integration correlates with reduced phagocytosis by THP-1 monocytes and increased escape from the human immune response [90].

In summary, Sa3int phages serve as a regulatory switch controlling expression of *hly* and human-specific immune evasion factors. During infection, restoration of functional Hly activity and phage excision is favored, resulting in increased virulence of *S. aureus*. For long-term colonization, immune escape mediated by integration of Sa3int prophages seems to be beneficial. This highlights the central role of Sa3int phages in the adaptation of *S. aureus* to the human host.

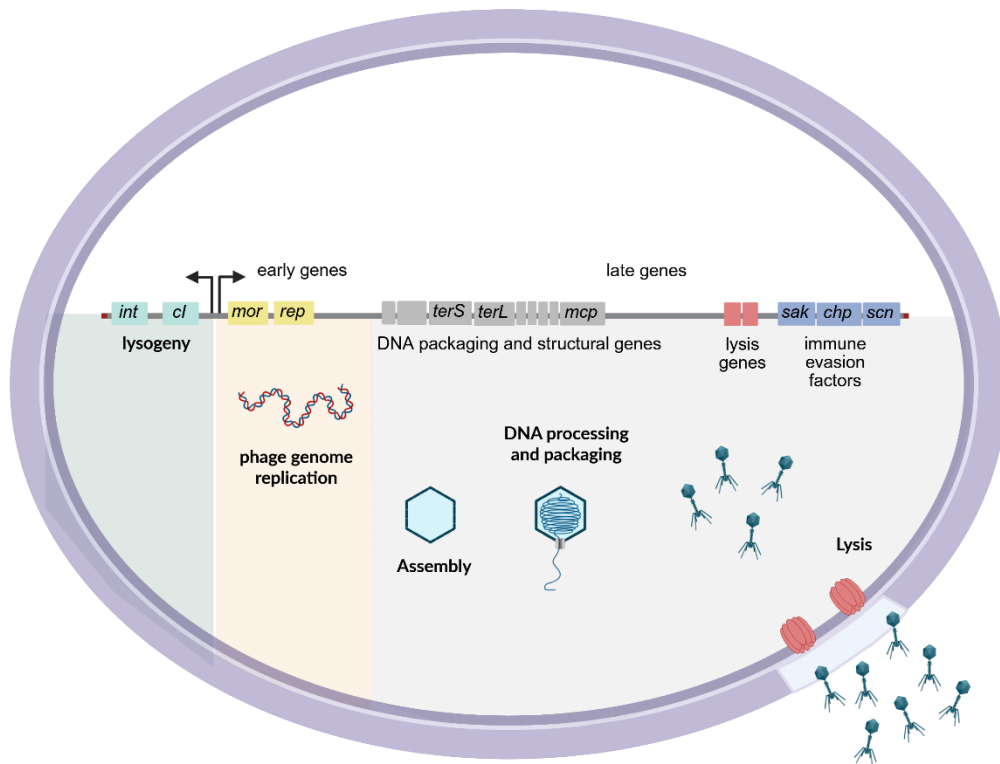


**Figure 2. Genetic organization and infection cycle of *S. aureus* Sa3int phage Φ13.** Schematic depiction of the modular genome architecture of phage Φ13. The lysogeny module (left, green) contains the integrase (*int*) and repressor (*ci*) genes responsible for integration and maintenance of the prophage state. Early lytic genes (yellow) involved in regulation (*mor*) and phage genome replication (e.g., *rep*), drive the initiation of the lytic lifecycle. Late lytic genes (light gray) encode DNA packaging and structural components, including small and large terminase subunits (*terS*, *terL*) and major capsid protein (*mcp*), which enable DNA processing, capsid assembly, and viral particle formation. Lysis genes mediate host cell wall degradation and release of progeny phages. The final module (blue) consists of immune evasion factors, including *sak*, *chp*, and *scn*, which encode proteins that modulate host immune defenses. Created with BioRender.com.

## **Aim of this thesis**

The adaptability of *Staphylococcus aureus* is strongly influenced by mobile genetic elements, particularly bacteriophages that enhance genetic diversity and introduce additional virulence determinants. Among these phages, Sa3int phages are the most prevalent in human *S. aureus* isolates. These phages, such as  $\Phi$ 13, function as regulatory switches by integrating into the *hlyB* locus while simultaneously expressing the immune evasion cluster, which encodes highly human-specific virulence factors. The dynamic integration and excision of these phages during infection enables *S. aureus* to modulate its virulence in response to changing environmental conditions.

The genomic organization of Sa3int phages and the switch from lysogenic to lytic life cycle upon host stress responses are well-characterized. However, the transcriptional regulation of late lytic stages and the contribution of host factors to phage replication remain poorly understood.

In this work, I aimed to characterize and reveal host-specific determinants that confer to differences in phage dynamics across diverse *S. aureus* strain backgrounds and thereby shape phage-host interactions. Comparative analyses of phage gene expression profiles were performed to uncover strain-dependent variations in transcriptional units and regulatory patterns. In addition, the influence of major global regulators of *S. aureus* virulence on phage regulation and replication was examined, given their potential role in coordinating the interactions necessary for stable phage-bacteria coexistence.

To gain deeper insight into the regulatory processes governing phage assembly and propagation, the transcriptional profile of  $\Phi$ 13 following induction was analyzed. Particular focus was placed on late-gene expression, as these genes encode essential components required for the formation of mature phage particles. By identifying both phage- and host-encoded regulators involved in the regulation of the phage life cycle, this work aimed to advance the understanding of the molecular mechanisms driving Sa3int phage dynamics and their impact on *S. aureus* pathogenicity.

## Results

### Part I: Influence of *Staphylococcus aureus* strain background on Sa3int phage life cycle switches

Carina Rohmer<sup>1,2,†</sup>, Ronja Dobritz<sup>1,†</sup>, Dilek Tuncbilek-Dere<sup>3,4</sup>, Esther Lehmann<sup>1</sup>, David Gerlach<sup>5</sup>, Shilpa Elizabeth George<sup>1</sup>, Taeok Bae<sup>6</sup>, Kay Nieselt<sup>3,4</sup>, Christiane Wolz<sup>1,3,\*</sup>

<sup>1</sup>Interfaculty Institute of Microbiology and Infection Medicine, University of Tübingen, 72074 Tübingen, Germany

<sup>2</sup>Fraunhofer Institute for Interfacial Engineering and Biotechnology IGB, 70569 Stuttgart, Germany

<sup>3</sup>Cluster of Excellence EXC 2124 “Controlling Microbes to Fight Infections”, University of Tübingen, 72074 Tübingen, Germany

<sup>4</sup>Institute for Bioinformatics and Medical Informatics, University of Tübingen, 72076 Tübingen, Germany

<sup>5</sup>Department of Microbiology, University of Würzburg, 97074 Würzburg, Germany

<sup>6</sup>Department of Microbiology and Immunology, Indiana University School of Medicine-Northwest, Gary, IN 46408, USA

\*Correspondence: [christiane.wolz@uni-tuebingen.de](mailto:christiane.wolz@uni-tuebingen.de)

†These authors contributed equally to this work

**Published:** Rohmer, C.; Dobritz, R.; Tuncbilek-Dere, D.; Lehmann, E.; Gerlach, D.; George, S.E.; Bae, T.; Nieselt, K.; Wolz, C. Influence of *Staphylococcus aureus* Strain Background on Sa3int Phage Life Cycle Switches. *Viruses* 2022, 14, 2471. <https://doi.org/10.3390/v14112471>

**Abstract:** *Staphylococcus aureus* asymptotically colonizes the nasal cavity of mammals, but it is also a leading cause of life-threatening infections. Most human nasal isolates carry Sa3 phages, which integrate into the bacterial *hly* gene encoding a sphingomyelinase. The virulence factor-encoding genes carried by the Sa3-phages are highly human-specific, and most animal strains are Sa3 negative. Thus, both insertion and excision of the prophage could potentially confer a fitness advantage to *S. aureus*. Here, we analyzed the phage life cycle of two Sa3 phages,  $\Phi$ 13 and  $\Phi$ N315, in different phage-cured *S. aureus* strains. Based on phage transfer experiments, strains could be classified into low (8325-4, SH1000, and USA300c) and high (MW2c and Newman-c) transfer strains. High-transfer strains promoted the replication of phages, whereas phage adsorption, integration, excision, or *recA* transcription was not significantly different between strains. RNASeq analyses of replication-deficient lysogens revealed no strain-specific differences in the *CI/Mor* regulatory switch. However, lytic genes were significantly upregulated in the high transfer strain MW2c  $\Phi$ 13 compared to strain 8325-4  $\Phi$ 13. By transcriptional start site prediction, new promoter regions within the lytic modules were identified, which are likely targeted by specific host factors. Such host-phage interaction probably accounts for the strain-specific differences in phage replication and transfer frequency. Thus, the genetic makeup of the host strains may determine the rate of phage mobilization, a feature that might impact the speed at which certain strains can achieve host adaptation.

**Keywords:** phage; virulence; induction; gene regulation; *Staphylococcus*; hemolysin

## Introduction

*Staphylococcus aureus* is a major human pathogen but also colonizes and infects different animal species [1–5]. Transmission of *S. aureus* between humans and livestock is of particular concern as *S. aureus* isolates from farmed animals are often antibiotic-resistant [6]. Adaptation to the different mammalian hosts occurs largely through the acquisition/loss of mobile genetic elements. *S. aureus* has jumped between species many times, resulting in the dynamic gain and loss of host-specific adaptive genes, many of which are prophage encoded [5,7–9]. Most prominent is the repeated loss of the temperate Sa3int phages upon the jump of *S. aureus* from humans to different animals [10]. In several instances, the animal-adapted strain was transmitted back to humans, where it often reacquired Sa3int phages, emphasizing their important role in human colonization [1,8–12]. Up to 96% of human nasal isolates were observed to carry Sa3int phages integrated into the *hly* locus, which encodes  $\beta$ -hemolysin (Hly), also named  $\beta$ -toxin [13]. These phages carry genes that encode human-specific immune evasion factors [14] and other potential virulence factors [10]. The observation that Hly is always functional after phage excision and that this process also occurs during human infections resulting in Hly-positive sub-populations [15], indicates that under certain infectious conditions, Hly is essential for bacterial survival.

Temperate staphylococcal phages belong to the family of *Siphoviridae*. The genomes of siphoviruses are typically organized into six functional modules: lysogeny, DNA replication, packaging, head, tail, and lysis. The evolution of phage lineages is driven by the lateral gene transfer of interchangeable genetic elements (modules), which consist of functionally related genes [8,13,16–19]. *S. aureus*-infecting siphoviruses have been classified according to polymorphisms of the integrase gene (*int*) [13,16,17,20]. The *int* type dictates chromosomal integration at cognate *attB* sites and is closely associated with the virulence gene content of the prophage [13]. However, due to the mosaic nature of *S. aureus* siphoviruses the distinct phage modules can show high homology between different Sa-Int phages. e.g., several open reading frames (ORFs) from the prototypic Sa3int phage  $\Phi$ 13 are homologous to those of PVL (Panton-Valentine leucocidin)-encoding Sa2int phages.

The molecular interactions between the *S. aureus* host and its temperate phages are largely unknown. The large number of phage genes encoding hypothetical proteins highlights how little is known about temperate phages and their influence on bacterial lifestyle switches. Likewise, we largely ignore which host factors influence the lysogenic-lytic cycle switch of temperate phages. Previous analysis of Sa2int phages revealed that the inducibility of the very same prophage can be significantly different when analyzed in diverse host genetic backgrounds [20]. Mobilization of the Sa2mw prophage from *S. aureus* strain MW2 or Newman was 100-fold higher than that from strain 8325-4.

Here, we investigated whether strain-specific features also impact the life cycle of Sa3int phages. For this, we constructed and integrated Sa3int phages into different phagecured *S. aureus* strains (8325-4, SH1000, USA300c, Newman-c, and MW2c). We focused on two prototypic Sa3int phages, namely  $\Phi 13$  and  $\Phi N315$ .  $\Phi 13$  is derived from the *S. aureus* reference strain 8325 of clonal complex (CC) 8.  $\Phi N315$  is derived from the methicillin-resistant strain N315 (CC5) and carries the *tarP* gene encoding for an alternative glycosyltransferase [21]. The strain background was found to impact phage transfer and replication. RNAseq analysis hint at specific interaction of host factors with the phage regulatory region located in the lytic module of the phage.

## Materials and Methods

### Growth Conditions

Unless otherwise stated, single-lysogens of *S. aureus* carrying  $\Phi 13_{kan}$  (Tang et al., 2017) or  $\Phi N315_{tet}$  were used. *S. aureus* cells were grown in Tryptic Soy Broth (TSB) (Oxoid), 37°C, 180 rpm. Precultures were supplemented with the appropriate antibiotics: kanamycin (KanA, 50  $\mu\text{g mL}^{-1}$ ), tetracycline (Tet, 3  $\mu\text{g mL}^{-1}$ ), erythromycin (Erm, 10  $\mu\text{g mL}^{-1}$ ), chloramphenicol (Chloro, 10  $\mu\text{g mL}^{-1}$ ), and streptomycin (Strep, 500  $\mu\text{g mL}^{-1}$ ).

### Strain Construction

Strains are listed in Supplementary Table S1, and oligonucleotides are listed in Supplementary Table S2.

### Selection of Strep Resistant Strains

*S. aureus* isolates were grown in TSB to  $OD_{600} = 0.7$  and supplemented with Strep (500  $\mu\text{g mL}^{-1}$ ). After 4 h of growth, serial dilutions were plated on TSB agar plates supplemented with Strep (500  $\mu\text{g mL}^{-1}$ ). Resistant colonies were sub-cultured and growth compared to the parental strain. Only streptomycin-resistant clones that were not impaired in growth were used in this study.

### Generation of Phage Cured USA300 (USA300c)

Native prophages (Sa2int and Sa3int) of *S. aureus* strain USA300 were deleted using plasmid pKOR1 as described for *S. aureus* Newman [22]. In brief: a 2 kb DNA fragment containing the respective *attB* sequences was PCR-amplified with the following primers (for Sa2int prophage: primer627 and primer628; for Sa3int prophage: primer434 and primer435) and inserted into pKOR1 and mutagenesis performed as described.

### Generation of Phage Lysates and Lysogens

Phage lysates of  $\Phi 13_{kan}$  or  $\Phi N315_{tet}$  were obtained after mitomycin C (500 ng  $\text{mL}^{-1}$ ) induction of 8325-4  $\Phi 13_{kan}$  or N315- $\Phi N315_{tet}$  in liquid culture ( $OD_{600} = 0.7$ ). After 2 h, 37°C additional mitomycin C (500 ng  $\text{mL}^{-1}$ ) was added and supernatant collected after further

incubation for 1 h (37°C). Supernatants were filtered (0.45 µm pore size (Merck)), and phage titer was enumerated by plaque assay. Single-lysogens were obtained by incubation of 10<sup>6</sup> phages with phage-cured *S. aureus* strains (10 mL) from the exponential growth phase (OD<sub>600</sub> = 0.7) for 4 h, 37°C. Selection of lysogens was performed on TSA plates containing KanA (50 µg mL<sup>-1</sup>) or Tet (3 µg mL<sup>-1</sup>), respectively. Single-lysogens were sub-cultivated four times, and phage integration at the cognate *att* site within *hly* verified by loss of β-hemolysin production and PCR using oligonucleotides hly675 and Sa3intfor.

### **Construction of Phage ΦN315tet**

Phage ΦN315 was labeled with a *tet* resistance cassette. *TetK* was amplified from plasmid pT181 using primer pair Tet2-F BamHI and Tet2-R BamHI. ΦN315 IEC specific overhangs were amplified using primer pair IEC:tet A+B and C+D. The three resulting fragments were fused using overlap extension PCR, ligated into plasmid pBASE6 [23], and cloned into *E. coli* DC10B. The vector was subsequently transferred into *S. aureus* N315 using electroporation and mutagenesis performed as described [23]. The mutation was verified by PCR and resulted in the replacement of phage-encoded *chp* and *scn* with the *tet* cassette.

### **Construction of Phage Φ13kan-Δrep**

Left and right flanking regions of prophage encoded replication factor (SAOUHSC\_02217) were amplified via PCR using oligonucleotides PiMAYrepdelrev/repdelrev and repdelfor/PiMAYrepdelfor (Supplementary Table S2) and cloned into shuttle vector piMAY [24] by Gibson assembly in *E. coli* DC10B. The vector was transferred from *E. coli* DC10B into 8325-4 Φ13kan and MW2c Φ13kan via electroporation and mutagenesis performed as previously described [24]. Gene deletion was verified by sequencing PCR amplicons spanning the mutation site. Further, lysogens were checked for β-hemolysin negative phenotype on blood agar plates.

### **Phage Transfer Assay**

Cultures of donor strains (single lysogens) and recipients (phage-cured, streptomycinresistant) were grown to exponential phase (OD<sub>600</sub> = 0.7), mixed at a ratio of 1:1, and co-cultivated for 4 h, 37°C, 180 rpm. Single and mixed cultures were diluted in PBS, and colony-forming units (CFU) were determined on blood agar plates (Oxoid) and TSA agar plates containing single antibiotics (KanA 50 µg mL<sup>-1</sup>, Tet 3 µg mL<sup>-1</sup>, Strep 500 µg mL<sup>-1</sup>) and double antibiotics (KanA 50 µg mL<sup>-1</sup>, Strep 500 µg mL<sup>-1</sup> or Tet 3 µg mL<sup>-1</sup>, Strep 500 µg mL<sup>-1</sup>), respectively. Phage transfer frequency was determined by CFU grown on double antibiotic-containing plates divided by CFU grown on TSA plates containing streptomycin (500 µg mL<sup>-1</sup>). Single colonies were analyzed for loss of Hly synthesis and phage integration by PCR. All tested double-resistant colonies carried the *hly* converting phage. Spontaneous resistance was monitored by

plating donor and recipient strains on selective agar plates and was many magnitudes lower than the observed transfer rates.

### **Lysogenization Assay**

Phage-cured derivatives of *S. aureus* isolates were grown to exponential growth phase ( $OD_{600} = 0.7$ ), and  $10^8$  bacteria per mL were infected with phages to a multiplicity of infection (MOI) of 0.1 or MOI 0.01 followed by incubation for 20 min or 4 h, 37°C, 180 rpm. CFU was determined on blood agar plates and TSA agar plates containing either KanA or Tet for the selection of lysogens. Single colonies were picked on a blood agar plate to verify loss of  $\beta$ -hemolysin activity. Lysogenization frequency was determined by CFU on antibiotic-containing plates divided by total CFU on blood plates.

### **Plaque Assay**

Phage titer was determined by agar overlay method using strain LS1 as indicator strain. Indicator strains were grown to  $OD_{600} = 0.1$  in TSB. In total, 100  $\mu$ L bacterial culture was mixed with 3 mL liquid phage soft agar (Casaminoacids 3 g L<sup>-1</sup>, Yeast Extract 3 g L<sup>-1</sup>, NaCl 5.9 g L<sup>-1</sup>, Agar 7.5 g L<sup>-1</sup>) and poured on TSA plate. After solidification, dilutions of sterile-filtered phage lysates were dropped on the lawn and incubated at 37°C to enumerate plaque-forming units (PFU).

### **Phage Adsorption Assay**

Phage adsorption assays were performed as described [25] with slight modifications. In brief, 100  $\mu$ L ( $3 \times 10^6$  phages) were incubated with  $3 \times 10^8$  bacteria in 1 mL TSB for 10 min at room temperature under non-shaking conditions. Bacteria were pelleted (5000 x g, 5 min), supernatant filtered (0.45  $\mu$ m pore size (Labsolute)), and used for PFU determination.

### **Prophage Spontaneous Induction or Induction Using Mitomycin C**

Single lysogens were grown to the exponential growth phase ( $OD_{600} = 0.7$ ) and split into 10 mL aliquots. Aliquots were further incubated with and without subinhibitory concentrations of mitomycin C (300 ng mL<sup>-1</sup>) for 1 h. Supernatants were filtered (0.45  $\mu$ m pore size (Merck)), PFU enumerated, and stored at -20 °C for qPCR. For absolute quantification of free phage DNA, 100  $\mu$ L of phage lysates were incubated with Proteinase K (100  $\mu$ g mL<sup>-1</sup>, AppliChem) for 1 h at 55°C, followed by heat inactivation at 95 °C for 10 min. Phage DNA was quantified by quantitative PCR (qPCR) using SYBR Green qPCR Kit (QIAGEN) and primers circlefor and circlerev spanning the reconstituted *attP* site of the phage. For quantification, standard molecules were obtained by PCR using primers phi13circlefor and phi13circlerev. The amplicons were purified, and DNA concentration was determined using  $A_{260}$ . For quantification of excised phages within bacteria, *attP* and the chromosomal *recA* (*recAF1* and *recA661*) were quantified using bacterial pellets. Bacteria were mechanically lysed using zirconia/silica beads in a high-speed homogenizer (6500 rpm, Fastprep). Lysed pellets were boiled for 10 min in

water bath and stored at  $-20^{\circ}\text{C}$ , and 1  $\mu\text{L}$  of a 1:100 dilution (RNase-free water, Ambion) was used for qPCR.

### **Northern Blot Analysis and Preparation of RNA-Probes**

Bacteria were grown to  $\text{OD}_{600} = 0.7$ , followed by 1 h incubation at  $37^{\circ}\text{C}$  with or without mitomycin C ( $300 \text{ ng mL}^{-1}$ ). In brief, the bacterial pellet was resuspended in TRIzol (Thermo Fisher Scientific, Waltham, MA, USA) and mechanically lysed using zirconia/silica beads in a high-speed homogenizer. For Northern blot analysis, RNA was isolated as recommended by the TRIzol manufacturer. Transcripts on Northern blots were hybridized with digoxigenin-labeled DNA probes generated by PCR (Supplementary Table S2). RNA probes were generated with specific primer pairs containing T7 promoter for in vitro transcription. In vitro transcription was performed with MEGAscript T7 kit following instructions with the exception that a nucleotide mix from Roche containing DIG-11-UTP was used for labeling of fragments with digoxigenin. For RNA-seq analysis, RNA from the aqueous phase was further purified using the ExpressArt® RNA ready Add-on Kit for TRIzol extraction (AmpTec, Hamburg, Germany) with the following modifications. After loading the sample on an RNAREady column, RNA was washed additionally with inhibitor removal buffer (5 M guanidine-HCl, 20 mM Tris-HCl pH 6.6, 37 % (v/v) EtOH). DNase digest of the sample was directly performed on the column.

### **TagRNAseq and RNAseq**

RNA aliquots were subjected to tagRNA-seq [26]. Experiments were conducted by Vertis Biotechnologie AG. Library preparation on rRNA depleted RNA samples was performed as follows: first Illumina TruSeq sequencing adapter (CTGAAGCT) was ligated to RNAs containing a 5' monophosphate end (resulting from processing events and thereby represent so-called processed start sites - PSS) followed by treatment with TEX (Terminator Exonuclease, Lucigen) to remove unligated 5' P-ends. Next, RNA 5' Polyphosphatase (5'PP, Lucigen) was used to convert triphosphate groups at 5'-RNA ends to monophosphate 5'-RNA ends. Formed monophosphate ends were then tagged by ligation of a second Illumina TruSeq sequencing adapter (TAATGCGC) (representing transcription start sites - TSS). After fragmentation, an oligonucleotide adapter was ligated to the 3' end of RNA fragments and cDNA synthesis performed using M-MLV reverse transcriptase. cDNA was PCR amplified within 16 cycles using high fidelity DNA polymerase. cDNA was purified using Agencourt AMPure XP Kit (Beckman Coulter Genomics). Last, the cDNA pool was single-read sequenced on an Illumina NextSeq 500 system using 75 bp read length. Output read data were assigned to three different sets based on the tags from sequencing: read-files assigned to either transcriptional start site (TSS), read-files assigned to processed start site (PSS), unassigned

read-files. The first two sets were used for transcription start site analysis, the latter was used for expression analysis.

### ***Differential Expression Analysis of Phage-Encoded Genes Using tagRNA-seq***

The reference genome of *S. aureus* 8325 (NCBI (NC\_007795.1) was manually phagecured,  $\Phi$ 13kan genome integrated and the sequence manually SNP-corrected based on resequencing of the 8325 strain [27]. Raw data files of reads (unassigned) were trimmed using the CLC genomics workbench (QIAGEN). Trimmed reads were mapped against the reference genome and then normalized for library depth and gene length, resulting in datasets containing expression values (RPKM-values). Raw data and processed files containing RPKM-values are available at <https://www.ncbi.nlm.nih.gov/geo/query/acc.cgi?acc=GSE214523> (accessed on 3 October 2022). Expression values were used for differential expression using the Wald test for statistical analysis. Significance was set to FDR-value of  $<0.05$  and log<sub>2</sub> fold change of lower than  $-1$  or higher than  $+1$ . From the resulting datasets of the whole genome, the prophage genome was extracted and analyzed (Supplementary Table S4). Read mapping was visualized to the  $\Phi$ 13 genome using Integrated Genome Viewer.

### ***Determination of TSSs***

To prepare the raw read data for TSS identification, reads were preprocessed and mapped, and a coverage per base was computed. For this, the RNA-seq analysis pipeline READemption version 0.5.0 [28] was used. All read samples were mapped to the respective reference sequence with the subcommand align, which integrates the mapper segemehl version 0.3.4 [29]. For the mapping, the following parameters were used: (`-adapter AGATCGGAAGAGCACACGTCTGAACTCCAGTCAC`, `-processes 4`, `-segemehl_accuracy 95`, `-segemehl_evalue 5.0`, `-poly_a_clipping`, `-min_phred_score 20` `-fastq`, `-progress`). The subcommand coverage calculates one position-based coverage file, also called wiggle files, resulting in three file sets: the unnormalized raw wiggle files, files normalized by the total number of mapped reads (TNOAR) and multiplied by one million (mil\_normalized), and files normalized by the total number of mapped read and multiplied by the lowest number of mapped reads taking all libraries in consideration (min\_normalized). The min\_normalized wiggle files were used for TSS calling. The TSS identification using the normalized wiggle files of the tagRNA-seq reads was conducted with TSSpredator 1.1 [30,31].

For all of the TSSpredator runs, the preset default parameters were used, except that matching replicates were set to 2. TSSpredator expects two types of reads, one from the so-called enriched library and one from the so-called normal or unenriched library. For the tagRNAseq data, we used the TSS-labeled reads as the enriched libraries and the PSS-labeled reads as the normal control libraries. The experimental setup of this study used three strains and compared two conditions. Therefore, TSSpredator was run both with the strain-setup and

condition-setup to analyze this data. For the cross-condition analysis, each strain was considered separately. For the cross-strain analysis, TSSpredator expects wiggle files normalized across all input libraries as input. For this, the lowest number of aligned reads over all replicates regarding both conditions was calculated, and then each library was multiplied by this minimum. From each TSSpredator run, the resulting MasterTables for each condition were combined manually, and the phage region was extracted (Supplementary Table S3). For the cross-condition analysis, each strain was considered separately. A detailed description of TSSpredator parameters, TSS classes, and output files can be taken from the user manual available at <https://tsspredator20-rtd.readthedocs.io/en/latest/index.html> (accessed on 3 November 2022).

### Statistical Analysis

Statistical analyses were performed using GraphPad Prism software. Differences between the two groups were evaluated using Student's t test. For multiple comparisons, statistical analysis was performed using one-way ANOVA (parametric) or Kruskal–Wallis test (non-parametric), with the Bonferroni test for parametric samples or Dunn's test for non-parametric samples as a post hoc test. Differences at  $p < 0.05$  were considered significant. All statistical analysis methods are based on independent biological replicates.

## Results

### Sa3int Phage Transfer during Co-Cultivation Depends on the Bacterial Host Strain

The Sa3int phage  $\Phi 13$  is derived from the *S. aureus* reference strain 8325. This strain was previously cured of all phages, and the phage-cured derivative 8325-4 is widely used as a prototypic *S. aureus* strain in many genetic studies. To facilitate the analysis of the phage life cycle, a kanamycin (*kan*) resistance cassette was introduced at the 3' end of  $\Phi 13$  [32]. To compare phage transfer/acquisition in different bacterial strains,  $\Phi 13_{kan}$  lysogens were generated in different phage-free host strains: 8325-4, SH1000, MW2c, Newman-c, USA300c (Supplementary Table S1). Phage transfer was monitored after 4 h of co-culture of the  $\Phi 13_{kan}$  single-lysogens with the isogenic, Strep-resistant and phage-free recipient under non-inducing conditions (Figure 1A). A high transfer rate was observed for strain MW2c and strain Newman-c, as enumerated by double resistance. Newly generated lysogens were Hlb-negative on blood agar plates, and phage integration into the *hIb* gene was verified by PCR using integration-specific oligonucleotides. Significantly lower phage transfer rates were observed for the 8325-4 or USA300c strain pairs as compared to Newman-c or MW2c. During the analyses, we observed that strain 8325-4 strain tended to aggregate during the incubation period. An *rsbU* repaired derivative of 8325-4 (strain SH1000) was described to form fewer aggregates [33]. To rule out any artifacts due to clumping, we also generated an SH1000  $\Phi 13_{kan}$  lysogen. This strain indeed did not aggregate but still showed a significantly lower phage transfer rate

compared to Newman-c or MW2c. In summary, we could confirm that the host background significantly influences phage lifecycle and pinpoint high (Newman-c and MW2-c) and low (8325-4, SH1000 and USA300) phage transfer strains (Figure 1A).

To analyze whether the strain background similarly determines the transfer rate of other phages, we included phage  $\Phi$ N315 derived from strain N315 in the analysis. The phage was labeled with a tet resistance cassette and mobilized into the same set of phage-cured strains. The phage transfer rate was lower compared to  $\Phi$ 13kan (Figure 1B). However, again strain Newman-c and MW2c exhibited higher phage transfer compared to the low-transfer strains SH1000 and USA300.

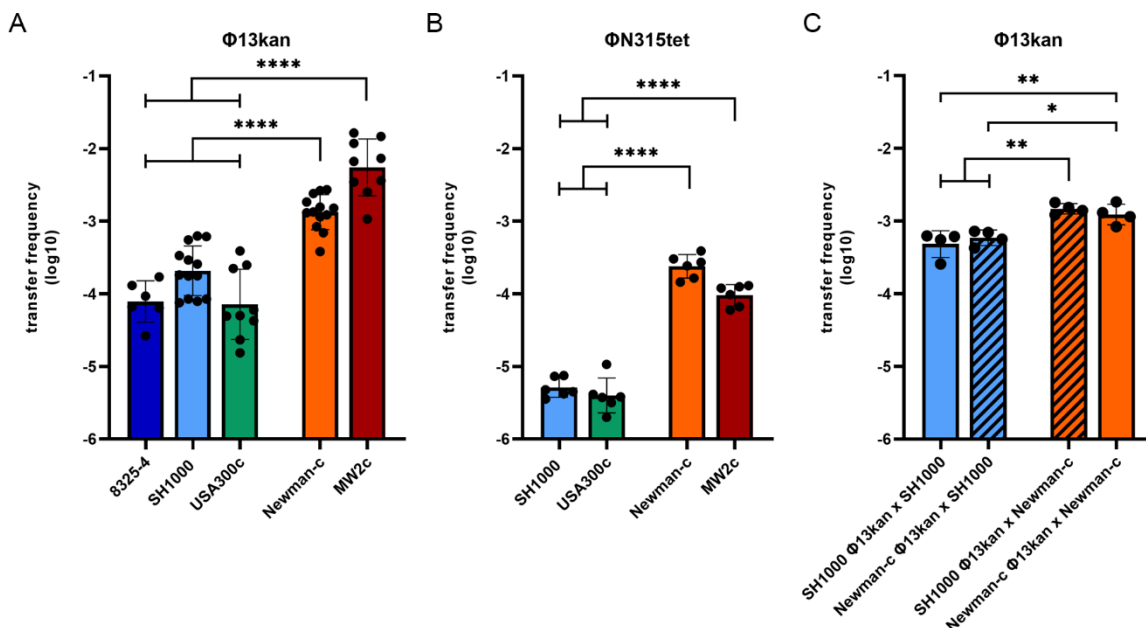


**Figure 1.** Phage transfer frequency of  $\Phi$ 13kan (A,C) or  $\Phi$ N315tet (B) is strain-dependent. Lysogens were mixed with isogenic, phage-cured, streptomycin-resistant recipients 8325-4 (dark blue), SH1000 (light blue), USA300c (green), Newman-c (orange), or MW2c (dark red) at a 1:1 ratio (4 h co-culture in tryptic soy broth) (A,B) or with non-isogenic recipients (C). Phage transfer frequency was determined by calculating the ratio of CFU of double-resistant colonies (kanamycin/streptomycin for  $\Phi$ 13kan or tetracycline/streptomycin for  $\Phi$ N315tet, respectively) divided by CFU on streptomycin (representing recipient). Values are independent biological replicates referring to mean  $\pm$  SD. Statistical analysis was performed on log-transformed data using one-way ANOVA. \*  $p \leq 0.05$ , \*\*  $p \leq 0.01$ , \*\*\*\*  $p \leq 0.0001$ .

**Strain-Dependent Differences in Sa3int Phage Transfer Are Determined by the Recipient**  
Strain 8325-4, SH1000, USA300, and Newman are assigned to the same CC 8 with no obvious restriction barrier [34]. MW2 belongs to CC1, and gene transfer between CC8 and CC1 strains is restricted due to different restriction/modification systems. Accordingly, phage transfer between CC8 strains and MW2 was found to be severely impaired (Supplementary Figure S1). We next analyzed whether transfer between low (SH1000) and high (Newman-c) transfer strains of the same CC is determined by the donor or by the recipient strain (Figure 1C). Strain

Newman as recipient showed higher phage acquisition when incubated with either SH1000  $\Phi$ 13kan or Newman-c  $\Phi$ 13kan. Strain SH1000 showed lower phage acquisition even when incubated with high transfer strain Newman-c  $\Phi$ 13kan. Thus, the different phage transfer rate among strains depends on the recipient.

### **Phage Adsorption Does Not Account for Strain Dependent Phage Integration**

We speculated that strain-dependent phage transfer may be the result of differential phage adsorption. Wall-teichoic acids (WTA) function as conserved phage receptor for *S. aureus* phages [8]. This could be verified for  $\Phi$ 13kan since phage adsorption was not detectable in the WTA-deficient strain USA300  $\Delta$ tagO (Supplementary Figure S2). All tested wild-type strains showed high phage adsorption with only minor differences between strains. Small differences in phage adsorption did not correlate with the observed strain dependent differences in lysogenicity efficiency. Thus, processes following initial phage adsorption are responsible for strain-specific differences in phage transfer and replication.

### **Strain Dependent Sa3int Lysogenization and Replication**

We next analyzed whether the various bacterial recipients differed in phage integration and/or replication rate. Newman-c lysogens were treated with mitomycin to induce prophage excision, and phage titer was enumerated by plaque assay. Phages were incubated with recipient strains, and phage integration was enumerated by the phage resistance marker. After 20 min co-incubation of  $\Phi$ 13kan with recipient strains, a similar fraction of SH1000 and Newman-c bacteria became lysogens (Figure 2A,B). This indicates that phage integration is equally efficient in both strains. However, after prolonged incubation (4 h), significantly more  $\Phi$ 13kan (Figure 2C) and  $\Phi$ N315tet (Figure 2D) lysogens were recovered in the high transfer strain Newman-c compared to the low transfer strain SH1000. We assumed that this is due to enhanced phage replication in strain Newman-c. To monitor phage replication, free phage titers were enumerated after the 4 h incubation period. Significantly higher phage replication of both phages ( $\Phi$ 13kan and  $\Phi$ N315tet) was observed after phage infection of strain Newman-c compared to strain SH1000 (Figure 2E,F). The phage titer of  $\Phi$ 13kan increased 650-fold in strain Newman-c and only 55-fold in strain SH1000.

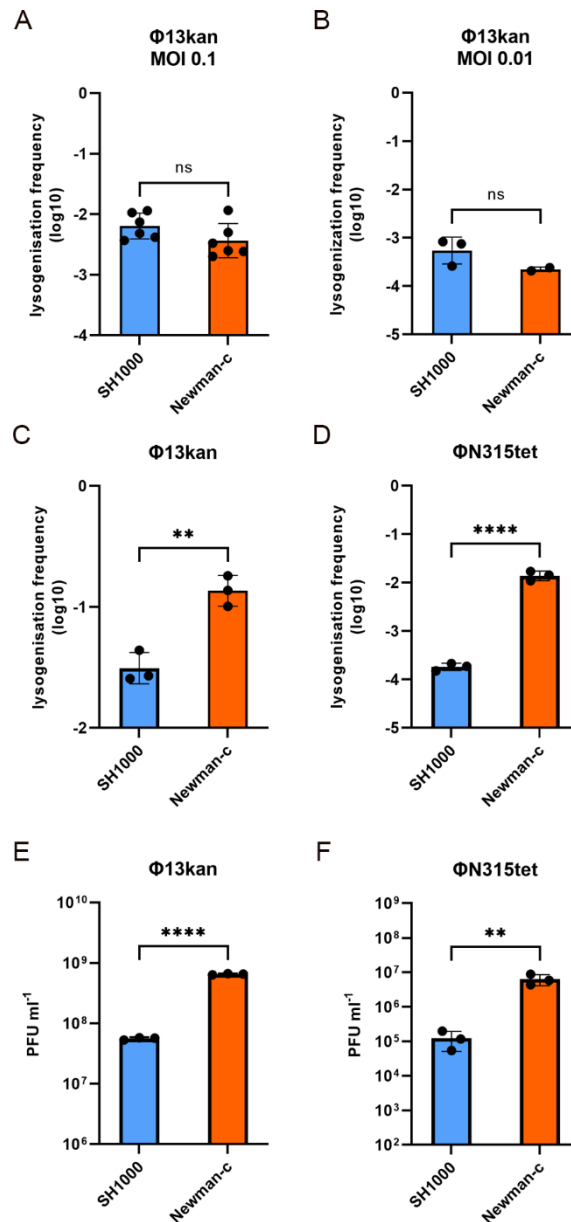


**Figure 2.** Strain-dependent lysogenization and replication of  $\Phi$ 13kan and  $\Phi$ N315tet. Lysogenization of phage-cured SH1000 (blue) and Newman-c (orange) with  $\Phi$ 13kan (A–C,E) or  $\Phi$ N315-tet (D,F) during exponential growth. Phages and phage-cured recipient bacteria were co-cultured to investigate lysogenization rates. Co-incubation was performed for 20 min at 37 °C and MOI of 0.1 (A) or 0.01 (B) or for 4 h at 37 °C and MOI of 0.01 (C–F). Lysogenization rates were determined by CFU on TSA plates containing kanamycin or tetracyclin (representing lysogenized colonies)/CFU on blood-agar plates. Replication of  $\Phi$ 13kan (E) and  $\Phi$ N315tet (F) was determined by enumerating phage particles in sterile filtrated supernatant by plaque assay 4 h post phage infection. Values are independent biological replicates referring to mean  $\pm$  SD. Statistical analysis was performed using t-test (A,B) and one-way ANOVA of log-transformed data (C–F). Data are back-transformed for visualization of phage titers (E,F). \*\*  $p \leq 0.01$ , \*\*\*\*  $p \leq 0.0001$ .

Thus, the integration efficiency seems not to differ between strains. However, in the high transfer strain, Newman-c phage replication is enhanced. The higher phage replication, in turn, increases the chance of phage integration, as seen in the later time points of infection.

### Phage Gene Expression Is Dependent on the Host Strain Background

Most of the genes carried by  $\Phi$ 13 encode proteins of unknown functions. Recently, a regulatory switch region was identified in the  $\Phi$ 13 genome [35]. The region is composed of a *Cl* coding repressor gene (*cl*) and a divergently transcribed *mor* (modulator of repression) gene. We monitored the transcription of lysogenic genes presumably initiating from the *cl* promoter and of the lytic genes initiating from *mor* by Northern blot analysis in MW2c- and 8325-4  $\Phi$ 13kan lysogens (Figure 3A). As expected, transcription of lytic genes (*mor*) was only detected after mitomycin treatment. One major transcript was detected, representing co-expression of *mor* with downstream lytic genes. Several additional bands were also visible, indicating the processing of the transcript. The expression of these lytic genes was mainly detectable in the MW2-c  $\Phi$ 13kan strain. This is consistent with higher replication observed in high phage transfer strain, i.e., Newman (Figure 2E). Higher phage replication in the MW2 background could be verified by quantification of phage copy numbers after mitomycin treatment via qPCR (Figure 3B). Phage replication also explains why the expression of genes within the lysogenic module, such as *cl* and *orfC*, was also increased after mitomycin treatment. Thus, multi-copy effect after phage replication impedes the interpretation of these results.

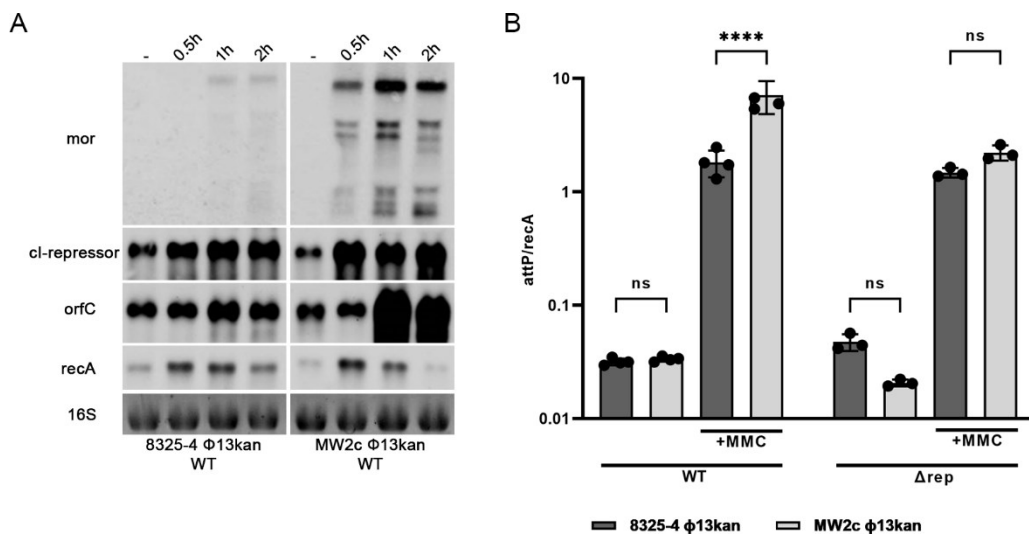


**Figure 3.** Phage replication is strain-dependent. Transcriptional analysis of phage-related genes (*cl*, *mor*, *orfC*) and chromosomally encoded *recA* under non-inducing and phage-inducing conditions (A). 8325-4  $\Phi$ 13kan and MW2c  $\Phi$ 13kan were grown to  $OD_{600} = 0.7$  and treated with mitomycin for 0.5 h, 1 h, or 2 h) or without mitomycin (1 h). RNA was hybridized with digoxigenin labeled DNA probes. Phage induction/replication in wild type (8325-4  $\Phi$ 13kan, MW2c  $\Phi$ 13kan) and replication-deficient derivatives ( $\Delta$ rep) under non-inducing and phage-inducing (1 h mitomycin, MMC) conditions (B). Phage excision/replication was enumerated as the ratio of excised, circularized phage copies (attP) per copy of bacterial chromosome (*recA*) as quantified by qPCR. \*\*\*\*  $p \leq 0.0001$ .

$\Phi$ 13 is likely induced following DNA damage-mediated RecA activation and subsequent CI autocleavage [35]. We speculated that MW2 might be more sensitive to RecA activation/SOS response compared to 8325-4. Therefore, we compared the induction of the SOS gene *recA* (preceded by a canonical LexA binding motif) in both strains. No difference in mitomycin-induced *recA* expression was observed between strains. In summary, the Northern blot analysis supported the hypothesis that RecA-independent bacterial factors promote phage replication in high-transfer strains.

### **Induction of $\Phi$ 13kan- $\Delta$ rep Is Not Strain Dependent**

To exclude multi-copy effects, we constructed replication-deficient mutants ( $\Phi$ 13kan- $\Delta$ rep) in different bacterial strain backgrounds. In such mutants, the phage can excise but not replicate (Figure 3B). No phage particles were detectable by plaque assays. Calculation of the excised prophage genomes per bacterial cell was performed by absolute quantification of *attP* in relation to *recA* (as a proxy for bacterial genome copy numbers) via qPCR. After mitomycin treatment, roughly one excised phage copy per bacterial genome was produced with no significant differences between strains. This indicates that phage induction is not significantly different between strains.

### **Transcriptional Start Site Prediction of $\Phi$ 13kan- $\Delta$ rep**

Besides the CI/Mor regulatory switch region, additional regulatory elements on the phage genome are likely involved in the phage-host cross-talk. So far, such putative regulatory elements and additional phage promoters are ill-defined. Therefore, we aimed to dissect phage transcriptional units in the replication-deficient lysogens 8325-4  $\Phi$ 13kan- $\Delta$ rep and MW2c  $\Phi$ 13kan- $\Delta$ rep using tagRNA-seq [26] followed by comparative analysis with putative TSSs as predicted by TSSpredator [31] (Figure 4, Supplementary Table S3).

We detected a total of 57 transcriptional start sites. For prediction, at least two replicates had to agree on the position of a TSS. The expression of corresponding genes is shown in Figure 4 and Supplementary Table S3. In general, transcription followed the expected orientation, namely leftwards in the lysogenic module and rightwards in the lytic/ structural modules.

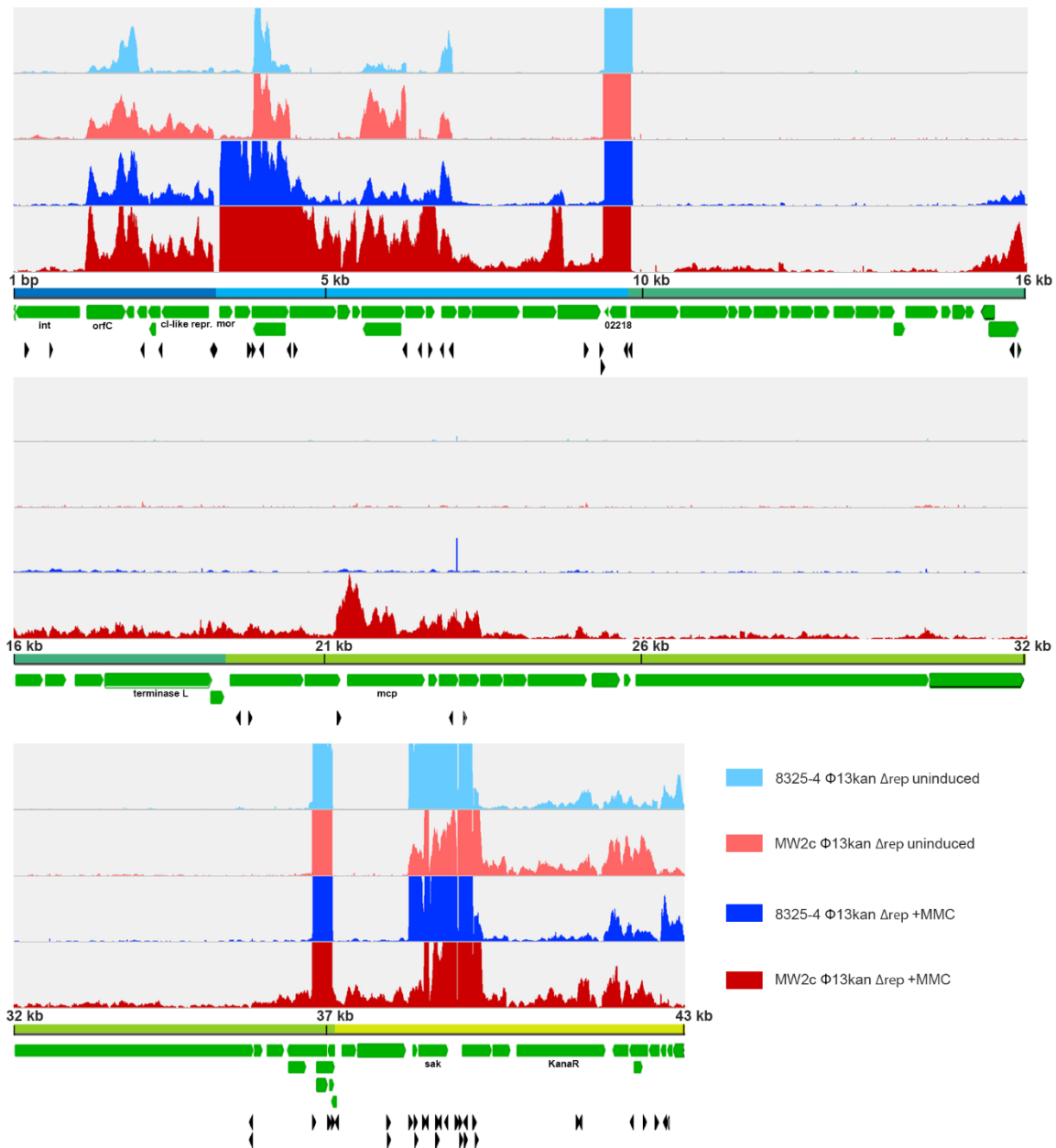


**Figure 4.** Visualization of predicted and enriched TSS and transcriptional profile of extracted Φ13 prophage region. Reads mapping to the phage genome are visualized for MW2c- and 8325-4 Φ13kan-Δrep strains under uninduced (light red and light blue, respectively) and induced (1 h mitomycin C treatment; dark red and dark blue) conditions from a representative sample out of 3 replicates. The maximum for the Y-axis in each panel is 200 counts. Protein coding genes are depicted in green and predicted TSS (Table S3) by black arrowheads.

The analysis also revealed several noncontiguous operons (operons containing a gene(s) that is transcribed in the opposite direction to the rest of the operon) (Figure 4, Supplementary Table S3), which were only recently acknowledged to play a role in gene regulation [36]. For instance, a single gene transcript (S861) located next to *ant* (putative antirepressor, SAOUHSC\_02229) is part of a lytic transcript but is also transcribed in anti-sense direction towards the lysogenic module (SAOUHSC\_02232) (Supplementary Table S4). A noncontiguous operon was also detected in the lysogenic module. *orfC* located between *int*

and the putative phage repressor *cl* is transcribed opposite to the expected lysogenic direction (Figure 5A). *Cl* transcription is initiated between *mor* and *cl* from the predicted promoter identified previously [35] (Figure 5). Northern blot analysis using strand-specific RNA probes confirmed that a transcript spanning *cl* and *orfC* is simultaneously detectable with a smaller *orfC* transcript starting from the opposite strand (Figure 5B).

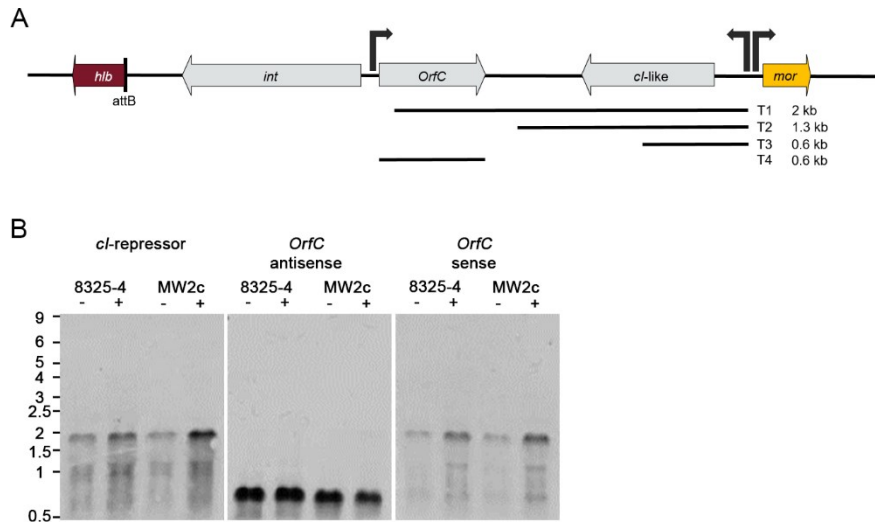


**Figure 5.** Transcriptional organization of the lysogenic modules of  $\Phi 13$ . Schematic representation of the lyosegenic module (A) of  $\Phi 13$ . Transcriptional units were visualized by hybridization of total RNA with digoxigenin-labeled RNA probes (B). Replication-deficient derivatives ( $\Delta rep$ ) of 8325-4  $\Phi 13kan$  and MW2c  $\Phi 13kan$  were grown to  $OD_{600} = 0.7$  and treated with (+) or without (-) mitomycin (1 h).

Thus, transcriptional regulation of phage genes seems highly complex, and gene expression is controlled at several levels. While most of the 57 TSSs were common to both strain backgrounds, strain-specific TSSs were also identified. In total, 14 of the predicted TSS are specific to 8325-4  $\Phi 13kan$  (5 TSS: uninduced, 8 TSS: +MMC, 1 TSS: both conditions) and 14 TSS to MW2c  $\Phi 13kan$  (1 TSS: uninduced, 12 TSS: +MMC, 1 TSS: both conditions).

### Strain-Dependent Gene Expression of $\Phi 13kan-\Delta rep$

Phage gene expression of  $\Phi 13kan-\Delta rep$  in 8325-4 and MW2c background was quantified by RNA-seq under non-induced and induced (1 h, mitomycin treatment) conditions (Supplementary Table S4). Under uninduced conditions, only nine phage genes were differentially expressed between both strains (Figure 6B). *OrfC* was expressed at higher levels in the 8325-background compared to the MW2-background. This is also evident in the Northern blot analysis of the  $\Phi 13kan-\Delta rep$  mutant (Figure 5B). The noncontiguous genes SAOUHSC\_02232 and SAOUHSC\_02218 were also more highly expressed in the 8325-4 background. Interestingly, these two genes of unknown function are transcribed in lysogenic direction although localized within the lytic phage region. Additionally, IEC genes showed

higher expression in 8325 compared to MW2 (e.g., *sak*, coding for staphylokinase, and the TA-system *sprGF1/sprF1*). The expression of *sak* was previously reported to be dependent on the host strain background, with expression being lower in MW2 compared to RN6390 (a derivative of 8325) background [20]. This is in agreement with previous work showing that Sa3int-encoded virulence genes are expressed independently from the phage lifecycle [10]. *Mcp* is the only gene that was found to be significantly higher expressed in strain MW2c than in 8325-4 under non-inducing conditions.

We next compared strain-dependent phage gene expression after mitomycin treatment (1 h), revealing a more profound difference in phage gene expression between the two strains. Most of the prophage genes either in 8325 (40 out of 73) and MW2 (56 out of 73) were significantly upregulated after mitomycin C treatment (Supplementary Table S4). However, upregulation was more pronounced in the MW2 background; 35 prophage-encoded genes were expressed at significantly higher levels in MW2 compared to the 8325 background (Figure 6C). Interestingly, no differences in the expression of *cl* and *mor* were observed between strains. Instead, most differences appeared in later genes assigned to regulation (blue), replication/packaging (dark green), and structural module (light green). Several TSSs were predicted within the lytic module, assuming that the expression of gene modules is dependent on different promoters (Figure 4 and Supplementary Tables S3 and S4), which are subject to strain-specific regulation.

Thus, the expression of lytic genes of prophage  $\Phi$ 13kan- $\Delta$ rep is more pronounced in the MW2 background compared to 8325 and probably accounts for the higher phage particle number observed in the MW2 background.

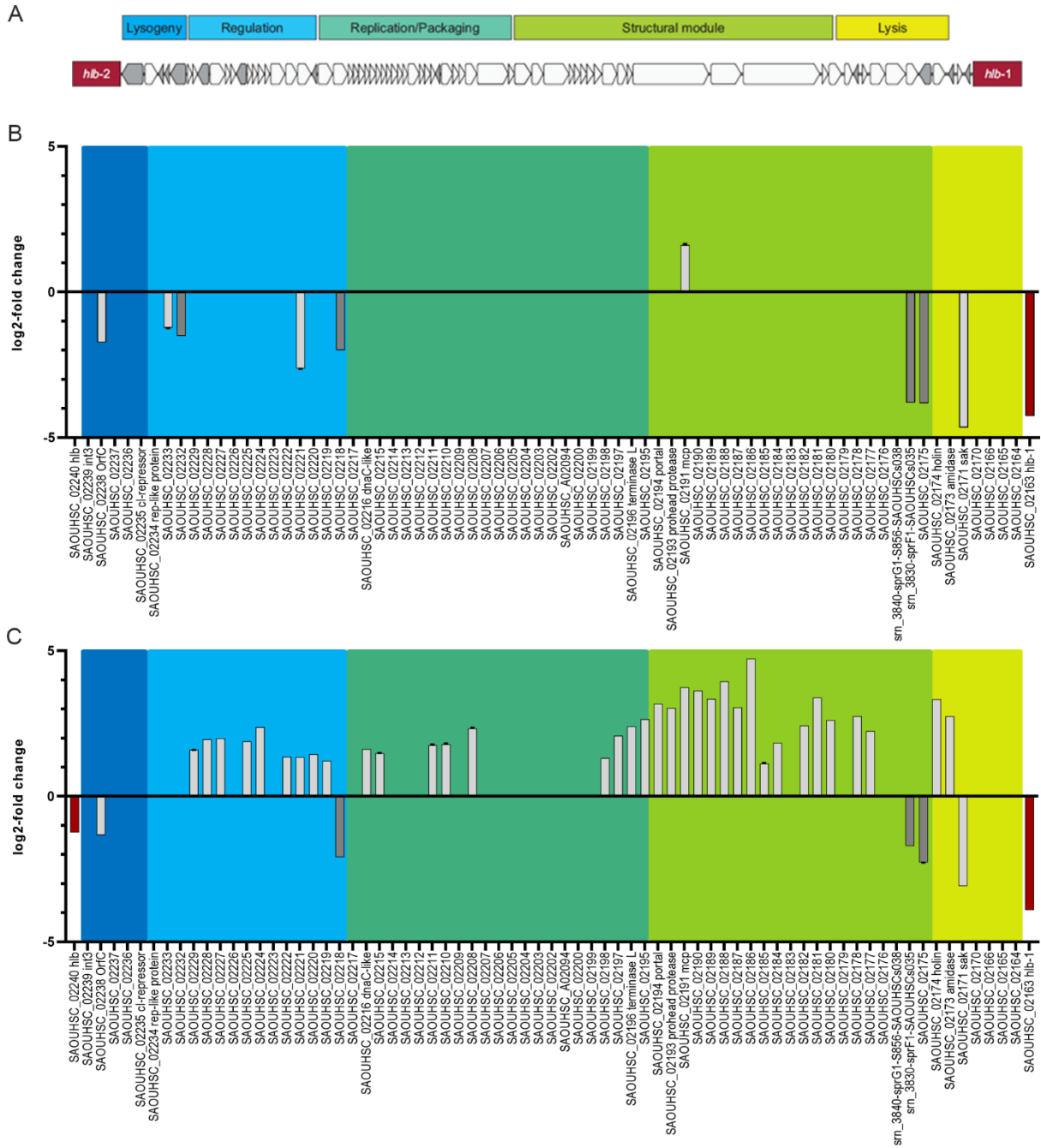


**Figure 6.** Module organization of  $\Phi 13kan$  (A). Comparison of  $\Phi 13kan$ - $\Delta rep$  gene expression between MW2- and 8325-background under uninduced conditions (B) and after mitomycin induction (C). Only genes with significant differences in gene expression are shown (FDR-value < 0.05; log<sub>2</sub>fold change > +1 and < -1). Negative values represent higher expression in 8325 background; positive values represent higher expression in MW2 background.

## Discussion

Here, we demonstrated that the lifecycle of *S. aureus* prophage is influenced by bacterial host factors. Replication of the *h1b* converting phages  $\Phi 13$  and  $\Phi N315$  was significantly enhanced in the Newman and MW2 strains compared to derivatives of the 8325 lineage or USA300. The higher replication rate correlated with higher spontaneous phage transfer events during co-culture. A similar dependence of phage replication on the host background was previously

shown for unrelated *pvl*-carrying  $\Phi$ Sa2mw phage [20]. The strain dependency is not due to differences in phage absorption (Supplementary Figure S2), phage integration (Figure 2), excision, or *recA* transcription (Figure 3). Interference with other phages could also be ruled out since all experiments were performed in single-lysogens.

To obtain more insights into the molecular mechanisms of the predicted phage–host interaction, we performed tagRNA-seq and determined the TSSs located on the  $\Phi$ 13kan- $\Delta$ rep phage and compared the expression of phage genes in 8325-4 and MW2c background. The decision between phage lifestyles is made by phage-encoded genetic switches best studied in phage  $\lambda$  of *Escherichia coli*. The transcriptional repressors CI and Cro can repress each other and compete for the same operator. Phage repressor CI represses transcription of lytic genes, whereas Cro relieves repression, thus facilitating the lytic life cycle. A CI/Cro-like switch region can be identified in  $\Phi$ N315 and  $\Phi$ Sa2mw2. However, in  $\Phi$ 13, the switch region is composed of an autocleavable CI repressor and a Mor homolog [35,37]. We confirmed the previously identified promoter regions as well as mitomycin sensitivity of  $\Phi$ 13. The CI repressor, which is expressed from the lysogenic promoter PR, represses the lytic promoter initiating *mor* expression. The small repressor MOR, first identified in lactococcal phages, functions as an anti-repressor of CI by protein-protein interaction but, on its own, does not directly influence transcription [37–39]. Thus, *S. aureus* phages can carry either CI/Mor ( $\Phi$ 13)- or CI/Cro-like switches ( $\Phi$ N315,  $\Phi$ Sa3mw) but nevertheless show similar strain dependency. It is thus unlikely that the proposed host factors influencing the phage life cycle target the canonical switch regions. Indeed, the expression of *ci* and *mor* genes was not significantly different between strains. Analysis of promoter fusions in *B. subtilis* also indicated that the decision switching by the minimal switch region of  $\Phi$  13 does not require *S. aureus*-specific host factors [35]. This is also in line with the observation that phage integration/excision seems to be independent of the strain background and likely only determined by RecA activity.

Nevertheless, replication and gene expression were elevated in the MW2 strain background, suggesting specific regulation downstream of the switch region. The TSS analysis points to many additional promoter regions that could be subject to gene regulation. The phage-derived mRNA landscape is further complicated by additional RNA processing sites. RNA processing might also be tightly controlled and functionally important [40,41]. Additionally, sRNAs or post-transcriptional regulation via, e.g., anti-termination [42] may be involved. Moreover, our analysis revealed several noncontiguous operons. Such a genetic arrangement was proposed to lead to mutual regulation of the expression of overlapping transcripts and to provide an additional strategy for coordinating the expression of functionally related genes within an operon [36].

Some TSSs were detected only in one strain background. Genes coding for structural phage proteins are more highly expressed in MW2 than in 8325-4. Thus, these TSSs are likely targets for host-dependent regulation. Post-excision regulation of phage replication and assembly, processes that are important to finalize the phage lytic phase, may also be a crucial determinant of the lysogenic-lytic cycle switch. Thus, under certain circumstances, the phages may just excise, leading to the reconstitution of the intact *hly* gene in the absence of complete phage assembly and host cell lysis. Such a process is reminiscent of the recently described process termed active lysogeny [43]. *L. monocytogenes* strain 10403S harbors a prophage in its *comK* gene. During infection of macrophage cells, the prophage lytic pathway is induced, but the phage lytic response is arrested, preventing the expression of the late genes. A phage-encoded LlgA transcription regulator (LlgA) and a DNA replicase are proposed to support the phage adaptive behavior [44]. No LlgA homolog could be identified, but functionally similar elements may be present in the *S. aureus* phages. The data strongly indicate that host factors interfere with such putative regulatory phage regions. Recently discussed xenogenic silencing factors might be involved in such a balance [45]. They promote tolerance of foreign genetic material and may play an important role in maintaining the lysogenic state. Those discovered so far are small, nucleoid-associated proteins that recognize and bind AT-rich DNA stretches (H-NS in Proteobacteria, MvaT/U in *Pseudomonas* species, Rok in *Bacillus subtilis* and Lsr2 in Actinobacteria). Of note, none of these factors is present in *S. aureus*. The phage-encoded virulence genes are known to be under the control of bacterial virulence regulatory systems such as the quorum sensing system, Agr, or the SaeRS two-component system [46]. From genome comparison between the low and high transfer strains, no obvious difference in known regulatory circuits, such as quorum sensing or transcriptional factors, was evident. Nevertheless, our data indicate that also phage structural genes are tightly controlled, although the mechanism remains to be determined.

Epidemiological data strongly indicate that Sa3int phages have co-evolved with the *S. aureus* host to facilitate the adaptation of the species to the human host. Adaptation is likely mediated by the phage-encoded virulence factors, which are specific to humans [10]. Of note, most *S. aureus* strains lack major phage defense systems such as CRISPR/Cas, cyclic-oligonucleotide-based anti-phage signaling systems [47] or phage-resistance mediating retrons [48]. This indicates that the species has likely evolved to tolerate phages and that the phages, to a large extent, are probably beneficial to the bacterial host. However, the phages remain highly mobile to relieve expression of the interrupted *hly* gene when needed, e.g., during infection [15,49]. This may occur either in the form of “active lysogeny” or prophage loss. Such switches must be controlled through firm molecular interactions between bacterial and phage factors. The postulated bacterial factors are highly strain-specific, and certain *S. aureus* strains may be more prone than others to support either a lysogenic or a lytic life

cycle. Thus, the genetic makeup of the host strains may determine the rate of phage mobilization during infection, a feature that might determine the speed at which certain strains can achieve host adaptation.

**Supplementary Materials:** The following supporting information can be downloaded at: <https://www.mdpi.com/article/10.3390/v14112471/s1>, **Table S3:** TSS prediction and corresponding gene expression; **Table S4:** Differential gene expression analysis of extracted prophage genomic region.

**Author Contributions:** Conceptualization, C.R., R.D. and C.W.; methodology, C.R., R.D., E.L., D.G. and S.E.G.; software, D.T.-D. and K.N.; validation, C.R., R.D., D.T.-D., K.N. and C.W.; formal analysis, C.R., R.D. and D.T.-D.; investigation, C.R., R.D., D.T.-D., D.G. and T.B.; writing—original draft preparation, C.R., R.D. and C.W.; writing—review and editing, C.R., R.D., C.W. and K.N.; visualization, C.R. and R.D.; supervision, C.W.; project administration, C.W.; funding acquisition, C.W. All authors have read and agreed to the published version of the manuscript.

**Funding:** This work was funded by Deutsche Forschungsgemeinschaft, GRK1708 to CW and CR (Project 174858087), Schwerpunktprogramm Spp2330 to CW (Project 464612409), and by infrastructural funding from the Deutsche Forschungsgemeinschaft (DFG), Cluster of Excellence EXC 2124 “Controlling Microbes to Fight Infections” (Project 390838134).

**Institutional Review Board Statement:** Not applicable.

**Informed Consent Statement:** Not applicable.

**Data Availability Statement:** RNAseq raw data and processed files containing RPKM-values are available at <https://www.ncbi.nlm.nih.gov/geo/query/acc.cgi?acc=GSE214523> (accessed on 3 October 2022).

**Acknowledgments:** We thank Natalya Korn and Vittoria Bisanzio for technical assistance, Libera Lo Presti for scientific discussions and editing of the manuscript, and Jeffrey J. Power for bioinformatic support.

**Conflicts of Interest:** The authors declare no conflict of interest.

## References

1. Matuszewska, M.; Murray, G.G.R.; Harrison, E.M.; Holmes, M.A.; Weinert, L.A. The Evolutionary Genomics of Host Specificity in *Staphylococcus aureus*. *Trends Microbiol.* 2020, 28, 465–477.
2. Balasubramanian, D.; Harper, L.; Shopsin, B.; Torres, V.J. *Staphylococcus aureus* pathogenesis in diverse host environments. *Pathog. Dis.* 2017, 75, ftx005.
3. Turner, N.A.; Sharma-Kuinkel, B.K.; Maskarinec, S.A.; Eichenberger, E.M.; Shah, P.P.; Carugati, M.; Holland, T.L.; Fowler, V.G., Jr. Methicillin-resistant *Staphylococcus aureus*: An overview of basic and clinical research. *Nat. Rev. Microbiol.* 2019, 17, 203–218.
4. Sakr, A.; Bregeon, F.; Mege, J.L.; Rolain, J.M.; Blin, O. *Staphylococcus aureus* Nasal Colonization: An Update on Mechanisms, Epidemiology, Risk Factors, and Subsequent Infections. *Front. Microbiol.* 2018, 9, 2419.
5. Haag, A.F.; Fitzgerald, J.R.; Penades, J.R. *Staphylococcus aureus* in Animals. *Microbiol. Spectr.* 2019, 7.
6. Richardson, E.J.; Bacigalupe, R.; Harrison, E.M.; Weinert, L.A.; Lycett, S.; Vrieling, M.; Robb, K.; Hoskisson, P.A.; Holden, M.T.G.; Feil, E.J.; et al. Gene exchange drives the ecological success of a multi-host bacterial pathogen. *Nat. Ecol. Evol.* 2018, 2, 1468–1478.
7. McCarthy, A.J.; Witney, A.A.; Lindsay, J.A. *Staphylococcus aureus* temperate bacteriophage: Carriage and horizontal gene transfer is lineage associated. *Front. Cell. Infect. Microbiol.* 2012, 2, 6.
8. Ingmer, H.; Gerlach, D.; Wolz, C. Temperate Phages of *Staphylococcus aureus*. *Microbiol. Spectr.* 2019, 7.
9. Chaguza, C.; Smith, J.T.; Bruce, S.A.; Gibson, R.; Martin, I.W.; Andam, C.P. Prophage-encoded immune evasion factors are critical for *Staphylococcus aureus* host infection, switching, and adaptation. *Cell Genom.* 2022.
10. Rohmer, C.; Wolz, C. The Role of hlb-Converting Bacteriophages in *Staphylococcus aureus* Host Adaptation. *Microb. Physiol.* 2021, 31, 109–122.
11. Bouiller, K.; Bertrand, X.; Hocquet, D.; Chirouze, C. Human Infection of Methicillin-Susceptible *Staphylococcus aureus* CC398: A Review. *Microorganisms* 2020, 8, 1737.
12. Sung, J.M.; Lloyd, D.H.; Lindsay, J.A. *Staphylococcus aureus* host specificity: Comparative genomics of human versus animal isolates by multi-strain microarray. *Microbiol. Read.* 2008, 154, 1949–1959.
13. Goerke, C.; Pantucek, R.; Holtfreter, S.; Schulte, B.; Zink, M.; Grumann, D.; Broker, B.M.; Doskar, J.; Wolz, C. Diversity of prophages in dominant *Staphylococcus aureus* clonal lineages. *J. Bacteriol.* 2009, 191, 3462–3468.
14. van Wamel, W.J.; Rooijackers, S.H.; Ruyken, M.; van Kessel, K.P.; van Strijp, J.A. The innate immune modulators staphylococcal complement inhibitor and chemotaxis inhibitory protein of *Staphylococcus aureus* are located on beta-hemolysin-converting bacteriophages. *J. Bacteriol.* 2006, 188, 1310–1315.
15. Goerke, C.; Wirtz, C.; Fluckiger, U.; Wolz, C. Extensive phage dynamics in *Staphylococcus aureus* contributes to adaptation to the human host during infection. *Mol. Microbiol.* 2006, 61, 1673–1685.
16. Deghorain, M.; Van Melderen, L. The Staphylococci phages family: An overview. *Viruses* 2012, 4, 3316–3335.
17. Kahankova, J.; Pantucek, R.; Goerke, C.; Ruzickova, V.; Holochova, P.; Doskar, J. Multilocus PCR typing strategy for differentiation of *Staphylococcus aureus* siphoviruses reflecting their modular genome structure. *Environ. Microbiol.* 2010, 12, 2527–2538.
18. Oliveira, H.; Sampaio, M.; Melo, L.D.R.; Dias, O.; Pope, W.H.; Hatfull, G.F.; Azeredo, J. Staphylococci phages display vast genomic diversity and evolutionary relationships. *BMC Genom.* 2019, 20, 357.
19. Zhou, W.; Wen, H.; Li, Y.; Gao, Y.; Zheng, X.; Yuan, L.; Zhu, G.; Yang, Z. Whole-Genome Analysis Reveals That Bacteriophages Promote Environmental Adaptation of *Staphylococcus aureus* via Gene Exchange, Acquisition, and Loss. *Viruses* 2022, 14, 1199.

20. Wirtz, C.; Witte, W.; Wolz, C.; Goerke, C. Transcription of the phage-encoded Panton-Valentine leukocidin of *Staphylococcus aureus* is dependent on the phage life-cycle and on the host background. *Microbiol. Read.* 2009, 155, 3491–3499.
21. Gerlach, D.; Guo, Y.; De Castro, C.; Kim, S.H.; Schlatterer, K.; Xu, F.F.; Pereira, C.; Seeberger, P.H.; Ali, S.; Codee, J.; et al. Methicillin-resistant *Staphylococcus aureus* alters cell wall glycosylation to evade immunity. *Nature* 2018, 563, 705–709.
22. Bae, T.; Baba, T.; Hiramatsu, K.; Schneewind, O. Prophages of *Staphylococcus aureus* Newman and their contribution to virulence. *Mol. Microbiol.* 2006, 62, 1035–1047.
23. Geiger, T.; Francois, P.; Liebeke, M.; Fraunholz, M.; Goerke, C.; Krismer, B.; Schrenzel, J.; Lalk, M.; Wolz, C. The stringent response of *Staphylococcus aureus* and its impact on survival after phagocytosis through the induction of intracellular PSMs expression. *PLoS Pathog.* 2012, 8, e1003016.
24. Monk, I.R.; Shah, I.M.; Xu, M.; Tan, M.W.; Foster, T.J. Transforming the untransformable: Application of direct transformation to manipulate genetically *Staphylococcus aureus* and *Staphylococcus epidermidis*. *mBio* 2012, 3, e00277-11.
25. Xia, G.; Corrigan, R.M.; Winstel, V.; Goerke, C.; Grundling, A.; Peschel, A. Wall teichoic Acid-dependent adsorption of staphylococcal siphovirus and myovirus. *J. Bacteriol.* 2011, 193, 4006–4009.
26. Innocenti, N.; Golumbeanu, M.; Fouquier d’Herouel, A.; Lacoux, C.; Bonnin, R.A.; Kennedy, S.P.; Wessner, F.; Serror, P.; Bouloc, P.; Repoila, F.; et al. Whole-genome mapping of 5′ RNA ends in bacteria by tagged sequencing: A comprehensive view in *Enterococcus faecalis*. *RNA* 2015, 21, 1018–1030.
27. Berscheid, A.; Sass, P.; Weber-Lassalle, K.; Cheung, A.L.; Bierbaum, G. Revisiting the genomes of the *Staphylococcus aureus* strains NCTC 8325 and RN4220. *Int. J. Med. Microbiol.* 2012, 302, 84–87.
28. Forstner, K.U.; Vogel, J.; Sharma, C.M. READemption—a tool for the computational analysis of deep-sequencing-based transcriptome data. *Bioinformatics* 2014, 30, 3421–3423.
29. Hoffmann, S.; Otto, C.; Kurtz, S.; Sharma, C.M.; Khaitovich, P.; Vogel, J.; Stadler, P.F.; Hackermüller, J. Fast mapping of short sequences with mismatches, insertions and deletions using index structures. *PLoS Comput. Biol.* 2009, 5, e1000502.
30. Bischler, T.; Tan, H.S.; Nieselt, K.; Sharma, C.M. Differential RNA-seq (dRNA-seq) for annotation of transcriptional start sites and small RNAs in *Helicobacter pylori*. *Methods* 2015, 86, 89–101.
31. Dugar, G.; Herbig, A.; Forstner, K.U.; Heidrich, N.; Reinhardt, R.; Nieselt, K.; Sharma, C.M. High-resolution transcriptome maps reveal strain-specific regulatory features of multiple *Campylobacter jejuni* isolates. *PLoS Genet.* 2013, 9, e1003495.
32. Tang, Y.; Nielsen, L.N.; Hvitved, A.; Haaber, J.K.; Wirtz, C.; Andersen, P.S.; Larsen, J.; Wolz, C.; Ingmer, H. Commercial Biocides Induce Transfer of Prophage Phi13 from Human Strains of *Staphylococcus aureus* to Livestock CC398. *Front. Microbiol.* 2017, 8, 2418.
33. Haaber, J.; Leisner, J.J.; Cohn, M.T.; Catalan-Moreno, A.; Nielsen, J.B.; Westh, H.; Penades, J.R.; Ingmer, H. Bacterial viruses enable their host to acquire antibiotic resistance genes from neighbouring cells. *Nat. Commun.* 2016, 7, 13333.
34. Moller, A.G.; Lindsay, J.A.; Read, T.D. Determinants of Phage Host Range in *Staphylococcus* Species. *Appl. Environ. Microbiol.* 2019, 85.
35. Kristensen, C.S.; Varming, A.K.; Leinweber, H.A.K.; Hammer, K.; Lo Leggio, L.; Ingmer, H.; Kilstrup, M. Characterization of the genetic switch from phage 13 important for *Staphylococcus aureus* colonization in humans. *Microbiol. Open* 2021, 10, e1245.
36. Saenz-Lahoya, S.; Bitarte, N.; Garcia, B.; Burgui, S.; Vergara-Irigaray, M.; Valle, J.; Solano, C.; Toledo-Arana, A.; Lasa, I. Noncontiguous operon is a genetic organization for coordinating bacterial gene expression. *Proc. Natl. Acad. Sci. USA* 2019, 116, 1733–1738.
37. Pedersen, M.; Neergaard, J.T.; Cassias, J.; Rasmussen, K.K.; Lo Leggio, L.; Sneppen, K.; Hammer, K.; Kilstrup, M. Repression of the lysogenic PR promoter in bacteriophage TP901-1 through binding of a CI-MOR complex to a composite OM-OR operator. *Sci. Rep.* 2020, 10, 8659.
38. Rasmussen, K.K.; Palencia, A.; Varming, A.K.; El-Wali, H.; Boeri Erba, E.; Blackledge, M.; Hammer, K.; Herrmann, T.; Kilstrup, M.; Lo Leggio, L.; et al. Revealing the mechanism of

- repressor inactivation during switching of a temperate bacteriophage. *Proc. Natl. Acad. Sci. USA* 2020, 117, 20576–20585.
39. Pedersen, M.; Hammer, K. The role of MOR and the CI operator sites on the genetic switch of the temperate bacteriophage TP901-1. *J. Mol. Biol.* 2008, 384, 577–589.
  40. Lacoux, C.; Fouquier d'Herouel, A.; Wessner-Le Bohec, F.; Innocenti, N.; Bohn, C.; Kennedy, S.P.; Rochat, T.; Bonnin, R.A.; Serror, P.; Aurell, E.; et al. Dynamic insights on transcription initiation and RNA processing during bacterial adaptation. *RNA* 2020, 26, 382–395.
  41. Marincola, G.; Schafer, T.; Behler, J.; Bernhardt, J.; Ohlsen, K.; Goerke, C.; Wolz, C. RNase Y of *Staphylococcus aureus* and its role in the activation of virulence genes. *Molecular Microbiol.* 2012, 85, 817–832.
  42. Yin, Z.; Kaelber, J.T.; Ebright, R.H. Structural basis of Q-dependent antitermination. *Proc. Natl. Acad. Sci. USA* 2019, 116, 18384–18390.
  43. Feiner, R.; Argov, T.; Rabinovich, L.; Sigal, N.; Borovok, I.; Herskovits, A.A. A new perspective on lysogeny: Prophages as active regulatory switches of bacteria. *Nat. Rev. Microbiol.* 2015, 13, 641–650.
  44. Pasechnek, A.; Rabinovich, L.; Stadnyuk, O.; Azulay, G.; Mioduser, J.; Argov, T.; Borovok, I.; Sigal, N.; Herskovits, A.A. Active Lysogeny in *Listeria monocytogenes* is a bacteriophage adaptive response in the mammalian environment. *Cell Rep.* 2020, 32, 107956.
  45. Pfeifer, E.; Hunnefeld, M.; Popa, O.; Frunzke, J. Impact of xenogeneic silencing on phage-host interactions. *J. Mol. Biol.* 2019, 431, 4670–4683.
  46. Xia, G.; Wolz, C. Phages of *Staphylococcus aureus* and their impact on host evolution. *Infect. Genet. Evol. J. Mol. Epidemiol. Evol. Genet. Infect. Dis.* 2014, 21, 593–601.
  47. Millman, A.; Melamed, S.; Amitai, G.; Sorek, R. Diversity and classification of cyclic-oligonucleotide-based anti-phage signalling systems. *Nat. Microbiol.* 2020, 5, 1608–1615.
  48. Millman, A.; Bernheim, A.; Stokar-Avihail, A.; Fedorenko, T.; Voichek, M.; Leavitt, A.; Oppenheimer-Shaanan, Y.; Sorek, R. Bacterial Retrons Function in Anti-Phage Defense. *Cell* 2020, 183, 1551–1561.e12.
  49. Goerke, C.; Matias y Papenberg, S.; Dasbach, S.; Dietz, K.; Ziebach, R.; Kahl, B.C.; Wolz, C. Increased frequency of genomic alterations in *Staphylococcus aureus* during chronic infection is in part due to phage mobilization. *J. Infect. Dis.* 2004, 189, 724–734.

## Supplementary Information

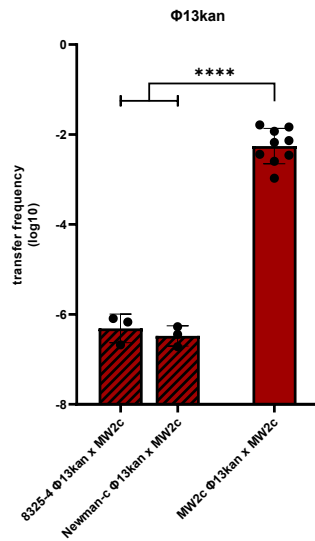


**Figure S1. Phage transfer frequency** between CC8 donors (8325-4 Φ13kan, Newman-c Φ13kan) and CC1 (MW2c) recipient strain is restricted. Lysogens were mixed with phage-cured, streptomycin-resistant recipients MW2c at a 1:1 ratio (4 h coculture in tryptic soy broth). Phage transfer frequency was determined by calculating the ratio of CFU of double-resistant colonies (kanamycin/streptomycin) divided by CFU on streptomycin (representing recipient). Values are independent biological replicates referring to mean  $\pm$  SD. Statistical analysis was performed on log-transformed data using one-way ANOVA.

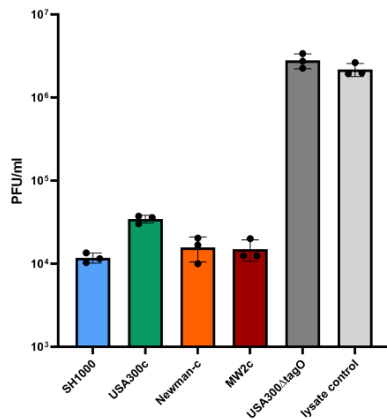


**Figure S2. Phage adsorption.**  $10^6$  Φphi13kan phage particles were incubated with  $10^8$  phage cured bacteria or a WTA deficient *tagO* mutant for 10 minutes. Unbound phages in the filtered supernatants were enumerated by plaque assays. Values are independent biological replicates with mean  $\pm$  SD.

**Table S1.** Strains used in this study

Bacterial strain	Clonal complex (CC)	Property	Origin
8325-4	CC8	Phage-cured	Dorte Frees, University of Copenhagen, Denmark
8325-4-Strep	CC8	Phage-cured, resistant against streptomycin	This study
8325-4Φ13-kana	CC8	Single-lysogen	This study
8325-4ΦN315-tet	CC8	Single-lysogen	This study
8325-4Φ13-kanaΔrep	CC8	Single-lysogen carrying replication-deficient mutant	This study
SH1000	CC8	Phage cured	Susanne Engelmann, TU Braunschweig, Germany
SH1000-Strep	CC8	Phage-cured, resistant against Streptomycin	This study
SH1000Φ13-kana	CC8	Single-lysogen	This study
SH1000ΦN315-tet	CC8	Single-lysogen	This study
USA300c	CC8	Phage-cured	This study
USA300c-Strep	CC8	Phage-cured, resistant against Streptomycin	This study
USA300cΦ13-kana	CC8	Single-Lysogen	This study
USA300cΦN315-tet	CC8	Single-lysogen	This study
Newman-c	CC8	Phage-cured	T. Bae et al., 2006
Newman-c-Strep	CC8	Phage-cured, resistant against Streptomycin	This study
Newman-cΦ13-kana	CC8	Single-Lysogen	This study
Newman-cΦN315-tet	CC8	Single-Lysogen	This study
MW2c	CC1	Phage-cured	Tang et al., 2017
MW2c-Strep	CC1	Phage-cured, resistant against Streptomycin	This study
MW2cpΦ13-kana	CC1	Single-Lysogen	This study
MW2cΦN315-tet	CC1	Single-lysogen	This study
MW2cΦ13-kanaΔrep	CC1	Single-lysogen carrying replication-deficient mutant	This study
USA300_ΔtagO	CC8	WTA-deficient isolate used as control for adsorption-assay	Wanner et al., 2008
<i>E. coli</i> DC10B	-	Used for cloning procedures	Monk et al., 2012

**Table S2.** Primer used in this study

Name	Sequence
circlefor	TTTTATTTTATATGGGGTATTATTGA
circlev	GTGTATTCTCATTTGTTAGAAGAAAA
h1b675	GCTATCATTATCGAATCCAC
h1b258	
IEC::tet_A	GACGAATTCGTGAAAAGGGTTGTTTATGGGGC
IEC::tet_B	CTTATATTTTGTCTAGGATCCCTGTGAATAGTCATAGGCGTCCATACATAATC
IEC::tet_C	GAGTTTTTAGAACAAGGATCCGGTAAAGAAAGTGTTAGGTTACTAGGCCACTTAAC
IEC::tet_D	CTCGAGCTCCCCTGGATTCAACTTAATTACAAAGG
phi13c1DIGfor	TCATACTTCGGATTTAGAGATACC
phi13c1DIGrev	CGAAACCTTATCAAAGAAACTAGG
phi13croDIGfor	CGGTAAAGTTGGTTGGAA
phi13croDIGrev	ATTGGAGTGGCGTTGATT
phi13sieDIGrev	GAAATCGCTACCAGCTGA
phi13sieDIGfor	CGCTTCTTCTTACAGGAGTT
Primer434	GGGGACAAGTTTGTACAAAAAAGCAGGCTCCGTTCCACAGTGATTGTGTATGG
Primer435	GGGGACCACTTTGTACAAGAAAGCTGGGTGCCTGCTACATAGAATGTAGTAGG
Primer627	GGGGACAAGTTTGTACAAAAAAGCAGGCTCAATTACATCATCAACTGTATTGTC
Primer628	GGGGACCACTTTGTACAAGAAAGCTGGGTGATGCGTTGAGTAAACTGATTAC
recAF1	GCTCAAGCATTAGGCGTAGAT
recA661	ATTTTAATGCACGTCACCTGG
sa3intfor	GAAAAACAAACGGTGCTAT
sa3intrev	TTATTGACTCTACAGGCTGA
phi13circlefor	TCTAGCTTTTGGGGTGTACATTCC
phi13circlev	GCTTTGAAATCAGCCTGTAGAG
p1MAYrepdelrev	TCGATAAGCTTGATATCGACTAGAAAACGGATATCCACT
p1MAYrepdelfor	GATCCCCCGGGCTGCAGGTCTCGCTCCCTGAAATCGTC
repdelfor	AAATGGCAACAGAAACACTTTTTTGGCAGT
repdelrev	GTGTTTCTGTTGCCATTTTCGTTATCTCCTTTCTG
Tet2-F BamHI	TTCACAGGGATCCTAGAACAAAATATAAG
Tet2-R BamHI	TCTTTACCGGATCCTTGTTCTAAAAACTC

**Table S3. TSS prediction and corresponding gene expression.** Table includes summarized information on predicted TSSs obtained from TSSpredator. Detailed description of included information are given in the user guide for TSSpredator V1.1 (<https://itnc.informatik.uni-tuebingen.de/index.php/s/en3s7fegaCzWQQy>). Information contained in Mastertable are given for each predicted TSS (listed in rows). TSS number (Column A), neighboring gene (Column B) or potential gene according to direction and position (Column O). Sequence -50 nt upstream + TSS (51nt) contains the base of the TSS and the 50 nucleotides upstream of the TSS (Column E). Column F-M indicate under which conditions the predicted TSS was enriched and the gene expression of the corresponding gene according to the direction and position of the TSS.

**Table S4. Differential gene expression analysis of extracted prophage genomic region.** Table contains combined data obtained from CLC genomics workbench (QIAGEN) including expression analysis for prophage genomic region for comparison of MW2 versus 8325 gene locus (**Column A**). Expression values of uninduced condition of MW2vs8325 comparison is marked in yellow (**Column D-F**), expression values for induced condition MW2vs8325 comparison are marked in green (**Column G-I**). Expression values for comparison of condition (induced versus control) are marked in dark blue for 8325 (**column J-L**) and dark red for MW2 (**Column M-O**). RPKM values are listed in Column P-AA and marked in light blue for 8325 and red for MW2 for both conditions.

**Part II: The phage  $\Phi$ 13-encoded transcriptional regulator Ltr controls phage assembly in *Staphylococcus aureus***

Ronja Dobritz<sup>1,2</sup>, Marcel Bäcker<sup>3</sup>, Carina Rohmer<sup>1</sup>, Natalya Korn<sup>1,2</sup>, Vittoria Bisanzio<sup>1,2</sup>, Christiane Wolz<sup>1,2,\*</sup>

<sup>1</sup>Interfaculty Institute of Microbiology and Infection Medicine, University of Tübingen, Germany

<sup>2</sup>Cluster of Excellence EXC 2124 “Controlling Microbes to Fight Infections”, University of Tübingen

<sup>3</sup>Institute of Biodiversity, Ecology and Evolution, Cluster of Excellence “Balance of the Microverse”, Friedrich Schiller University, Jena, Germany

\*Correspondence: [christiane.wolz@uni-tuebingen.de](mailto:christiane.wolz@uni-tuebingen.de)

**Submitted Manuscript:** Ronja Dobritz, Marcel Bäcker, Carina Rohmer, Natalya Korn, Vittoria Bisanzio, Christiane Wolz. The phage  $\Phi$ 13-encoded transcriptional regulator Ltr controls phage assembly in *Staphylococcus aureus*.

bioRxiv 2025.11.28.691083 <https://doi.org/10.1101/2025.11.28.691083>

Submitted to Virology Journal.

**Abstract:** Temperate phages play a central role in evolution and pathogenicity of *Staphylococcus aureus*. Sa3int phages, in particular, contribute highly human-specific virulence factors that promote immune evasion and survival within the host. The reversible excision of these phages which occurs without phage production and bacterial lysis allows the simultaneous expression of phage virulence genes and the *hly* gene where they usually integrate. The regulatory mechanisms controlling phage assembly remain poorly understood. In this study, we analyzed the regulatory mechanism controlling late gene transcription in Sa3int phage  $\Phi$ 13. We identified a functional promoter, P<sub>23</sub>, located upstream of the late phage genes that control DNA processing and packaging, capsid assembly, bacterial lysis and immune evasion. SAOUHSC\_02200, the gene located upstream of P<sub>23</sub>, encodes for a late transcriptional regulator (Ltr). Mutating the P<sub>23</sub> TATA-box or the *ltr* gene abolished P<sub>23</sub> activity and formation of mature intact phage particles, thus confirming the role of Ltr in regulating P<sub>23</sub> activity. Four direct repeats upstream of the P<sub>23</sub> transcriptional start site were identified as potential Ltr binding sites. RT-qPCR analysis confirmed that Ltr-dependent P<sub>23</sub> activation is essential for expression of late genes and the subsequent propagation of  $\Phi$ 13. Furthermore, comparative analysis of P<sub>23</sub> activity and *ltr* expression in different host strain backgrounds revealed strain-specific differences that appear to depend on the alternative sigma factor SigB and its downstream effector SpoVG. These findings establish Ltr as the major regulator of late gene expression in  $\Phi$ 13 and reveal bacterial host factors that control successful phage assembly, and bacterial lysis.

**Importance:** The dynamic integration and excision of highly prevalent Sa3int phages in *Staphylococcus aureus* is considered a regulatory switch that enables bacterial adaptation to specific niches. These phages carry several human-specific virulence genes and integrate into the *hly* virulence gene. It was assumed that they undergo a mechanism termed 'active lysogeny', which allows the phages to be excised reversibly without phage production or bacterial lysis. Here, we have identified a new phage-encoded 'late transcriptional regulator' (Ltr) that controls the expression of all late phage genes and thus phage assembly and lysis. We found that Ltr activity is regulated by the alternative sigma factor B and its downstream effector SpoVG. Restriction of SpoVG, and consequently phage assembly, likely contributes to the maintenance of Sa3int phages, even under phage-inducing conditions. This may be relevant in certain infectious conditions where both the phage-encoded virulence genes and the gene that is usually interrupted by the phage are required for infectivity.

**Keywords:** *Staphylococcus aureus*; phage assembly; active lysogeny; pseudo-lysogeny; late transcriptional regulators

## Introduction

*Staphylococcus aureus* is a major opportunistic pathogen that asymptotically colonizes the nose of up to 30% of the human population and can cause severe infectious diseases. The virulence of *S. aureus* can be influenced by mobile genetic elements, such as pathogenicity islands, plasmids and bacteriophages that encode accessory virulence factors (1). All known temperate staphylococcal phages belong to the family of *Siphoviridae*, which are characterized by an icosahedral head, a long, non-contractile tail and dsDNA. The phage genomes are organized into functional modules for lysogeny, replication, DNA packaging, structural genes encoding for head and tail proteins and lysis (2-6). *S. aureus* can carry several prophages at the same time, some of those encode for various staphylococcal virulence factors (6, 7). Phages infecting *S. aureus* have been classified into seven major groups based on the encoded *integrase* gene (*Sa-int* type). The *int* type dictates the *attB* site for integration of the prophage into the bacterial genome (3).

With up to 96% abundance, Sa3int phages are the most prevalent temperate phages in human nasal isolates of *S. aureus* (3, 8). Phages of this group integrate into the *hly* locus, disrupting the *hly* gene encoding a sphingomyelinase ( $\beta$ -hemolysin) (3, 9). On the other hand, Sa3int phages carry a set of genes for human-specific virulence factors, including a staphylokinase, as well as chemotaxis- and complement inhibitors, on the so called Immune Evasion Cluster (10, 11).

Sa3int phages are repeatedly lost when *S. aureus* is transferred from humans to animals, confirming the importance of these phages for the adaptation of *S. aureus* to the human host. Interestingly, when animal-adapted strains were transmitted back to humans, they often re-acquire Sa3int phages (11, 12). It was also found that Sa3int phages are more prevalent in strains that colonize the human nose than in infectious strains (13).

Depending on the host environment, both the insertion and excision of prophages may confer a fitness advantage to the host bacterium. Recently, it was demonstrated that the integration of Sa3int prophages significantly reduced the uptake into human macrophages, thereby mediating escape from human innate immune cells (14). On the other hand, the excision of Sa3int phage  $\Phi$ 13 is a critical step in the pathogenesis of *S. aureus* during murine infections (15) and spontaneous Hly-positive variants are selected during murine skin colonization (16) or infective endocarditis in rabbits (17). Sa3int phages may also undergo pseudo-lysogeny/active lysogeny a process during which a phage is temporally excised from the chromosome without forming intact phage particles (18-21). This is consistent with the observation that infection of *S. aureus* with Sa3int phages usually does not result in the lysis of the bacterial population (22). Through this process, bacteria can simultaneously activate

phage virulence genes as well as the gene that is typically inactivated by phage integration (23).

Molecular cross-talk between Sa3int phages and their *S. aureus* host and regulatory processes controlling active lysogeny remain largely unknown. Previous studies revealed that prophage excision, replication and transfer is highly strain dependent (24, 25) Comparative RNA-Seq analysis of high (MW2c) and low transfer (8325-4) strains revealed significant differences in the expression of structural module genes (24). Thus, so far unidentified bacterial factors are crucial determinants for the phage life cycle.

Here, we investigated the transcriptional regulation of Sa3int phages to uncover the mechanisms that control phage assembly. We identified an essential promoter region within the phage genome that regulates late phage genes and discovered strain-specific differences in its activity. Moreover, we identified SAOUHSC\_02200 as an activating regulator, with similarity to Family IV of the previously described late transcriptional regulators (Ltrs). Strain-specific differences in  $P_{23}$  activity implicated that the alternative sigma factor B (SigB) and its downstream effector SpoVG play a role in the regulation of  $P_{23}$  dependent phage gene expression and consequently phage assembly.

## Results

### The predicted promoter region P<sub>23</sub> in the Φ13 genome is functional and exhibits strain-specific activity

In previous work, we identified 57 transcriptional start sites (TSS) across the Φ13 genome analyzed in low and high phage transfer strains (24). TSS23 became of interest, as it is located upstream of the structural module and precedes genes (*SAOUHSC\_02198* to *SAOUHSC\_02177*) that were significantly upregulated in the high-transfer strain MW2c. TSS23 is located in an intergenic region in between two genes of unknown function (upstream: *SAOUHSC\_02200*; downstream: *SAOUHSC\_02199*). Late phage genes including DNA-packaging genes (*endonuclease*, small (*terS*) and large terminase (*terL*)) and structural genes (*mcp*) are located downstream of TSS23. Sequence analysis of the region upstream of TSS23 revealed a putative TATA-box, suggesting the presence of a functional promoter. To analyze the activity and regulation of this putative promoter region (designated P<sub>23</sub>), we constructed reporter plasmids, covering 200 bp upstream and 50 bp downstream of the predicted TSS23 (Figure 1A). The P<sub>23</sub> promoter region was fused to *yfp*, allowing fluorescence measurements to assess P<sub>23</sub> activity.

Promoter activity was measured for 24 h in four different Φ13K single-lysogenic *S. aureus* strains. Under uninduced conditions, P<sub>23</sub> activity remained undetectable, indicating the promoter remains inactive in the lysogenic state (Supplemental Figure S1). Upon addition of subinhibitory concentrations of mitomycin C (MMC) to induce the bacterial SOS response and phage excision, strain-specific differences in P<sub>23</sub> activity were obvious. The highest P<sub>23</sub> activity was found in high-transfer strain MW2c Φ13K, while intermediate fluorescent signals were detected in Newman-c Φ13K and SH1000 Φ13K, and the lowest activity in 8325-4 Φ13K (Figure 1B). To assess strain-specific differences independently of growth effects, we measured P<sub>23</sub> activity at single time-points with adjusted optical densities. Measurement at 4 hours after induction with MMC revealed the same strain-specific differences in P<sub>23</sub> activity (Figure 1C).

To confirm promoter functionality and characteristics of P<sub>23</sub>, we replaced the putative TATA-box (position -15 to -5 relative to TSS23) with Cs and Gs (Figure 1A). The substitutions abolished P<sub>23</sub> promoter activity, confirming that the region contains a functional TATA-box at the proposed position, which is required for promoter activity (Figure 1C, Supplemental Figure S1).

To investigate the role of P<sub>23</sub> in phage replication and production, we mutated the TATA-Box in the P<sub>23</sub> promoter region of the Φ13 genome. This resulted in a loss of phage particle production under uninduced and MMC induced conditions as determined by plaque assay (Figure 1D).

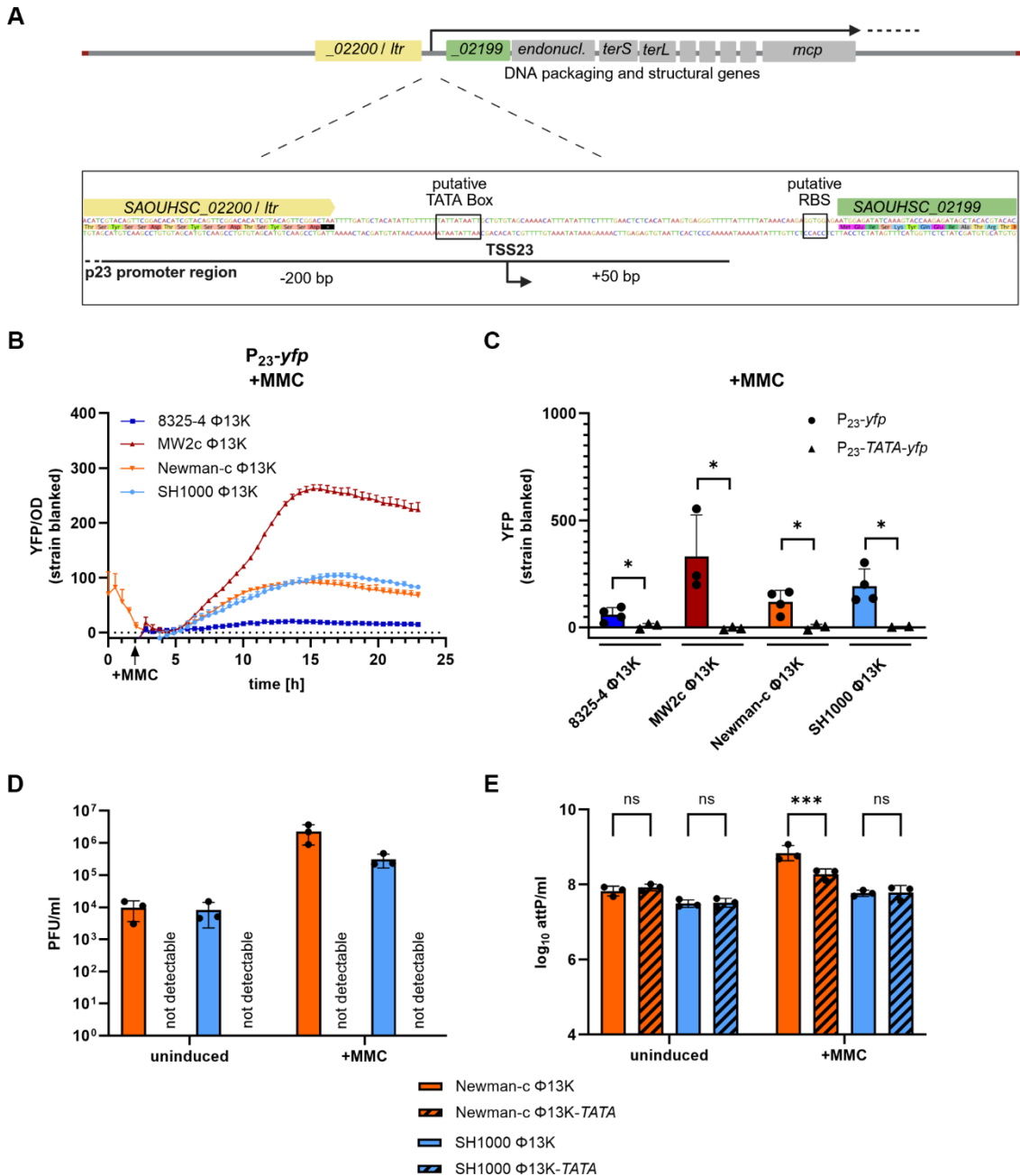


**Figure 1: P<sub>23</sub> is a functional and essential promoter of Φ13 with strain-specific activity.** (A) Schematic depiction of P<sub>23</sub> promoter region and transcriptional start site 23 (TSS23). (B) P<sub>23</sub> promoter activity measurement over time after mitomycin C (MMC) addition. Single-lysogenic strains were grown to exponential growth phase and induced with a subinhibitory concentration of mitomycin C (300 ng ml<sup>-1</sup>). Optical density and fluorescence were measured for further 24 hours. Arbitrary units of fluorescence (YFP) are shown normalized to OD<sub>600</sub> after subtracting strain-specific background fluorescence. (C) Single time point measurement of P<sub>23</sub> promoter activity without (P<sub>23</sub>-yfp) and with mutant TATA-Box (P<sub>23</sub>-TATA-yfp). Single-lysogenic strains were grown to exponential phase, induced with a subinhibitory concentration of MMC, and grown for additional 4 hours. Bacteria were harvested to OD<sub>600</sub> of 2 and resuspended in PBS. Fluorescence was measured. Arbitrary units of fluorescence (YFP) are shown; strain-specific background fluorescence was subtracted. Data shown are mean ± SD (n ≥ 3). Statistical significance was determined by unpaired t-tests within strains. (D,E) Phage replication in strains carrying Φ13K (wild type) and Φ13K-TATA (TATA-box mutation) under uninduced and induced (+MMC) conditions. Single-lysogenic Φ13K strains were induced with subinhibitory MMC in exponential phase and incubated for 60 min. Phage numbers were determined by plaque assay (D) and phage genome numbers by qPCR on the attachment site (*attP*) (E). Data shown are mean ± SD (n = 3). Statistical significance was determined by 2way ANOVA tests on log<sub>10</sub> transformed data (\*\*\*p-value < 0.001, \*p-value < 0.05, ns > 0.05).

However, phage genome replication, quantified by qPCR still occurred in the TATA-Box mutant phage. Since no infectious phage particles were detectable, we assume that phage genomes are likely released into the supernatant through phage-independent mechanisms of bacterial cell lysis. Upon addition of MMC, no (SH1000) or only a slight increase (Newman-c, factor 2) in phage genome copy numbers was observed for the  $\Phi$ 13K-*TATA* phage mutant (Figure 1E). These results indicate that the phage loses its ability to produce intact mature phage particles through  $P_{23}$  disruption. However, phage genome replication was largely independent of  $P_{23}$  activity.

These findings confirm that the  $P_{23}$  promoter region is functional and essential for  $\Phi$ 13 propagation. Our data also indicates strain-specific differences in  $P_{23}$  activity potentially caused by host-dependent regulatory factors.

### ***sigB* and *spoVG* dependent $P_{23}$ regulation**

*S. aureus* SH1000, which exhibited intermediate  $P_{23}$  activity, and *S. aureus* 8325-4, which showed the lowest activity, differ only by a defective *rsbU* gene in 8325-4. Since RsbU is responsible for the activation of SigB, 8325-4 is considered SigB-deficient. This was confirmed by analyzing the expression of *asp*, a prototypic SigB target gene (Figure 2A). This observation led us to investigate the involvement of SigB in  $P_{23}$  regulation.

Deletion of the whole *sigB* operon ( $\Delta mazEFrsbUVWsigB$ ) in single-lysogenic strains resulted in a decrease of  $P_{23}$  activity to levels comparable to those of the natural SigB-deficient strain 8325-4 (Figure 2B).  $P_{23}$  activity after 4 hours of induction with MMC was fourfold lower in the *sigB* deleted SH1000 single-lysogen than in the wild type. Since  $P_{23}$  promoter region does not contain a SigB consensus motif, the SigB effect is likely mediated by one of its downstream effectors. Expression of the putative regulator *spoVG* is directly regulated through SigB and might serve as SigB effector. Indeed, mutation of *spoVG* resulted in a similar decrease in  $P_{23}$  promoter activity to that observed for the *sigB* mutation (Figure 2C). Deletion of either *sigB* or *spoVG* also resulted in significantly reduced phage particle numbers as quantified by plaque assay (Figure 2D). However, the number of phage genome copies decreased more profoundly in the *sigB* mutant than in the *spoVG* mutant indicating that SigB exerts some additional SpoVG-independent effects on phage replication (Figure 2E).

Overall, these results demonstrate that SigB and its downstream effector SpoVG directly or indirectly modulate  $P_{23}$  activity and subsequent phage propagation.

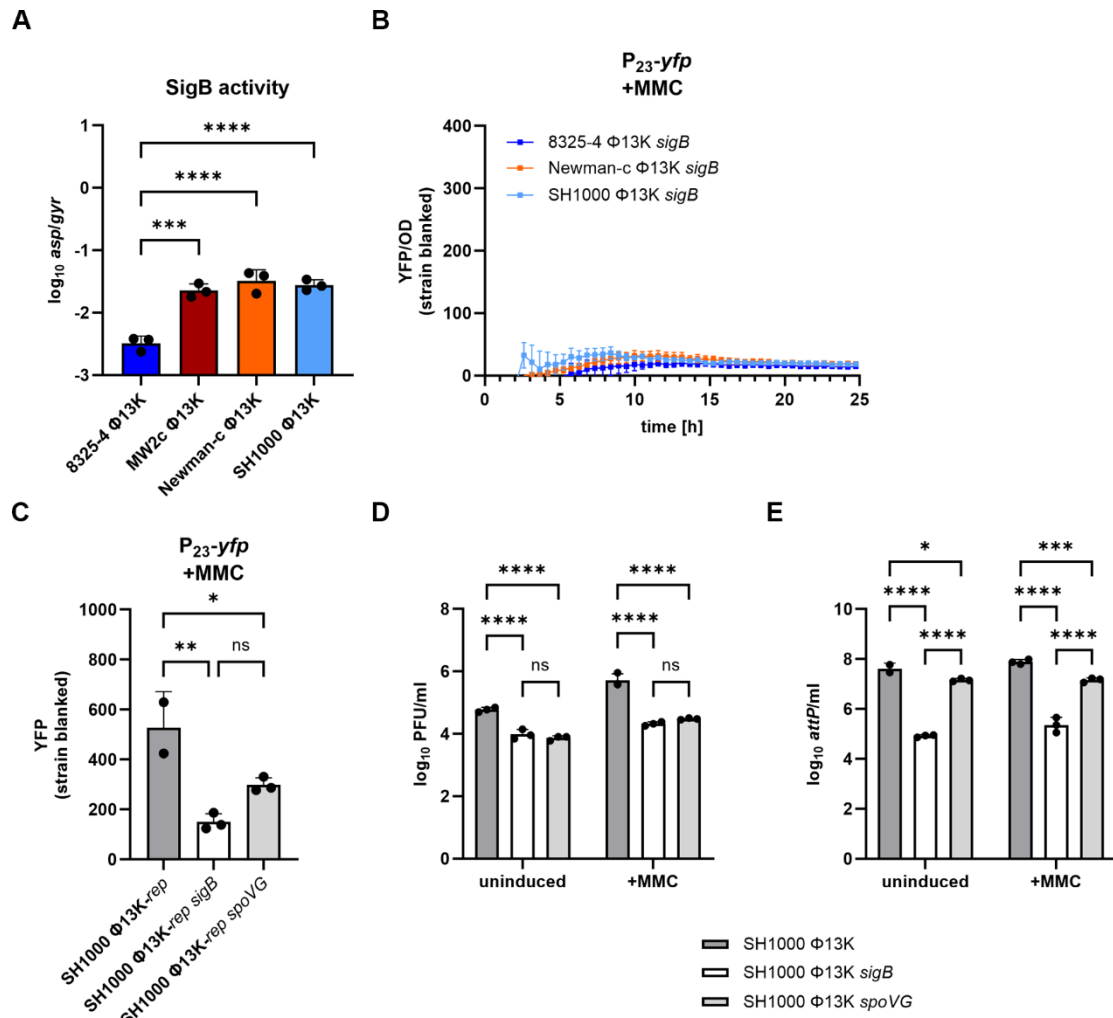


**Figure 2: SigB and SpoVG impact P<sub>23</sub> promoter activity and phage production.** (A) Strain-specific SigB activity under induced conditions. Single-lysogenic strains were grown to exponential phase, induced with a subinhibitory concentration of mitomycin C (MMC) (300 ng ml<sup>-1</sup>), and grown for further 4 hours. Bacteria were harvested for RNA isolation and RT-qPCR was performed. The expression of *asp* was normalized to *gyrB* expression. Data shown are mean ± SD (n = 3). Statistical significance was determined by ordinary one-way ANOVA test on log<sub>10</sub> transformed data. (B) P<sub>23</sub> promoter activity in a *sigB*-deficient background over time after MMC addition. Single-lysogenic strains were grown to exponential phase and induced with a subinhibitory concentration of MMC. Optical density and fluorescence were measured for further 24 h. Arbitrary units of fluorescence (YFP) are shown normalized to OD<sub>600</sub>; strain-specific background fluorescence was subtracted. (C) Single time point measurement of P<sub>23</sub> promoter activity in SH1000 (wild type), SH1000 *sigB* (*sigB::tet* deletion), and SH1000 *spoVG* (*spoVG::erm* deletion). Single-lysogenic strains were grown to exponential phase, induced with a subinhibitory concentration of MMC and grown for further 4 hours. Bacteria were harvested to OD<sub>600</sub> of 2 and resuspended in PBS. Fluorescence was measured. Arbitrary units of fluorescence (YFP) are shown; strain-specific background fluorescence was subtracted. Data shown are mean ± SD. Statistical significance was determined by ordinary one-way ANOVA. (D,E) Phage replication in single-lysogenic SH1000 (wild type), SH1000 *sigB* (*sigB::tet* deletion) and SH1000 *spoVG* (*spoVG::erm* deletion) under uninduced and induced (+MMC) conditions. Single-lysogenic Φ13K strains were induced with subinhibitory MMC in exponential growth phase and incubated for 60 min. Phage numbers were determined by plaque assay (D) and phage genome numbers by qPCR on the attachment site (*attP*) (E). Data shown are mean ± SD (n = 3). Statistical significance was determined by 2way ANOVA tests on log<sub>10</sub> transformed data. (\*\*\*\*p-value < 0.0001, \*\*\*p-value < 0.001, \*\*p-value < 0.01, \*p-value < 0.05).

### **A phage factor is required for P<sub>23</sub> activity**

We further analyzed whether phage factors are involved in P<sub>23</sub> activity. Therefore, using the reporter plasmid with the wild type promoter region, we analyzed P<sub>23</sub> activity in bacterial strains carrying various prophage mutants, as well as in a prophage-free background. Promoter activity was significantly increased in single-lysogens carrying either the P<sub>23</sub>-disrupted prophage mutant ( $\Phi$ 13K-*TATA*) or the replication-deficient prophage ( $\Phi$ 13K-*rep*) (Figure 3A). We speculate that the enhanced promoter activity may be the result of increased binding of a regulatory factor to the reporter plasmid in the absence of a functional target site in the prophage genome (for  $\Phi$ 13K-*TATA*) or due to a reduced number of genomic promoter copies in  $\Phi$ 13K-*rep*.

In contrast to the analyzed phage mutants, a phage-free background resulted in promoter inactivation, confirming that a phage-encoded factor is required for P<sub>23</sub> activity (Figure 3A). This effect was observed for all four tested strains (Supplemental Figure S2).

### **SAOUHSC\_02200 is a late transcriptional regulator of the Ltr family IV**

To identify the phage factor activating the P<sub>23</sub> promoter, we compared the genomic organization of  $\Phi$ 13 with other phages. Since late phage genes are located downstream of P<sub>23</sub>, we mined the phage genome for the presence of late transcriptional regulators (Ltrs), which activate late phage gene expression. Quiles-Puchalt et al. described four families of Ltrs in addition to the RinA homologs identified in *S. aureus* phage  $\Phi$ 11. These Ltrs are characterized as small basic proteins encoded at the end of the early phage gene cluster and positioned directly upstream of the promoter they regulate (26).

Due to the localization of *SAOUHSC\_02200* upstream of P<sub>23</sub> promoter region, we aligned the protein sequence of *SAOUHSC\_02200* (UniProt ID: Q2FWT0) with those of representative members of the different Ltr families. Sequence analysis revealed 59% similarity to the ORF34 of phage  $\Phi$ 55 (UniProt ID: Q4ZB49), encoding a member of the Ltr family IV, and 100% identity to hypothetical protein PVL\_60 of *S. aureus* phage PVL (UniProt ID: O80099) (Supplemental Figure S3). These alignment results support the hypothesis that *SAOUHSC\_02200* encodes a late transcriptional regulator belonging to the Ltr family IV (LtrC-homologs).

### **SAOUHSC\_02200-encoded Ltr regulates P<sub>23</sub> promoter**

To verify the role of the putative Ltr in P<sub>23</sub> regulation, we generated a genomic *ltr*-deficient mutant by introducing a stop codon into *SAOUHSC\_02200* without altering the P<sub>23</sub> promoter region. In the absence of functional Ltr, no P<sub>23</sub> activity was detected, proving that P<sub>23</sub> activation is dependent on Ltr (Figure 3B). Similar to the  $\Phi$ 13K-*TATA* mutant, the  $\Phi$ 13K-*ltr* mutant failed to produce intact phage particles. However, phage genome replication appeared unaffected under uninduced conditions. Following MMC induction, a greater number of genome copies were detectable for the wild type phage than for the *ltr* mutant phage, for which no increase in

phage genome copies was detectable (Figure 3C,D). This is likely because only the wild type phage propagates and lyses its hosts.

After identifying Ltr (SAOUHSC\_02200) as a regulator and activator of promoter P<sub>23</sub>, we analyzed the expression of *ltr* in different single-lysogenic strain backgrounds under uninduced conditions and 4 h post MMC-induction. Replication-deficient phage mutants ( $\Phi$ 13K-*rep*) were used to avoid multi copy effects. As expected, *ltr* expression was undetectable under uninduced conditions. Upon MMC induction, strain-specific differences in *ltr* expression were detected, with the 8325-4 single-lysogen showing significantly lower expression than the other strains (Figure 3E). These differences correlated with differences in SigB activity (see Figure 2A).

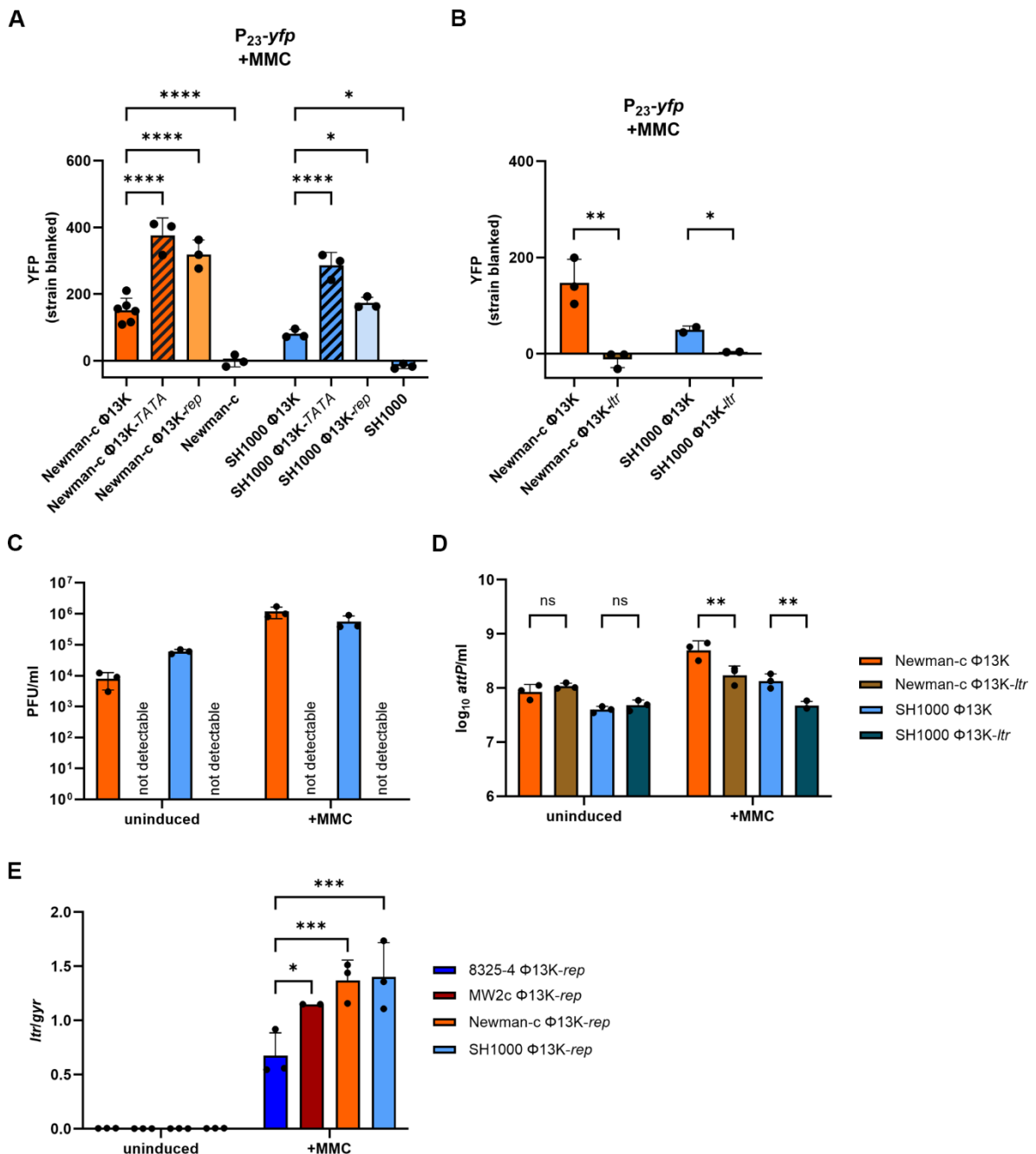


**Figure 3: P<sub>23</sub> promoter region is controlled by the phage-encoded late transcriptional regulator (Ltr).** (A) Single timepoint measurement of P<sub>23</sub> promoter activity in single-lysogens carrying  $\Phi$ 13K (wild type),  $\Phi$ 13K-TATA (TATA-box mutation), or  $\Phi$ 13K-*rep* (replication deficient), and in phage-free strains. Strains were grown to exponential phase, induced with a subinhibitory concentration of mitomycin C (MMC) (300 ng ml<sup>-1</sup>) and grown for further 4 hours. Bacteria were harvested to OD<sub>600</sub> of 2 and resuspended in PBS. Fluorescence was measured. Arbitrary units of fluorescence (YFP) are shown; strain-specific background fluorescence was subtracted. Data shown are mean  $\pm$  SD (n  $\geq$  3). Statistical significance was determined by ordinary one-way ANOVA. (B) Single time point measurement of P<sub>23</sub> promoter activity in single-lysogens carrying  $\Phi$ 13K (wild type), or  $\Phi$ 13K-*ltr* (*ltr* deletion). Data shown are mean  $\pm$  SD. Statistical significance was determined by unpaired t-tests for comparisons within strains. (C,D) Phage replication in strains carrying  $\Phi$ 13K (wild type) or  $\Phi$ 13K-*ltr* (*ltr* deletion) under uninduced and induced (+MMC) conditions. Single-lysogenic  $\Phi$ 13K strains were induced with subinhibitory MMC in exponential phase and incubated for 60 min. Phage numbers were determined by plaque assay (C) and phage genome numbers by qPCR on the attachment site (*attP*) (D) Data shown are mean  $\pm$  SD. Statistical significance was determined by 2way ANOVA on log<sub>10</sub> transformed data. (E) Strain specific *ltr* gene expression. Single-lysogenic strains were grown to exponential phase, induced with a subinhibitory concentration of MMC and grown for further 4 hours. Bacteria were harvested for RNA Isolation and RT-qPCR was performed. *ltr* gene expression was normalized to *gyrB* expression. Data shown are mean  $\pm$  SD. Statistical significance was determined by 2way ANOVA. (\*\*\*\*p-value < 0.0001, \*\*\*p-value < 0.001, \*\*p-value < 0.01, \*p-value < 0.05, ns > 0.05).

In summary, these results confirm Ltr (encoded by *SAOUHSC\_02200*) as the activator of promoter P<sub>23</sub> and demonstrate that a functional Ltr is essential for production of intact mature phage particles. The variation in *ltr* expression in different strain backgrounds indicates that host factors, particularly SigB, contribute to its regulation.

### Repeat motifs in the P<sub>23</sub> promoter region are essential for activation

Previous studies have shown that Ltrs generally bind to four imperfect repeats within their target promoter regions (26). Sequence analysis of P<sub>23</sub> promoter region revealed three perfect 18 bp repeats and an additional partial repeat corresponding to the first 9 bp (Figure 4A). Deletion of this repeated sequence in the reporter plasmid abolished P<sub>23</sub> activity (Figure 4B). This confirmed the importance of this repeated sequence for promoter activation, likely due to impaired binding of Ltr in the absence of the repeat motif.

### P<sub>23</sub> activation by Ltr is essential for late phage gene expression

We next determined the impact of Ltr on P<sub>23</sub> dependent gene expression. Therefore, gene expression across the phage genome in absence of functional P<sub>23</sub> or Ltr (Figure 5A) was assessed using RT-qPCR analyses on RNA isolated from single-lysogenic SH1000 strains carrying replication-deficient  $\Phi$ 13K-*rep* or its derivatives with mutated P<sub>23</sub> ( $\Phi$ 13K-TATA), or lacking *ltr* ( $\Phi$ 13K-*ltr*) (Figure 5B-I).

Expression of the genetic switch genes *cl* and *mor* were unaffected by disruption of P<sub>23</sub> or mutation of *ltr*, indicating that early phage gene expression and induction of the lytic life cycle are Ltr-independent. Similarly, *ltr* itself showed no significant change in expression in the phage mutants, suggesting the absence of regulatory feedback on *ltr* expression.

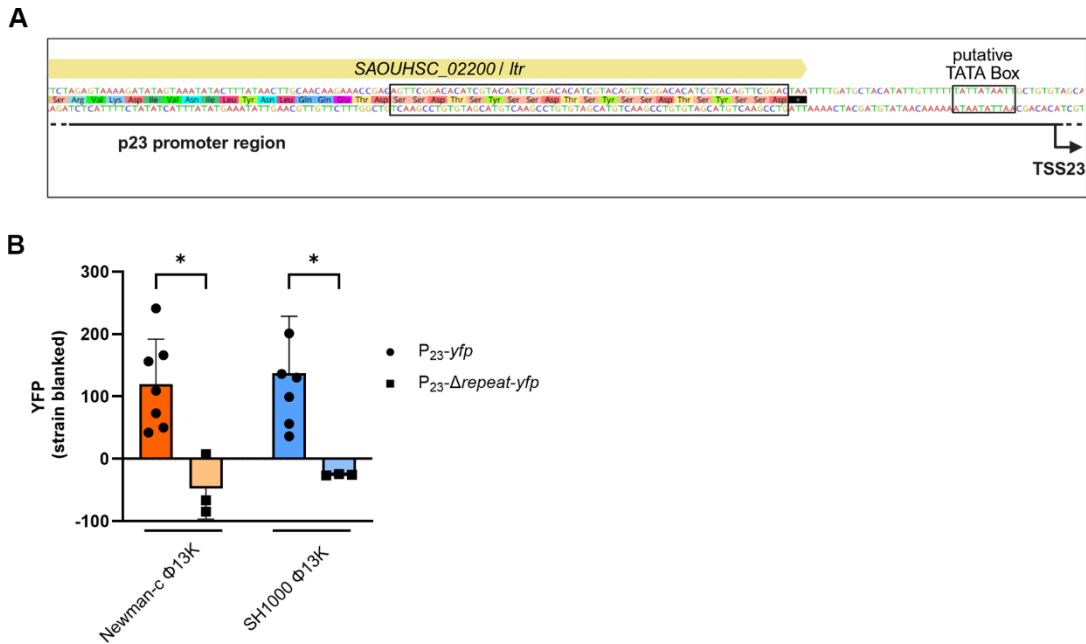


**Figure 4: The repeated sequence in the P<sub>23</sub> promoter region is required for promoter activation.** (A) Schematic depiction of repeated sequence in P<sub>23</sub> promoter region upstream of the putative TATA-box. (B) Single time point measurement of the promoter activity of wild type (P<sub>23</sub>-yfp) or mutant P<sub>23</sub> (P<sub>23</sub>-Δrepeat-yfp), lacking the repeated region. Single-lysogenic strains were grown to exponential phase, induced with a subinhibitory concentration of MMC and grown for further 4 hours. Bacteria were harvested to OD<sub>600</sub> of 2 and resuspended in PBS. Fluorescence was measured. Arbitrary units of fluorescence (YFP) are shown; strain-specific background fluorescence was subtracted. Data shown are mean ± SD (n ≥ 3). Statistical significance was determined by ordinary one-way ANOVA. (\*p-value < 0.05).

In contrast, the expression of late phage genes involved in DNA-processing and packaging (*endonuclease*, *terL*), as well as the major capsid protein gene (*mcp*), was significantly reduced in both the Φ13K-*rep-TATA* and Φ13K-*rep-ltr* phage mutants compared to the wild type Φ13K-*rep*. The expression of late phage genes required for bacterial lysis and phage release, such as *holin* was also significantly reduced, alongside the expression of the immune evasion factor staphylokinase (*sak*), located downstream of the lysis genes.

Overall, the expression of all the analyzed late genes downstream of the P<sub>23</sub> promoter including the immune evasion cluster proved to be dependent on P<sub>23</sub> and Ltr. Moreover, MMC induction did not induce late gene expression in the mutants, confirming that Ltr is required for late gene activation during the lytic cycle.

Previous studies have shown that late transcriptional regulators activate the transcription of a single large transcript covering all late phage genes (26). Northern Blot analysis using DNA-probes targeting transcripts of *terL* and *mcp* revealed multiple transcripts in different sizes, including a shared transcript of ~ 6 kb, which indicated co-transcription of *terL* and *mcp* from the P<sub>23</sub> promoter. However, no larger transcript covering all late phage genes was detected (Figure 5J).

# Results Part II

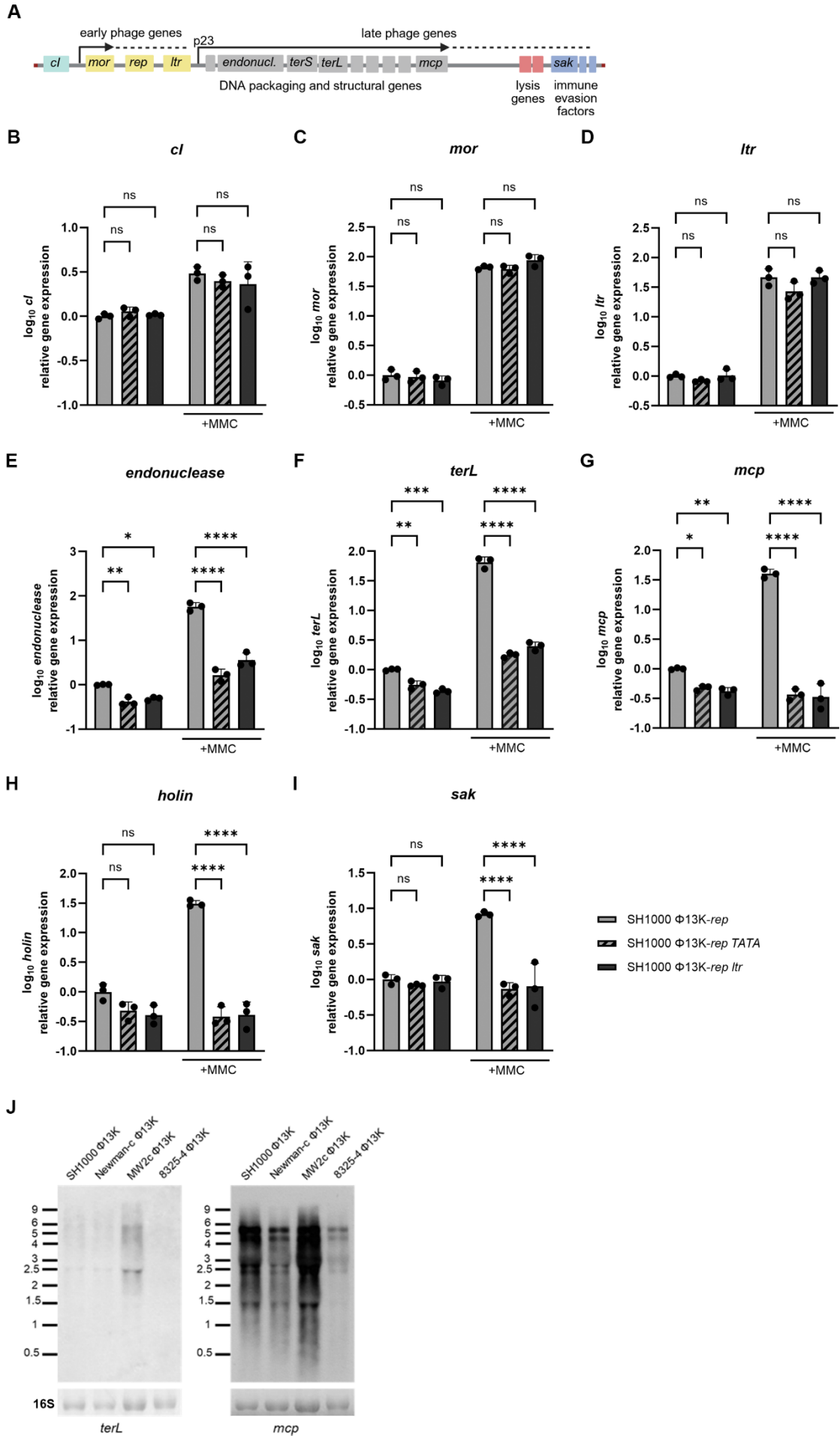


**Figure 5: P<sub>23</sub> promoter activation by Ltr is required for late gene expression.** (A) Schematic depiction of the phage genome, indicating early and late phage genes. (B-I) Gene expression analysis of early (*cl*, *mor* and late transcriptional regulator (*ltr*)) and late phage genes (*endonuclease*, large terminase (*terL*), major capsid protein (*mcp*), *holin* and staphylokinase (*sak*)) under uninduced and induced (+MMC) conditions. Strains carrying  $\Phi$ 13K-*rep* (wild type, replication deficient),  $\Phi$ 13K-*rep-TATA* (TATA-box mutation), or  $\Phi$ 13K-*rep-ltr* (*ltr* deletion) were grown to exponential phase, induced with a subinhibitory concentration of mitomycin C (MMC) and grown for 60 min. Bacteria were harvested for RNA isolation, transcripts were quantified by RT-qPCR and normalized to *gyrB* expression by  $\Delta\Delta$ Ct method. Data shown are mean  $\pm$  SD. Statistical significance was determined by ordinary one-way ANOVA on log<sub>10</sub> transformed data. (\*\*\*\*p-value < 0.0001, \*\*\*p-value < 0.001, \*\*p-value < 0.01, \*p-value < 0.05, ns > 0.05). (J) Northern Blot analysis for *terL* and *mcp* transcripts. Single-lysogens were grown to exponential phase, induced with a subinhibitory concentration of mitomycin C (MMC) and grown for 60 min. Bacteria were harvested for RNA isolation. Blots were hybridized by using digoxigenin-labeled DNA-probes generated by PCR. 16S RNA was detected for loading control. Millenium Marker (ThermoFisher Scientific) was included for size comparison.

Although additional transcriptional start sites and transcriptional units were identified for late genes (24), our data indicate Ltr as major phage regulator of late phage gene expression from the P<sub>23</sub> promoter.

## Discussion

The impact of host factors such as RecA or SarA on  $\Phi$ 13 excision and replication have been previously described (22, 27). Here we focused on regulatory mechanisms controlling phage assembly. We identified Ltr as a key regulator of late gene transcription. Ltr, encoded by the final gene on the early phage module, activates P<sub>23</sub> and thereby initiates the expression of genes involved in capsid assembly, DNA processing and packaging, lysis, and immune evasion. Both *ltr* expression and P<sub>23</sub> activity exhibit strain-specific differences, which appear to be dependent on the alternative sigma factor SigB and its downstream effector SpoVG. We propose that Ltr could be a regulatory target for the switch between the lytic phage life cycle and active lysogeny (Figure 6).

### Ltr (SAOUHSC\_02200) regulates late phage gene expression in $\Phi$ 13

Phage gene regulation is tightly temporally controlled to ensure that genome replication is complete before particle assembly and host lysis occur. The first step in genetic activation is the transition from the lysogenic to the lytic life cycle. In the model phage  $\lambda$ , this genetic switch is regulated by the interplay between the CI repressor and Cro anti-repressor. Similarly, in the Sa3int phage  $\Phi$ 13 this switch involves a cleavable CI-repressor and the small anti-repressor Mor, originally described in lactococcal phages (27, 28). Activation of the SOS-response induces RecA-dependent auto-cleavage of CI, leading to de-repression of early lytic genes and phage genome replication. Subsequently, late phage genes are expressed to enable the assembly of mature phage particles, and bacterial lysis.

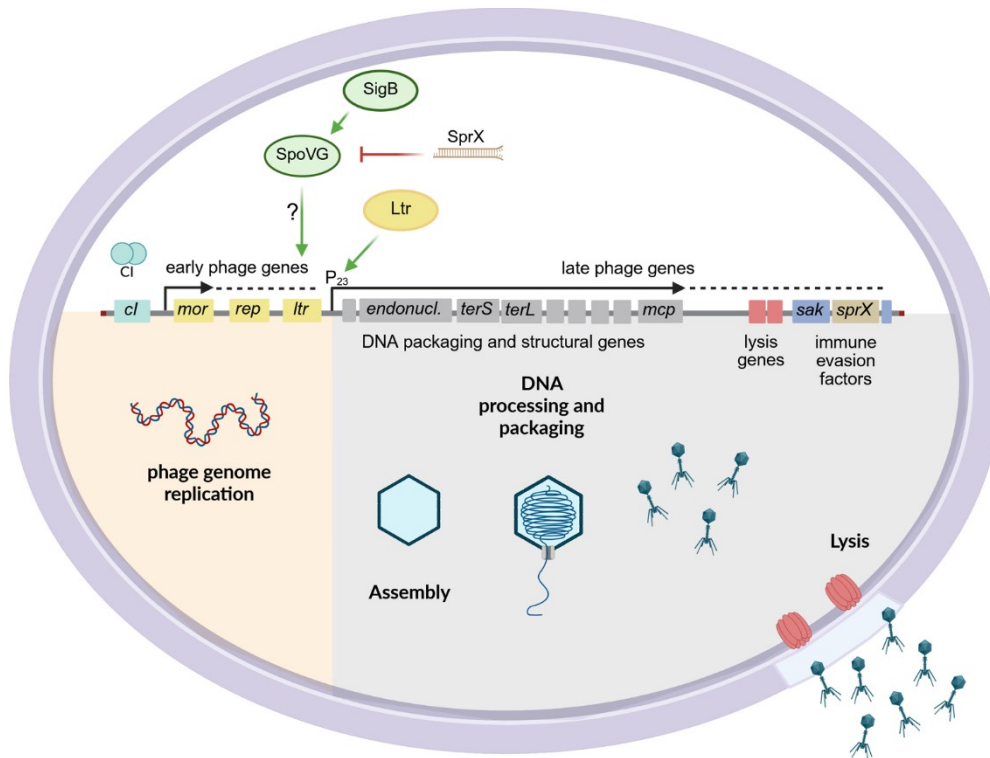


**Figure 6: Temporal control of phage gene expression within the bacterial host.** Genetic organization of the bacteriophage  $\Phi 13$ . Release of CI from the *mor* promoter results in derepression of the lytic cycle and expression of early lytic genes, including the replication factor (*rep*) and late transcriptional regulator (*ltr*). Subsequently, late expression of DNA-packaging (*endonuclease*, *terS*, *terL*) and structural genes (e.g. *mcp*) leads to DNA-processing, capsid assembly and DNA-packaging. The products of lysis genes enable host cell lysis, releasing mature phage particles, while immune evasion factors (e.g. *sak*) aid in escaping the host immune system. These late phage genes are transcribed from the  $P_{23}$  promoter, which is activated by the Ltr transcriptional regulator encoded by *ltr*. Ltr expression and  $P_{23}$  activity are regulated in a SigB and SpoVG-dependent manner. Small RNA SprX provides a feedback for post-transcriptional SpoVG repression.

In *S. aureus* phage  $\Phi 11$ , the expression of late genes is controlled by the transcriptional regulator RinA, located upstream of the *terS* gene. Deletion of *rinA* abolishes the production of functional phage particles and reduces late gene expression (29). Quiles-Puchalt et al. described four additional families of late transcriptional regulators (Ltrs), which share the size of about 130 aa and a similar localization within the phage genome, although they show no sequence similarity to RinA or known bacterial transcription factors (26).

Here, the Ltr of  $\Phi 13$  was identified based on the localization upstream of the endonuclease gene and the predicted TSS<sub>23</sub>. Mutation of *ltr* or  $P_{23}$  abolished the production of functional phage particles and significantly reduced the expression of all genes downstream of  $P_{23}$ . Moreover,  $P_{23}$  activity was completely lost in phages lacking a functional *ltr* gene, confirming Ltr as the key regulator of late gene expression in  $\Phi 13$ . Sequence alignment to the different Ltr families revealed 30% identity and 59% similarity with ORF34 of phage  $\Phi 55$  (Ltr IV family) and 100% identity to hypothetical protein PVL\_60 of Staphylococcal phage PVL. Pantone-Valentine leucocidin (PVL), the bi-component pore-forming cytotoxin encoded by phage PVL

and several other phages, contributes to the virulence of *S. aureus* by targeting and lysing host immune cells such as macrophages and neutrophils (30, 31). Comparative genome analysis revealed extensive sequence identity between  $\Phi$ 13K and staphylococcal phage PVL (Supplemental Figure S3). For instance, one 19 kb region spans from the  $P_{23}$  promoter region up to a locus upstream of the lysis genes. Another conserved region includes the genetic switch genes *cl* and *mor*. Phage genomes are known to have interchangeable modules fulfilling the same functions, which lead to mosaicism within phage genomes (3). The high degree of conservation between  $\Phi$ 13K and staphylococcal phage PVL in regions important for transcriptional regulation, suggests a similar phage-host interaction for both phages in *S. aureus*.

Previous studies have shown that repeated sequences in the promoter region serve as recognition targets for Ltr binding (26, 29). In *Lactococcus lactis* phage TP901-1, sharing the anti-repressor MOR with  $\Phi$ 13, the late transcriptional regulator Alt binds to four imperfect direct repeats located -76 to -32 bp upstream of the transcriptional start site (32, 33). The promoter region downstream of  $\Phi$ 13-Ltr also consists of four repeats located at the 3' end of the regulator's coding sequence. Deletion of this repeat region, between position -107 and -42 bp relative to the TSS, abolished  $P_{23}$  activity, confirming that binding of  $\Phi$ 13-Ltr to this sequence is required for promoter activation.

### **Transcriptional organization and regulation of late phage genes in $\Phi$ 13**

For both RinA- and Ltr-homologous regulators, transcription from their respective promoters results in a single transcript for DNA-packaging, structural and lysis genes (26, 29). Consistent with this, Northern blot analysis confirmed co-transcription of *terL* and *mcp*, however, no transcript spanning across the phage genome from  $P_{23}$  to the immune evasion cluster was detected. In  $\Phi$ 13, additional transcriptional start sites were identified downstream of TSS23, indicating a more complex regulatory network. These include TSS located upstream of *mcp* (TSS25, 26), lysis genes (TSS30) and immune evasion factors (TSS36) (24). Previous work suggested co-transcription of the lysis gene *amidase* and the immune evasion factor *sak* (34). Transcript size analysis by Northern blot revealed a transcript of 3 kb hybridizing with a *sak*-specific probe, confirming the presence of additional transcriptional start sites within the late genetic modules. The major regulatory factor, however, appears to be *ltr*, as phages lacking *ltr* or carrying disruptions in  $P_{23}$  did not express late phage genes, including *sak* and lysis genes. These findings suggest that potential additional regulatory processes are dependent on initial Ltr activation of promoter  $P_{23}$ .

### **Regulatory mechanisms controlling Ltr and $P_{23}$ activity**

The post-transcriptional inhibition of LlgA (a Ltr family protein) activity has been shown to block late gene transcription in *Listeria monocytogenes* phage  $\Phi$ 10403S in the intracellular niche.

This interruption of the phage replication process induces a pseudo-lysogenic state that allows prophage excision and subsequent *comK* expression required for phagosomal escape (35). Although the bacterial factors mediating LlgA regulation remained unidentified, it was proposed that LlgA activity is under host-dependent control for beneficial regulation of the phage life cycle in different stages of infection.

We observed strain-specific differences in  $P_{23}$  activity and *ltr* expression pattern also indicating a strong impact of bacterial host factors on the fate of the phage. Interestingly, SigB activity within the different strains correlated with *ltr* expression differences, indicating a regulatory effect of the host factor SigB on *ltr* expression.  $\Phi 13$  or PVL phage Sa2mw integrated into the SigB deficient 8325-4 lysogens were previously shown to exhibit reduced mobility compared to other SigB-positive strains (24, 25). RinA, the late transcriptional regulator of  $\Phi 11$ , exhibits the highest expression in the late-exponential phase (36) which is consistent with SigB activity during later growth phases (37).

However, no SigB consensus sequences could be identified in the promoter initiating *ltr* or  $P_{23}$ . Deletion of *spoVG* resulted in reduced  $P_{23}$  activity and phage assembly similar to SigB deletion. SpoVG acts as a downstream effector of SigB and was proposed to activate transcription of SigB-dependent genes lacking a SigB consensus sequence (38, 39). Thus, SpoVG likely mediates the impact of SigB on phage gene regulation. SpoVG is broadly conserved, especially among Gram-positive bacteria. *L. monocytogenes* SpoVG was shown to bind RNA with a greater affinity than DNA and it was suggested that the protein is mainly acting as RNA-binding protein thereby functioning as a global post-transcriptional gene regulator (40). SpoVG in *S. aureus* is post-transcriptionally suppressed through interference with a small RNA, SprX (41), which is located within several Sa3int phages downstream of *sak*. Thus, there seems to be a strong feedback mechanism whereby upon phage replication the increase of SprX likely restricts SpoVG-dependent phage assembly. Under certain infectious conditions the SOS response and SigB activity are activated, which then may promote SpoVG activity to overcome SprX restriction and enable the phage to escape from the bacterial host. However, additional host factors likely contribute to the regulation of phage late gene expression. TSS prediction showed additional strain-specific TSSs in MW2c and 8325-4. Furthermore, the high  $P_{23}$  activity of MW2 compared to other SigB-positive strains could not be linked to higher SigB activity in MW2 and thus remain unclear.

## Material and Methods

### Growth conditions

Strains used in this work are listed in Table S1. If not stated differently, strains were grown in Tryptic Soy Broth (TSB) (Oxoid) at 37°C and 200 rpm. For strains carrying resistance genes, antibiotics (erythromycin (erm) 10 µg ml<sup>-1</sup>, tetracyclin (tet) 3 µg ml<sup>-1</sup>, kanamycin (kan) 50 µg ml<sup>-1</sup>, chloramphenicol (cm) 10 µg ml<sup>-1</sup>) were added in precultures and for selection on agar plates.

### Generation of strains and mutants

Oligonucleotides and plasmids used for generation of mutants are listed in Table S2 and Table S3.

### Promoter fusion constructs for promoter activity measurements

By Gibson Assembly, promoter regions of genes of interest ( $P_{\text{gene}}$ ) were cloned into reporter plasmids upstream of a strong ribosomal binding site (RBS) followed by a gene coding for a yellow fluorescent protein (*yfp*: gpVenus). To generate  $P_{23}$ -*yfp* (pCG896) 50 bp downstream of the predicted transcriptional start site 23 (TSS23) and 200 bp upstream were amplified by PCR with the primer pair pCG896gibfor/pCG896gibrev (24). The amplified promoter regions were cloned into the reporter plasmid pCG725 digested with Sall and SphI (24, 42). To generate  $P_{23}$ -TATA-*yfp* (pCG910) the bases of the putative TATA Box of promoter region 23 in pCG896 were replaced with Cs and Gs by site directed mutagenesis (SDM) using the primer pair pCG910SDMfor/pCG910SDMrev. To generate  $P_{23}$ - $\Delta$ repeat-*yfp* (pCG943) the repeated sequence of 65 bp was deleted from pCG896 by SDM using the primer pair pCG943SDMfor/pCG943SDMrev. Site directed mutagenesis was performed according to the manufacturers instructions (Q5 Site-Directed Mutagenesis Kit).

Promoter fusion plasmids were verified by sequencing and introduced into the final bacterial strains by transduction via *S. aureus* RN4220 or direct electroporation. Final strains were verified by PCR on the reporter plasmids.

### Late transcriptional regulator (*ltr*) mutant ( $\Phi$ 13K-*ltr*)

Flanking regions were amplified by PCR using primer pairs pCG926insert1gibfor/pCG926insert1gibrev and pCG926insert2gibfor/pCG926insert2gibrev. The overlapping primers pCG926insert1gibrev and pCG926insert2gibfor contained point mutations to introduce a stop codon into SAOUHSC\_02200. Both fragments were cloned into BamHI digested pIMAY-Z vector and transformed into *E. coli* DC10B. After verification by sequencing, the plasmid was transformed into the final *S. aureus* strains by electroporation. pIMAY-Z mutagenesis for genomic integration was performed as described before (43).

### Generation of phage $\Phi$ 13K-*rep*

Replication deficient phage mutants were generated as described before (24).

**Generation of mutants (*sigB*, *spoVG*)**

For the generation of *sigB::tet* and *spoVG::erm* mutants, recipient strains were transduced with  $\Phi 11$  phage lysates, generated by using strains included in Table S1. Deletions were verified by PCR on the flanking regions within the resistance cassettes and on the respective gene.

**Promoter activity measurement*****Time measurement of promoter activity***

Promoter activity over time was analyzed in a Tecan Spark plate reader as following. Cultures were inoculated in 96-well plate (Greiner, F-Bottom, clear) to OD<sub>600</sub> of 0.05, grown for 2 h at 37°C and induced with subinhibitory concentration of mitomycin C (MMC, 300 ng ml<sup>-1</sup>). Optical density (absorbance: 600 nm) and fluorescence (gpVenus: excitation 500 nm, emission 545 nm) were measured in 30 min time-intervals for 24 hours. Fluorescence measurements were normalized to OD<sub>600</sub> and strain-background fluorescence was subtracted.

***Single time point measurement of promoter activity***

For single time point measurements of promoter activity, measurements were performed as described before (22). In brief, 4 hours after induction with MMC bacteria were harvested, adjusted to OD<sub>600</sub> of 2 in PBS and fluorescence was measured in the plate reader using the same settings as mentioned for time measurement of promoter activity. For analysis, strain-specific background fluorescence was subtracted.

**Prophage induction and phage replication**

Phage replication following induction was analyzed as described before (24). In short, single-lysogenic strains were grown to OD<sub>600</sub> of 0.7, induced with a subinhibitory concentration of MMC (300 ng ml<sup>-1</sup>) and incubated for further 1 or 4 h. Subsequently, supernatants were harvested by centrifugation and sterile filtrated (0.45  $\mu$ m). Analysis of phage replication of transposon strains was performed in 24 well plates shaking at 130 rpm. Phage numbers in the supernatant were quantified by quantitative PCR (qPCR) and plaque assays.

**Plaque assay**

Phage titer were determined in the supernatants by the agar overlay method. Phage top agar (Casaminoacids 3 g l<sup>-1</sup>, Yeast Extract 3 g l<sup>-1</sup>, NaCl 5.9 g l<sup>-1</sup>, Agar 7.5 g l<sup>-1</sup>) was mixed with *S. aureus* LS1 grown to OD<sub>600</sub> of 0.1 and poured onto NB2 agar plates supplemented with CaCl<sub>2</sub>. Supernatants were diluted in phage buffer (Tris 50 mM, CaCl<sub>2</sub> 4 mM, MgSO<sub>4</sub> 1mM, NaCl 5.9 g l<sup>-1</sup>, gelatine 1 g l<sup>-1</sup>) and spotted onto the bacterial lawn. Phage titers were calculated as plaque-forming units (PFU) per ml, after overnight incubation at 37°C.

**qPCR for phage genome quantification**

Quantification of phage genomes within sterile filtered culture supernatants was performed as described before (22). In brief, supernatants were treated with proteinase K and diluted 1:10

in nuclease-free water. QuantiFAST SYBR Green PCR Kit (Qiagen) was used for qPCRs, with primers spanning the attachment site (*attP*) on the phage genome.

Oligonucleotides used for qPCR are listed in Table S2.

### **RNA isolation and RT-qPCR**

For RNA isolation, bacteria were harvested and resuspended in 1 ml TRIzol (Thermo Fisher Scientific). Cells were lysed using a high-speed homogenizer (6500 rpm) and zirconia/silica beads (0.1 mm diameter). RNA was isolated as recommended by the TRIzol manufacturer. Five  $\mu$ g of the isolated RNA were DNase-treated (Roche) and subsequently diluted 1:10 in nuclease-free water for RT-qPCR.

To determine gene expression of target genes, RT-qPCR was performed with QuantiFast SYBR Green RT-PCR Kit (Qiagen) using the Quantstudio3 system (Applied Biosystems) with the recommended settings. For strain comparisons gene expression was normalized to *gyrB* expression. Relative gene expression, comparing wild type to mutants, was calculated using the  $\Delta\Delta$ CT method with *gyrB* as the housekeeping gene for normalization. Uninduced wild type bacteria were used as control condition.

Oligonucleotides used for RT-qPCR are listed in Table S2.

### **Northern Blot**

Northern Blot analysis was done as described before (44). Transcripts on Northern blots were hybridized with digoxigenin-labelled DNA probes generated by PCR (Supplementary Table S2).

### **Statistical analysis**

Statistical analyses were performed using GraphPad Prism 10.3.1 software. All data represent values from independent biological replicates. Tukey's multiple comparisons tests were performed post-hoc for ANOVA tests. P-values < 0.05 were considered significant.

Schematic depictions were created in <https://BioRender.com>.

**Acknowledgements:** We thank Libera Lo Presti for editing of the manuscript. We thank Janes Krusche for helpful scientific discussions.

**Funding:** CW and RD were supported by the Deutsche Forschungsgemeinschaft program SPP2330 (grant numbers 464612409 to C. Wo.) and infrastructural funding Cluster of Excellence EXC 2124 Controlling Microbes to Fight Infections (grant number 390838134).

## References

1. Hatoum-Aslan A. 2021. The phages of staphylococci: critical catalysts in health and disease. *Trends Microbiol* 29:1117-1129.
2. Deghorain M, Van Melderen L. 2012. The Staphylococci phages family: an overview. *Viruses* 4:3316-35.
3. Goerke C, Pantucek R, Holtfreter S, Schulte B, Zink M, Grumann D, Broker BM, Doskar J, Wolz C. 2009. Diversity of prophages in dominant *Staphylococcus aureus* clonal lineages. *J Bacteriol* 191:3462-8.
4. Kahánková J, Pantůček R, Goerke C, Růžičková V, Holochová P, Doškař J. 2010. Multilocus PCR typing strategy for differentiation of *Staphylococcus aureus* siphoviruses reflecting their modular genome structure. *Environ Microbiol* 12:2527-38.
5. Oliveira H, Sampaio M, Melo LDR, Dias O, Pope WH, Hatfull GF, Azeredo J. 2019. Staphylococci phages display vast genomic diversity and evolutionary relationships. *BMC Genomics* 20:357.
6. Ingmer H, Gerlach D, Wolz C. 2019. Temperate Phages of *Staphylococcus aureus*. *Microbiol Spectr* 7.
7. Xia G, Wolz C. 2014. Phages of *Staphylococcus aureus* and their impact on host evolution. *Infect Genet Evol* 21:593-601.
8. Verkaik NJ, Benard M, Boelens HA, de Vogel CP, Nouwen JL, Verbrugh HA, Melles DC, van Belkum A, van Wamel WJ. 2011. Immune evasion cluster-positive bacteriophages are highly prevalent among human *Staphylococcus aureus* strains, but they are not essential in the first stages of nasal colonization. *Clin Microbiol Infect* 17:343-8.
9. Coleman DC, Sullivan DJ, Russell RJ, Arbutnott JP, Carey BF, Pomeroy HM. 1989. *Staphylococcus aureus* bacteriophages mediating the simultaneous lysogenic conversion of beta-lysin, staphylokinase and enterotoxin A: molecular mechanism of triple conversion. *J Gen Microbiol* 135:1679-97.
10. van Wamel WJ, Rooijackers SH, Ruyken M, van Kessel KP, van Strijp JA. 2006. The innate immune modulators staphylococcal complement inhibitor and chemotaxis inhibitory protein of *Staphylococcus aureus* are located on beta-hemolysin-converting bacteriophages. *J Bacteriol* 188:1310-5.
11. Rohmer C, Wolz C. 2021. The Role of hlb-Converting Bacteriophages in *Staphylococcus aureus* Host Adaption. *Microb Physiol* 31:109-122.
12. Chaguza C, Smith JT, Bruce SA, Gibson R, Martin IW, Andam CP. 2022. Prophage-encoded immune evasion factors are critical for *Staphylococcus aureus* host infection, switching, and adaptation. *Cell Genom* 2.
13. Goerke C, Wirtz C, Fluckiger U, Wolz C. 2006. Extensive phage dynamics in *Staphylococcus aureus* contributes to adaptation to the human host during infection. *Mol Microbiol* 61:1673-85.
14. Nepal R, Houtak G, Bouras G, Feizi S, Shaghayegh G, Shearwin K, Ramezanpour M, Psaltis AJ, Wormald PJ, Vreugde S. 2025. A  $\phi$ Sa3int (NM3) Prophage Domestication in *Staphylococcus aureus* Leads to Increased Virulence Through Human Immune Evasion. *MedComm* (2020) 6:e70313.
15. Poupel O, Kenanian G, Touqui L, Abrial C, Msadek T, Dubrac S. 2025. Timely excision of prophage  $\Phi$ 13 is essential for the *Staphylococcus aureus* infectious process. *Infect Immun* doi:10.1128/iai.00314-25:e0031425.
16. Katayama Y, Baba T, Sekine M, Fukuda M, Hiramatsu K. 2013. Beta-hemolysin promotes skin colonization by *Staphylococcus aureus*. *J Bacteriol* 195:1194-203.
17. Salgado-Pabón W, Herrera A, Vu BG, Stach CS, Merriman JA, Spaulding AR, Schlievert PM. 2014. *Staphylococcus aureus*  $\beta$ -toxin production is common in strains with the  $\beta$ -toxin gene inactivated by bacteriophage. *J Infect Dis* 210:784-92.
18. Huang W, Tian X, Zhu K, Lu S, Zhao Y, Zhou J, He T, Li C, Li M, Zhou R, Li G. 2025. Glucose-induced active lysogeny of prophage  $\Phi$ Sa3XN promotes *Staphylococcus aureus* virulence. *Virology* 22:371.

19. Goerke C, Wirtz C, Flückiger U, Wolz C. 2006. Extensive phage dynamics in *Staphylococcus aureus* contributes to adaptation to the human host during infection. *Mol Microbiol* 61:1673-85.
20. Tran PM, Feiss M, Kinney KJ, Salgado-Pabón W. 2019.  $\phi$ Sa3mw Prophage as a Molecular Regulatory Switch of *Staphylococcus aureus*  $\beta$ -Toxin Production. *J Bacteriol* 201.
21. Deutsch DR, Utter B, Verratti KJ, Sichtig H, Tallon LJ, Fischetti VA. 2018. Extra-Chromosomal DNA Sequencing Reveals Episomal Prophages Capable of Impacting Virulence Factor Expression in *Staphylococcus aureus*. *Front Microbiol* 9:1406.
22. Dobritz R, Rohmer C, Niepoth E, Egle V, Korn N, Bisanzio V, Bojer MS, Ingmer H, Wolz C. 2025. Multiple effects of the bacterial DNA-binding protein SarA on the life cycle of *Staphylococcus aureus* phages. *J Bacteriol* doi:10.1128/jb.00279-25:e0027925.
23. Feiner R, Argov T, Rabinovich L, Sigal N, Borovok I, Herskovits AA. 2015. A new perspective on lysogeny: prophages as active regulatory switches of bacteria. *Nat Rev Microbiol* 13:641-50.
24. Rohmer C, Dobritz R, Tuncbilek-Dere D, Lehmann E, Gerlach D, George SE, Bae T, Nieselt K, Wolz C. 2022. Influence of *Staphylococcus aureus* Strain Background on Sa3int Phage Life Cycle Switches. *Viruses* 14.
25. Wirtz C, Witte W, Wolz C, Goerke C. 2009. Transcription of the phage-encoded Panton-Valentine leukocidin of *Staphylococcus aureus* is dependent on the phage life-cycle and on the host background. *Microbiology (Reading)* 155:3491-3499.
26. Quiles-Puchalt N, Tormo-Más M, Campoy S, Toledo-Arana A, Monedero V, Lasa I, Novick RP, Christie GE, Penadés JR. 2013. A super-family of transcriptional activators regulates bacteriophage packaging and lysis in Gram-positive bacteria. *Nucleic Acids Res* 41:7260-75.
27. Kristensen CS, Varming AK, Leinweber HAK, Hammer K, Lo Leggio L, Ingmer H, Kilstrup M. 2021. Characterization of the genetic switch from phage 13 important for *Staphylococcus aureus* colonization in humans. *Microbiologyopen* 10:e1245.
28. Pedersen M, Hammer K. 2008. The role of MOR and the CI operator sites on the genetic switch of the temperate bacteriophage TP901-1. *J Mol Biol* 384:577-89.
29. Ferrer MD, Quiles-Puchalt N, Harwich MD, Tormo-Más M, Campoy S, Barbé J, Lasa I, Novick RP, Christie GE, Penadés JR. 2011. RinA controls phage-mediated packaging and transfer of virulence genes in Gram-positive bacteria. *Nucleic Acids Res* 39:5866-78.
30. Genestier AL, Michallet MC, Prévost G, Bellot G, Chalabreysse L, Peyrol S, Thivolet F, Etienne J, Lina G, Vallette FM, Vandenesch F, Genestier L. 2005. *Staphylococcus aureus* Panton-Valentine leukocidin directly targets mitochondria and induces Bax-independent apoptosis of human neutrophils. *J Clin Invest* 115:3117-27.
31. Kaneko J, Kamio Y. 2004. Bacterial two-component and hetero-heptameric pore-forming cytolytic toxins: structures, pore-forming mechanism, and organization of the genes. *Biosci Biotechnol Biochem* 68:981-1003.
32. Brøndsted L, Pedersen M, Hammer K. 2001. An activator of transcription regulates phage TP901-1 late gene expression. *Appl Environ Microbiol* 67:5626-33.
33. Pedersen M, Kilstrup M, Hammer K. 2006. Identification of DNA-binding sites for the activator involved in late transcription of the temperate lactococcal phage TP901-1. *Virology* 345:446-56.
34. Goerke C, Köller J, Wolz C. 2006. Ciprofloxacin and trimethoprim cause phage induction and virulence modulation in *Staphylococcus aureus*. *Antimicrob Agents Chemother* 50:171-7.
35. Pasechnek A, Rabinovich L, Stadnyuk O, Azulay G, Mioduser J, Argov T, Borovok I, Sigal N, Herskovits AA. 2020. Active Lysogeny in *Listeria Monocytogenes* Is a Bacteria-Phage Adaptive Response in the Mammalian Environment. *Cell Rep* 32:107956.
36. Jiang M, Li Y, Sun B, Xu S, Pan T, Li Y. 2023. Phage transcription activator RinA regulates *Staphylococcus aureus* virulence by governing sarA expression. *Genes Genomics* 45:191-202.
37. Pane-Farre J, Jonas B, Forstner K, Engelmann S, Hecker M. 2006. The sigmaB regulon in *Staphylococcus aureus* and its regulation. *Int J Med Microbiol* 296:237-58.

38. Bischoff M, Dunman P, Kormanec J, Macapagal D, Murphy E, Mounts W, Berger-Bächi B, Projan S. 2004. Microarray-based analysis of the *Staphylococcus aureus* sigmaB regulon. *J Bacteriol* 186:4085-99.
39. Schulthess B, Bloes DA, François P, Girard M, Schrenzel J, Bischoff M, Berger-Bächi B. 2011. The  $\sigma$ B-dependent yabJ-spoVG operon is involved in the regulation of extracellular nuclease, lipase, and protease expression in *Staphylococcus aureus*. *J Bacteriol* 193:4954-62.
40. Burke TP, Portnoy DA. 2016. SpoVG Is a Conserved RNA-Binding Protein That Regulates *Listeria monocytogenes* Lysozyme Resistance, Virulence, and Swarming Motility. *mBio* 7:e00240.
41. Eyraud A, Tattevin P, Chabelskaya S, Felden B. 2014. A small RNA controls a protein regulator involved in antibiotic resistance in *Staphylococcus aureus*. *Nucleic Acids Res* 42:4892-905.
42. Keinhorster D, Salzer A, Duque-Jaramillo A, George SE, Marincola G, Lee JC, Weidenmaier C, Wolz C. 2019. Revisiting the regulation of the capsular polysaccharide biosynthesis gene cluster in *Staphylococcus aureus*. *Mol Microbiol* 112:1083-1099.
43. Monk IR, Tree JJ, Howden BP, Stinear TP, Foster TJ. 2015. Complete Bypass of Restriction Systems for Major *Staphylococcus aureus* Lineages. *mBio* 6:e00308-15.
44. Goerke C, Campana S, Bayer MG, Döring G, Botzenhart K, Wolz C. 2000. Direct quantitative transcript analysis of the agr regulon of *Staphylococcus aureus* during human infection in comparison to the expression profile in vitro. *Infect Immun* 68:1304-11.

## Supplementary Information

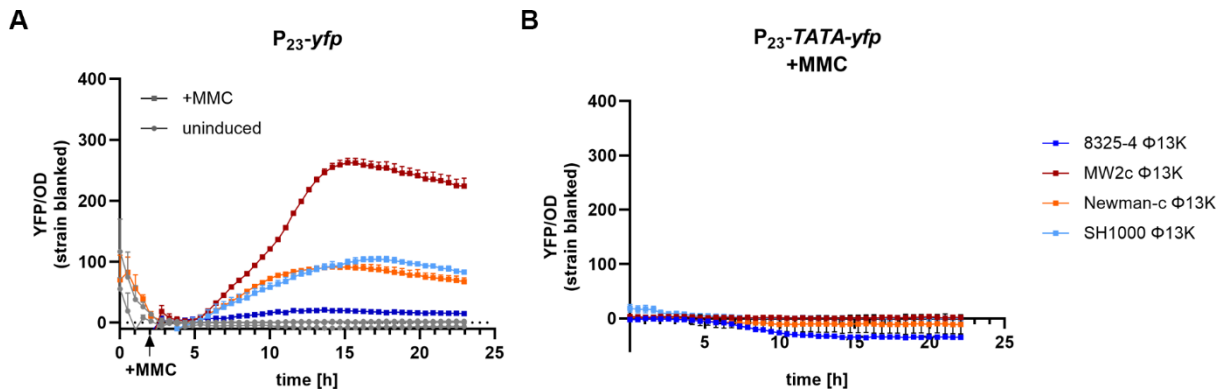


**Figure S1:  $P_{23}$  promoter activity measurement over time.** Strains carrying (A) the wild type ( $P_{23}$ -yfp: pCG896) or (B) the TATA mutant reporter plasmid ( $P_{23}$ -TATA-yfp: pCG910) were grown to exponential phase, induced with subinhibitory mitomycin C (MMC), and incubated for 24 h. Optical density and fluorescence were measured. Arbitrary units of fluorescence (YFP) are shown normalized to  $OD_{600}$ ; strain-specific background fluorescence was subtracted. (A) Comparison of strain-specific activity of the wild type  $P_{23}$  promoter under uninduced and induced (+MMC) conditions. (B) Promoter activity of  $P_{23}$  with mutated TATA-box ( $P_{23}$ -TATA-yfp).

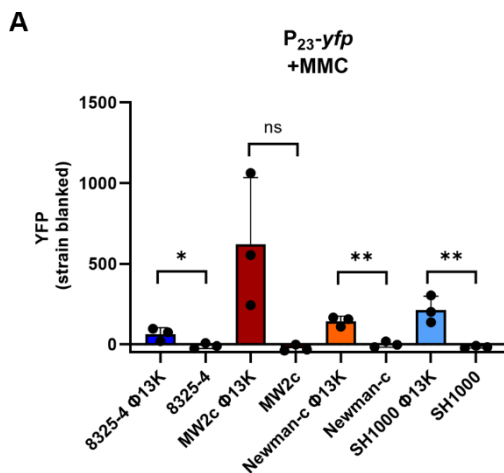


**Figure S2:  $P_{23}$  activity in single-lysogenic and phage-free background.** (A) Single time point measurement of  $P_{23}$  promoter activity in single-lysogens carrying  $\Phi$ 13K (wild type) and in phage-free strains. Strains were grown to exponential phase, induced with a subinhibitory concentration of mitomycin C (MMC) ( $300 \text{ ng ml}^{-1}$ ), and grown for further 4 hours. Bacteria were harvested to  $OD_{600}$  of 2 and resuspended in PBS. Fluorescence was measured. Arbitrary units of fluorescence (YFP) are shown, strain-specific background fluorescence was subtracted. Data shown are mean  $\pm$  SD ( $n = 3$ ). Statistical significance was determined by unpaired t-tests within strains. (\*\*p-value < 0.01, \*p-value < 0.05, ns > 0.05).

## Results Part II

**A**

CLUSTAL O(1.2.4) multiple sequence alignment

```

tr|Q4ZB49|Q4ZB49_9CAUD      MYSKESIVNMIGTHKMKCNVLADVIPEYDSNSIAQYGIQATLPKPQGENSKVEDVVRL      60
tr|Q2FWT0|Q2FWT0_STAA8      MYNRKEIREMIDNYKMKNIIDSKVYDNESTIAQYGYQSAMPKAGTTSNKVLVKVINK      60
                              **.:.:* :**.:* *.:. . : :*.***** *.:** :* .*.** *:.
tr|Q4ZB49|Q4ZB49_9CAUD      ERANKRYAQLKKEVEFINQSQRRLG-HVDFCFLELLKKGYNRDAIKKMPNSKLNRRNFL      119
tr|Q2FWT0|Q2FWT0_STAA8      NKALRKYDYLIKKIADFIDEYEEYITNEKDYHILQMLKQRESHNR---IMSIDIGRDNFY      117
                              :.* :.* :.*.: **.: **.: : : :*. :.*.:**.: :. : * .:.*:**
tr|Q4ZB49|Q4ZB49_9CAUD      ARRDELAEKIYLLQ----- 133
tr|Q2FWT0|Q2FWT0_STAA8      SRVKDIVNLYNLQQETDSSDTSYSSDTSYSSDTSYSSD      156
                              :* .:.: :.* **
    
```

**B**

CLUSTAL O(1.2.4) multiple sequence alignment

```

tr|Q2FWT0|Q2FWT0_STAA8      MYNRKEIREMIDNYKMKNIIDSKVYDNESTIAQYGYQSAMPKAGTTSNKVLVKVINK      60
tr|O80099|O80099_9CAUD      MYNRKEIREMIDNYKMKNIIDSKVYDNESTIAQYGYQSAMPKAGTTSNKVLVKVINK      60
                              *****
tr|Q2FWT0|Q2FWT0_STAA8      NKALRKYDYLIKKIADFIDEYEEYITNEKDYHILQMLKQRESHNRIMSILDIGRDNFYSRV      120
tr|O80099|O80099_9CAUD      NKALRKYDYLIKKIADFIDEYEEYITNEKDYHILQMLKQRESHNRIMSILDIGRDNFYSRV      120
                              *****
tr|Q2FWT0|Q2FWT0_STAA8      KDIVNLYNLQQETDSSDTSYSSDTSYSSDTSYSSD      156
tr|O80099|O80099_9CAUD      KDIVNLYNLQQETDSSDTSYSSDTSYSSDTSYSSD      156
                              *****
    
```

**C**

	Phage PVL		Φ13K		Identities	Gaps	Strand	Position
	start	end	start	end				
Range 1	1	19285	17031	36331	19100/19301 (99%)	16/1903 (0%)	Plus	Structural module
Range 2	26435	29608	2235	5411	3149/3179 (99%)	7/3179 (0%)	Plus	Genetic switch
Range 3	39707	41401	15345	17039	1688/1695 (99%)	0/1695 (0%)	Plus	Ltr, p23 region
Range 4	25538	26417	1124	2002	849/880 (96%)	1/880 (0%)	Plus	OrfC
Range 5	36683	37336	12399	13059	596/665 (90%)	15/665 (2%)	Plus	
Range 6	21316	21664	39619	39969	323/351 (92%)	2/351 (0%)	Plus	
Range 7	30281	30814	6581	7113	432/548 (79%)	29/548 (5%)	Plus	
Range 8	37340	37588	13812	14060	216/249 (87%)	0/249 (0%)	Plus	
Range 9	38758	38896	15204	15343	133/140 (95%)	1/140 (0%)	Plus	
Range 10	38372	38530	14982	15140	146/160 (91%)	2/160 (1%)	Plus	
Range 11	29966	30013	4383	4430	46/48 (96%)	0/48 (0%)	Plus	
Range 12	29989	30028	6247	6286	40/40 (100%)	0/40 (0%)	Plus	

**Figure S3: Alignment of Ltrs and phage genomes (A,B)** Protein sequence alignment of putative Φ13-Ltr (SAOUHSC\_02200, UniProt ID: Q2FWT0) and ORF34 of phage Φ55 (UniProt ID: Q4ZB49) (A) and hypothetical protein PVL\_60 (UniProt ID: O80099) (B). Symbols below sequences indicate the degree of conservation, with ‘\*’ indicating fully conserved residues, ‘.’ indicating conservation between groups of strongly similar properties (Gonnet PAM 250 > 0.5), ‘:’ indicating conservation between groups of weakly similar properties (Gonnet PAM 250 ≤ 0.5), and a space indicating non-conserved residues. (C) Overview of nucleotide alignment results of phage Φ13K genome (see Supplement) and phage PVL genome (Accession number: NC\_002321).







**Table S1:** Strains

Strain	Description	Reference/ Origin
<b><i>Escherichia coli</i></b>		
DC10B		(1)
<b><i>Staphylococcus aureus</i></b>		
8325-4 (RN0450)	NCTC8325 cured of $\Phi$ 11, $\Phi$ 12 and $\Phi$ 13	(2)
8325-4 $\Phi$ 13K	Single-lysogen, <i>kan<sup>R</sup></i>	(3)
8325-4 $\Phi$ 13K- <i>rep</i>	Single-lysogen, carrying replication deficient phage mutant (3), <i>kan<sup>R</sup></i>	(3)
SH1000	<i>rsbU</i> repaired derivative of 8325-4	(4) Susanne Engelmann, TU Braunschweig, Germany
SH1000 $\Phi$ 13K	Single-lysogen, <i>kan<sup>R</sup></i>	(3)
SH1000 $\Phi$ 13K- <i>rep</i>	Single-lysogen, carrying replication deficient phage mutant (3), <i>kan<sup>R</sup></i>	(5)
Newman-c	Phage-cured	(6)
Newman-c $\Phi$ 13K	Single-lysogen, <i>kan<sup>R</sup></i>	(3)
Newman-c $\Phi$ 13K- <i>rep</i>	Single-lysogen, carrying replication deficient phage mutant (3), <i>kan<sup>R</sup></i>	This study
MW2c	Phage-cured	(7)
MW2c $\Phi$ 13K	Single-lysogen, <i>kan<sup>R</sup></i>	(3)
MW2c $\Phi$ 13K- <i>rep</i>	Single-lysogen, carrying replication deficient phage mutant (3), <i>kan<sup>R</sup></i>	(3)
SH1000 $\Phi$ 13K-TATA	Single-lysogen, <i>p23</i> TATA-Box substitution, <i>kan<sup>R</sup></i>	(5)
Newman-c $\Phi$ 13K-TATA	Single-lysogen, <i>p23</i> TATA-Box substitution, <i>kan<sup>R</sup></i>	(5)
SH1000 $\Phi$ 13K- <i>ltr</i>	Single-lysogen, carrying <i>ltr</i> deficient phage mutant, <i>kan<sup>R</sup></i>	This study
Newman-c $\Phi$ 13K- <i>ltr</i>	Single-lysogen, carrying <i>ltr</i> deficient phage mutant, <i>kan<sup>R</sup></i>	This study
RN4220-331	$\Delta mazEFrsbUVWsigB::tetM$	(8)
8325-4 $\Phi$ 13K <i>sigB</i>	Single-lysogen, <i>sigB::tetM</i>	This study
SH1000 $\Phi$ 13K <i>sigB</i>	Single-lysogen, <i>sigB::tetM</i>	This study
Newman-c $\Phi$ 13K <i>sigB</i>	Single-lysogen, <i>sigB::tetM</i>	This study
SM2	Newman <i>spoVG::erm</i> , <i>yabJ-spoVG</i> mutant, <i>erm<sup>R</sup></i>	(9) Markus Bischoff
SH1000 $\Phi$ 13K <i>spoVG</i>	Single-lysogen, <i>spoVG::erm</i>	This study
LS1		(10) Löffler, Münster, Germany
RN4220	restriction deficient derivate of 8325-4, rK-mK+	(11)

**Table S2:** Oligonucleotides

Oligonucleotide	Sequence	Used for
pCG896gibfor	gctggcggcccgtgcatgGGATCAT	Cloning pCG896

Results Part II

	GAGCATTCTTGATATAGGC	
pCG896gibrev	cataaataatcatcctcctaagCCCTC ACTTAATGTGAGAGTTCA	Cloning pCG896
pcllyfpoutsidecontrolfor	GGACAGGTATCCGGTAAGCG	Cloning
pcllyfpcontrolrev	TGACAAGTGTGGCCATGGA	Cloning
pCG896insidecontrolfor	GGACACATCGTACAGTTCGG	Cloning
pCG910SDMfor	cggccGCTGTGTAGCAAACATTTA TATTTT	Cloning pCG910, pCG925
pCG910SDMrev	cggcgAAAAACAATATGTAGCATCA AAATTAG	Cloning pCG910, pCG925
pCG943SDMfor	TAATTTTGTATGCTACATATTGTTTT TTATTATAATTG	Cloning pCG943
pCG943SDMrev	CGGTTTCTTGTTGCAAG	Cloning pCG943
pIMAYcontrolfor	CCAGCCCCCTCACTACAT	Cloning pCG925, pCG926
pIMAYcontrolrev	ATCACCCGACGCACTTTG	Cloning pCG925, pCG926
pCG925gibfor	aattcctgcagcccggggCTATGACTATT GTATTTGCTATATTGCT	Cloning pCG925
pCG925gibrev	gccgctctagaactagtgGCACATCACTC CTTGTCGAC	Cloning pCG925
pCG925outsidecontrolfor	GCGGAGGTAAGTGAGTGA	Cloning pCG925
pCG925outsidecontrolrev	GGATGACCACATCGCTTCA	Cloning pCG925
pCG926insert1gibfor	aattcctgcagcccggggAGACATC TTAGATCGAGTTAAGGAGG	Cloning pCG926
pCG926insert1gibrev	ttcctgtttTACATGCAATACCT CCGATA	Cloning pCG926
pCG926insert2gibfor	ttgcatgtaAAACAGGAAAGAAA TACGTGA	Cloning pCG926
pCG926insert2gibrev	gccgctctagaactagtgAATAGACA ATGCACATCACTCCT	Cloning pCG926
926outsidecontrolfor	CGACCAACTCATTGACGC	Cloning pCG926
926outsidecontrolrev	AACCATAGTCGCTTGATTGCCACA	Cloning pCG926
circlefor	TTTTATTTTATATGGGGTATTATTGA	qPCR (Φ13)
circclerev	GTGTATTCTCATTTGTTAGAAGAAAA	qPCR (Φ13)
SAOUHSC_02200qPCRfor	GGCAGACTAGCAATAAA	RT-qPCR ( <i>ltr</i> )
SAOUHSC_02200qPCRrev	GTCTCTGCCTATATCAAGAAT	RT-qPCR ( <i>ltr</i> )
clqPCRfor	AGAACGTCAAGATGAAACGA	RT-qPCR ( <i>cl</i> )
clqPCRrev	AATTCTTCTCCTATGCCAGC	RT-qPCR ( <i>cl</i> )
SAOUHSC02234DIGfor	TAATACGACTCACTATAGGGAG ATGCAAATTGACTGAGTGC	RT-qPCR ( <i>mor</i> )
SAOUHSC02234DIGrev	ATGTGTTACGACTACTCACG	RT-qPCR ( <i>mor</i> )
SAOUHSC02196for2	CACGAATCAAACGGCATTAA	RT-qPCR ( <i>terL</i> )
SAOUHSC02196rev2	ACAACAATCGAATCAATGGC	RT-qPCR ( <i>terL</i> )
SAOUHSC02191for	TTTGCATCTTCGATTGCTTC	RT-qPCR ( <i>mcp</i> )
SAOUHSC02191DIGrev	TACGACAATCAGAAGTTGCA	RT-qPCR ( <i>mcp</i> )
RTqPCRamidasefor	AAATAGGTGATGTGGCTGTA	RT-qPCR ( <i>amidase</i> )
RTqPCRamidaserev	AGTGAGTACAGCCGTAATAATT	RT-qPCR ( <i>amidase</i> )
holin255for	ATGATTAATTGAAAATTAGAA	RT-qPCR ( <i>holin</i> )
holin255rev	CTAGTATTTTCTTCTTGTTCT	RT-qPCR ( <i>holin</i> )
sakLClo	CATCAAGTTCATTCGACAAAGGAAA	RT-qPCR ( <i>sak</i> )
sak-A	TGTAGTCCCAGGTTTAATAGG	RT-qPCR ( <i>sak</i> )
asp493f	AAAATTGCTGGTATCGCTGC	RT-qPCR ( <i>asp</i> )
asp848r	TGAAACCTTGTCTTTCTTGGT	RT-qPCR ( <i>asp</i> )

T7-SAOUHSC02196DIGfor	TAATACGACTCACTATAGGGAG ATTAGGGTCTGGAAGCATTTTC	DIG-probe Northern Blot ( <i>terL</i> )
SAOUHSC02196DIGrev	ATGGTTGCCATTGGGATAAT	DIG-probe Northern Blot ( <i>terL</i> )
T7-SAOUHSC02191DIGfor	TAATACGACTCACTATAGGGA GATTTGCATCTTCGATTGCTTC	DIG-probe Northern Blot ( <i>mcp</i> )
SAOUHSC02191DIGrev	TACGACAATCAGAAGTTGCA	DIG-probe Northern Blot ( <i>mcp</i> )

**Table S3:** Plasmids

Plasmid	Description	Resistance cassette	Reference/ Origin
pIMAY-Z	Mutagenesis vector	<i>cm</i>	(12)
pCG725	$P_{cap}$ - <i>yfp</i>	<i>cm</i>	(8)
pCG896	Promoter construct $P_{23}$ - <i>yfp</i>	<i>cm</i>	This study
pCG910	Promoter construct $P_{23}$ - <i>TATA-yfp</i>	<i>cm</i>	This study
pCG925	Mutagenesis vector for p23 TATA Box mutation (pIMAY-Z)	<i>cm</i>	(5)
pCG926	Mutagenesis vector for <i>ltr</i> mutation (pIMAY-Z)	<i>cm</i>	This study
pCG943	Promoter construct $P_{23}$ - $\Delta$ <i>repeat-yfp</i>	<i>cm</i>	This study

**References (Supplementary Information)**

1. Monk IR, Shah IM, Xu M, Tan MW, Foster TJ. 2012. Transforming the untransformable: application of direct transformation to manipulate genetically *Staphylococcus aureus* and *Staphylococcus epidermidis*. *mBio* 3.
2. Novick R. 1967. Properties of a cryptic high-frequency transducing phage in *Staphylococcus aureus*. *Virology* 33:155-66.
3. Rohmer C, Dobritz R, Tuncbilek-Dere D, Lehmann E, Gerlach D, George SE, Bae T, Nieselt K, Wolz C. 2022. Influence of *Staphylococcus aureus* Strain Background on Sa3int Phage Life Cycle Switches. *Viruses* 14.
4. Horsburgh MJ, Aish JL, White IJ, Shaw L, Lithgow JK, Foster SJ. 2002. sigmaB modulates virulence determinant expression and stress resistance: characterization of a functional rsbU strain derived from *Staphylococcus aureus* 8325-4. *J Bacteriol* 184:5457-67.
5. Dobritz R, Rohmer C, Niepoth E, Egle V, Korn N, Bisanzio V, Bojer MS, Ingmer H, Wolz C. 2025. Multiple effects of the bacterial DNA-binding protein SarA on the life cycle of *Staphylococcus aureus* phages. *J Bacteriol* doi:10.1128/jb.00279-25:e0027925.
6. Bae T, Baba T, Hiramatsu K, Schneewind O. 2006. Prophages of *Staphylococcus aureus* Newman and their contribution to virulence. *Mol Microbiol* 62:1035-47.
7. Tang Y, Nielsen LN, Hvitved A, Haaber JK, Wirtz C, Andersen PS, Larsen J, Wolz C, Ingmer H. 2017. Commercial Biocides Induce Transfer of Prophage  $\Phi$ 13 from Human Strains of *Staphylococcus aureus* to Livestock CC398. *Front Microbiol* 8:2418.
8. Keinhörster D, Salzer A, Duque-Jaramillo A, George SE, Marincola G, Lee JC, Weidenmaier C, Wolz C. 2019. Revisiting the regulation of the capsular polysaccharide biosynthesis gene cluster in *Staphylococcus aureus*. *Mol Microbiol* 112:1083-1099.
9. Meier S, Goerke C, Wolz C, Seidl K, Homerova D, Schulthess B, Kormanec J, Berger-Bächi B, Bischoff M. 2007. sigmaB and the sigmaB-dependent arlRS and yabJ-spoVG loci affect capsule formation in *Staphylococcus aureus*. *Infect Immun* 75:4562-71.
10. Bremell T, Abdelnour A, Tarkowski A. 1992. Histopathological and serological progression of experimental *Staphylococcus aureus* arthritis. *Infect Immun* 60:2976-85.
11. Kreiswirth BN, Lofdahl S, Betley MJ, O'Reilly M, Schlievert PM, Bergdoll MS, Novick RP. 1983. The toxic shock syndrome exotoxin structural gene is not detectably transmitted by a prophage. *Nature* 305:709-12.
12. Monk IR, Tree JJ, Howden BP, Stinear TP, Foster TJ. 2015. Complete Bypass of Restriction Systems for Major *Staphylococcus aureus* Lineages. *mBio* 6:e00308-15.

**Part III: Multiple effects of the bacterial DNA-binding protein SarA on the life cycle of *Staphylococcus aureus* phages**

Ronja Dobritz<sup>1,2</sup>, Carina Rohmer<sup>3</sup>, Elena Niepoth<sup>1,2</sup>, Valentin Egle<sup>1</sup>, Natalya Korn<sup>1,2</sup>, Vittoria Bisanzio<sup>1,2</sup>, Martin Saxtorph Bojer<sup>4</sup>, Hanne Ingmer<sup>4</sup>, Christiane Wolz<sup>1,2,\*</sup>

<sup>1</sup>Interfaculty Institute of Microbiology and Infection Medicine, University of Tübingen, Germany

<sup>2</sup>Cluster of Excellence EXC 2124 “Controlling Microbes to Fight Infections”, University of Tübingen, Germany

<sup>3</sup>Fraunhofer Institute for Interfacial Engineering and Biotechnology IGB, Stuttgart, Germany

<sup>4</sup>Department of Veterinary and Animal Sciences, University of Copenhagen, Denmark

\*Correspondence: [christiane.wolz@uni-tuebingen.de](mailto:christiane.wolz@uni-tuebingen.de)

**Published:** Dobritz R, Rohmer C, Niepoth E, Egle V, Korn N, Bisanzio V, Bojer MS, Ingmer H, Wolz C. 2025. Multiple effects of the bacterial DNA-binding protein SarA on the life cycle of *Staphylococcus aureus* phages. *J Bacteriol* 207:e00279-25.

<https://doi.org/10.1128/jb.00279-25>

**Abstract:** *Staphylococcus aureus* is a major opportunistic pathogen in humans and animals. More than 90% of human nasal *S. aureus* isolates carry Sa3int-phages that integrate into the bacterial *hly* gene coding for a sphingomyelinase. Sa3int-phages encode highly human-specific virulence factors that enable *S. aureus* to adapt to the human host. Thus, balancing mechanisms are necessary for the phage-bacteria coexistence. However, the factors that coordinate these interactions have yet to be discovered. Here, we elucidate the impact of the DNA-binding protein SarA on the life cycle of two prototypic *S. aureus* phages, Sa3int  $\Phi$ 13 and Sa5int  $\Phi$ 11. SarA promotes the propagation of both phages, albeit via different mechanisms. SarA promotes  $\Phi$ 11 propagation by repressing the glycosyltransferase TarM, which affects the glycosylation pattern of the phage receptor, wall teichoic acid, thereby improving phage adsorption. SarA also dampens the DNA damage response as indicated by the downregulation of the *ci* and *mor* phage promoters and the *umuC* SOS target gene, as well as inhibition of  $\Phi$ 11 inducibility. For  $\Phi$ 13, however, SarA promotes phage replication rather than inhibiting phage induction. The replication-deficient phage  $\Phi$ 13K-*rep* was SarA-insensitive and phage gene expression was unaltered in the *sarA* mutant. These results highlight SarA as a regulator of temperate phage propagation and support its role as a DNA structural protein that promotes phage replication.

**Importance:** The dynamic gain and loss of temperate phages is crucial for bacteria to adapt to specific niches. In *Staphylococcus aureus* Sa3int phages are highly prevalent in human strains but are missing in most animal strains. The mechanisms that balance phage-bacteria coexistence are only partially understood. We demonstrate that the DNA-binding protein SarA is a key regulator of the phage life cycle. SarA protects bacteria from phage induction in response to DNA damage, yet it can also promote phage propagation by altering the phage receptor or interfering with phage replication. SarA likely functions not only as a transcriptional factor, but also as a bacterial chromosome structural component, that controls the phage life cycle at different levels.

**Keywords:** *Staphylococcus aureus*; phage; SOS-response; DNA-binding proteins; SarA; Hly

## Introduction

*Staphylococcus aureus* is a major opportunistic pathogen in humans and animals. This bacterium asymptotically colonizes the nasal mucosa of healthy individuals but can cause life-threatening acute and chronic infections (1, 2). *S. aureus* has jumped between species many times, resulting in the dynamic gain and loss of host-specific adaptive genes many of which are prophage encoded (2-5). Most prominent is the repeated loss of the temperate Sa3int phages after transfer of *S. aureus* from humans to different animals (6). In several instances, animal-adapted strains were transmitted back to humans, where they often reacquired Sa3int phages, emphasizing the importance of these temperate phages in human colonization (7). Up to 96% of human nasal *S. aureus* isolates carry Sa3int phages integrated into the *hlyB* locus, which encodes the toxin  $\beta$ -hemolysin (HlyB). While phage integration disrupts an important virulence factor of *S. aureus*, Sa3int phages carry genes that encode human-specific immune evasion factors and other potential virulence factors (6). The phage encoded factors mediate the escape of *S. aureus* from human innate immunity (8). The observation that HlyB is always functional after phage excision and that this process also occurs during human infections, resulting in HlyB positive sub-populations (9), indicates that under certain infectious conditions, HlyB is essential for bacterial survival. Recently, it was confirmed that phage excision enhances pathogenesis in mice (10). All temperate phages of *S. aureus* are classified as siphophages (4). They can be discriminated into different groups based on their integrase gene allele (Sa-int groups) (11). The siphophage genomes are usually organized into six functional modules: lysogeny, DNA replication, packaging, head, tail, and lysis. The best-studied temperate phages from *S. aureus*, Sa5int phage  $\Phi$ 11 and the Sa3int phage  $\Phi$ 13, originate from the same host bacteria *S. aureus* NCTC 8325. Previously, we analysed the life cycle of two Sa3int phages,  $\Phi$ 13 and  $\Phi$ N315, in different phage-cured *S. aureus* strains. *S. aureus* strains could be classified into low (8325-4, SH1000, USA300c) and high (MW2c, Newman-c) transfer strains (12). Host-phage interactions probably account for the observed strain specific differences in phage replication, assembly, and transfer frequency. The CI/Cro lysogenic/lytic switch in temperate phages is the best studied regulatory switch to control phage mobilisation and has been extensively characterized in the *Escherichia coli* phage  $\lambda$ . RecA-dependent cleavage of the CI repressor initiates phage induction and derepression of the lytic genes.  $\Phi$ 11 contains a  $\lambda$ -like CI/Cro switch region (13). In  $\Phi$ 13 the switch region is composed of a cleavable CI repressor and a Mor homologue (14). The small antirepressor Mor, first identified in lactococcal phages, functions as an anti-repressor of CI by protein-protein interaction (15, 16). The lytic state requires MOR-CI complex formation. Molecular circuits controlling the expression of late phage genes are only partially understood. Nevertheless, additional phage and host factors beside the “classical lytic switch” module are likely important for phage-host interaction. Active lysogeny or pseudolysogeny (13, 17) may be common for Sa3int phages

and refers to the process whereby a prophage is temporarily excised from the chromosome without forming intact phage particles or the prophage is not integrated following infection. This allows bacteria to simultaneously express phage-encoded virulence genes as well as the gene that is usually inactivated by prophage integration, e.g., the *hly* gene (9).

Recently described xenogenic silencing factors (XS) may contribute to balancing bacteria-phage co-existence (18), particularly favouring and maintaining the lysogenic state. The XS factors discovered so far are small, nucleoid-associated proteins that recognize and bind AT-rich DNA stretches. Of note, none of the described factors are present in *S. aureus*. We speculated that SarA family proteins might fulfil a XS-like function. SarA recognizes and binds AT-rich DNA motifs and is usually seen as a transcriptional factor controlling gene expression (19, 20). However, SarA seems to bind the chromosome more frequently than one might expect for a bona fide transcription factor. SarA is present at intracellular concentrations far exceeding any classical transcription factor and its concentration remains unchanged during different growth phases (21). SarA was therefore suggested to be a histone-like protein that may alter DNA topology (21, 22).

Here we analyzed the role of SarA in the life cycle of two prototypic siphophages,  $\Phi$ 11 and  $\Phi$ 13. Our data indicate that SarA promotes propagation of both phages, albeit in different ways. By inhibiting the expression of glycosyltransferase TarM, SarA alters the glycosylation pattern of the phage receptor wall teichoic acid (WTA) and promotes  $\Phi$ 11 adsorption. In contrast, the positive impact of SarA on  $\Phi$ 13 replication can be attributed to the promotion of a step between prophage excision and viral particle assembly, which most likely requires the function of SarA as a DNA structural protein rather than a transcription factor.

## Results

### **SarA promotes propagation of siphophages $\Phi$ 11 and $\Phi$ 13**

We analyzed SarA-dependent phage propagation using two phage-cured *S. aureus* strains (SH1000 and Newman-c). *SarA* mutants were generated, and mutants were complemented by integration of the *sarA* expressing plasmid into the *geh* locus. We first analysed the infection dynamics of phage  $\Phi$ 13K-*int* (23), a kanamycin resistant derivative of  $\Phi$ 13, the native phage of the SH1000 ancestor NCTC 8325 (12). Unlike  $\Phi$ 13K,  $\Phi$ 13K-*int* lacks the integrase and thus produces clear plaques because it cannot enter the lysogenic life cycle. After infection at a multiplicity of infection (MOI) of 1, phage replication was significantly lower in the *sarA* mutants compared to wild type strains (SH1000, Newman-c) or complemented mutants (Fig. 1A, 1C). Despite phage propagation, little or no concomitant bacterial lysis was detectable after infection and bacterial numbers continued to increase up to 6 h post-infection (Fig. 1B, 1D). This is probably due to the phage infecting only a sub-population of bacteria or to phage replication/assembly being somehow inhibited in most of the bacterial population. However, in

strain Newman a slight but significant SarA-dependent inhibition of bacterial replication was detectable in the wild type and complemented strains 3 h post-infection. These data indicate that host derived factors modulate  $\Phi$ 13K-*int* propagation.

We next analyzed the infection dynamics of  $\Phi$ 11, a phage from the Sa5int group. Like  $\Phi$ 13, this phage is also derived from the SH1000 parental strain NCTC 8325. Following phage infection, significantly fewer phage copies were detectable in the *sarA* mutant 3 h post-infection (Fig. 1E). However, in contrast to  $\Phi$ 13K-*int*, infection resulted in bacterial lysis of the wild type and complemented strain (Fig. 1F). In the *sarA* mutant, bacterial lysis was partial and detectable only after > 3 h of infection. Thus, SarA promotes phage propagation of  $\Phi$ 13K-*int* and  $\Phi$ 11, despite phage-specific differences in host cell lysis.

### **SarA supports adsorption of $\Phi$ 11 but not $\Phi$ 13K**

We next analyzed the impact of SarA on phage adsorption, a prerequisite for phage propagation. After 10 min of phage adsorption, the number of unbound phages was determined by qPCR on phage genomes (Fig. 2A). While phage adsorption of  $\Phi$ 13K-*int* was not altered in the *sarA* mutant, adsorption of  $\Phi$ 11 to the *sarA* mutant was significantly reduced. WTA serves as a receptor for all *S. aureus* phages, although differences exist between phages with respect to the specific WTA moiety bound (24).  $\Phi$ 11 adsorption is dependent on WTA glycosylation whereas  $\Phi$ 13 binds to the RboP-WTA backbone, irrespective of its glycosylation pattern. Glycosylation is catalysed by the glycosyltransferases TarM and/or TarS. We speculated that SarA might impact expression of *tarS* and/or *tarM* and thereby modulating  $\Phi$ 11 adsorption. Expression of *tarM* was found to be significantly increased in the *sarA* mutant whereas *tarS* expression was SarA-independent (Fig. 2B, 2C). Complementation of the *sarA* mutant restored *tarM* expression to the level of the wild type (Suppl. Fig. S1). Since SarA controls the activity of the quorum-sensing system Agr (25) and Agr inhibits *tarM* expression (26), we speculated that SarA effect on  $\Phi$ 11 adsorption is due to Agr-dependent dysregulation of *tarM*. Indeed, *sarA* and an isogenic *agr* mutant were similarly diminished in  $\Phi$ 11 adsorption (compare Fig. 2A and Fig. 2D). Furthermore, incubating the *sarA* mutant with the autoinducing peptide AIP-I counteracted the SarA-mediated inhibition of phage adsorption (Fig. 2E).

Interestingly,  $\Phi$ 13 adsorption was also found to be *agr* dependent, although *sarA* deletion did not significantly alter phage binding (compare Fig. 2A and Fig. 2D).

The data indicate that SarA-dependent promotion of  $\Phi$ 11 propagation is due to enhanced phage adsorption, likely due to Agr-mediated inhibition of *tarM*. However, adsorption of  $\Phi$ 13 is glycosylation insensitive and SarA-independent. Thus, SarA likely impacts  $\Phi$ 13 life cycle via mechanism(s) unrelated to phage adsorption or other Agr mediated effects.

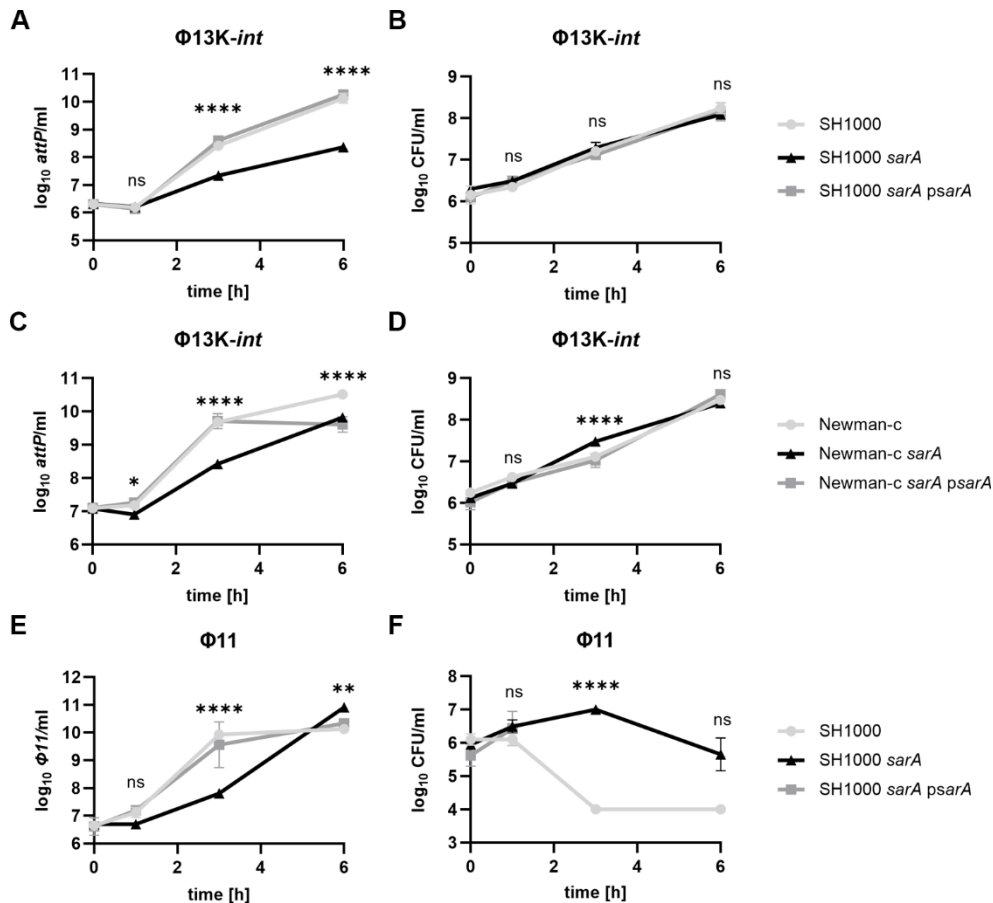


**FIG 1** SarA promotes propagation of  $\Phi 11$  and  $\Phi 13$ . Phage replication and bacterial growth in wild type, *sarA* (*sarA::ermC* deletion), and *sarA psarA* (*sarA* complementation) following phage infection. Phage-free strains were grown to an  $OD_{600}$  of 0.5, then  $1 \times 10^6$  bacteria per milliliter were infected with integrase-deficient  $\Phi 13K-int$  (A, B, C, D) or  $\Phi 11$  (E, F) at MOI 1 and incubated for up to 6 h. Phage replication was analyzed by enumerating free phage genomes in the supernatant by quantitative PCR (qPCR) (copies of *attP*) (A, C, E), and bacterial growth was monitored by colony-forming unit (CFU) determination (B, D, F). Data shown are mean  $\pm$  SD ( $n = 3$ ). Statistical significance was determined by two-way ANOVA tests on  $\log_{10}$ -transformed data for multiple comparisons for each time point (Tukey's multiple comparison test). Statistical results for wild type vs *sarA* comparison are shown (\*\*\*\* $P$  value  $< 0.0001$ , \*\* $P$  value  $< 0.01$ , ns  $> 0.05$ ).

### SarA promotes replication of $\Phi 13K$ but not $\Phi 11$

To further analyze the impact of SarA on the phage life cycle, *sarA* mutants were created in single-lysogens of strain SH1000. We first analyzed induction of  $\Phi 13K$  with and without the inducing agent mitomycin C (MMC). The extracellular genome copies of released  $\Phi 13K$  from culture supernatants were quantified by attachment site (*attP/ml*) qPCR. SarA deletion significantly reduced the number of released  $\Phi 13K$  copies (239-fold decrease under uninduced and 278-fold under induced conditions), a phenotype that was fully reverted to wild type in the complemented strain (Fig. 3A). Interestingly, no difference in replication of  $\Phi 13K$  between wild type and *agr* mutant was observed, supporting the hypothesis that the effect of SarA on phage replication is Agr independent (Suppl. Fig. S2).

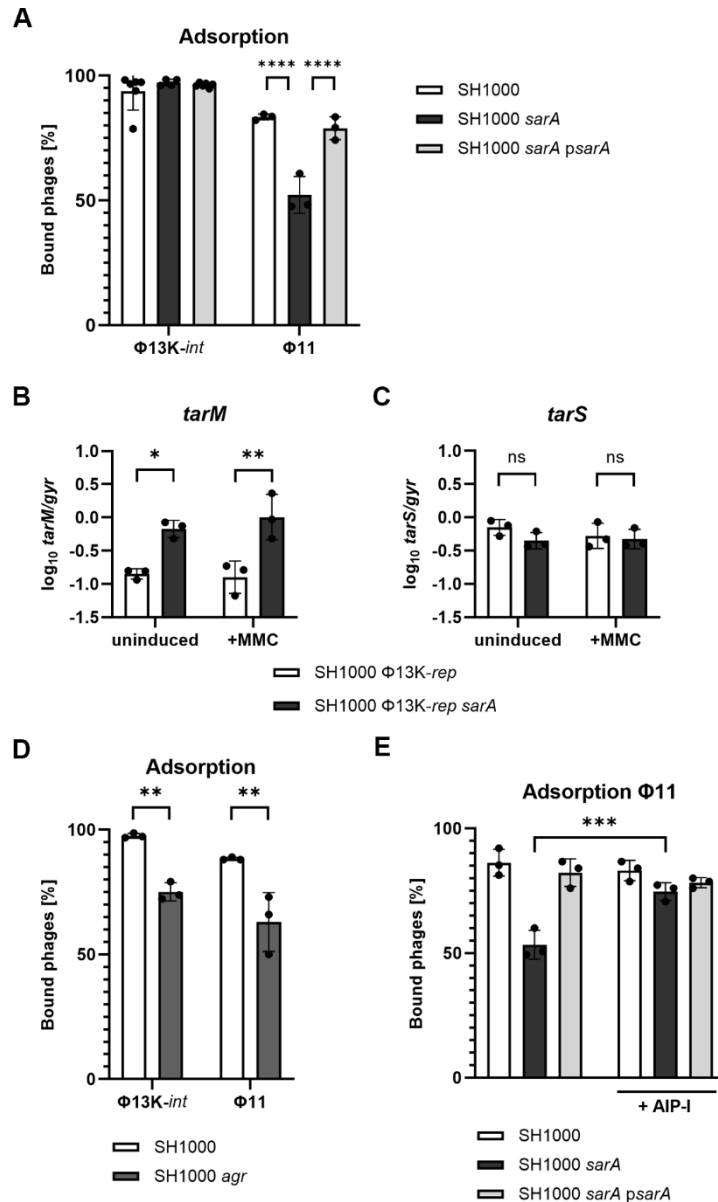


**FIG 2** *sarA* deletion results in reduced binding of Φ11 and altered expression of WTA glycosyl transferase *tarM*. (A) Phage adsorption of Φ13K-*int* and Φ11 to SH1000 (wild type), SH1000 *sarA* (*sarA::ermC* deletion), and SH1000 *sarA psarA* (*sarA* complementation). Phage-free strains were grown to an OD<sub>600</sub> of 1, and 1 × 10<sup>8</sup> bacteria per milliliter were incubated for 10 min with phages at MOI 0.01. Unbound phages were enumerated by qPCR on the phage genome and compared to media control to calculate the number of bound phages. (B, C) Gene expression analysis of *tarM* (α-1,4 GlcNAc) and *tarS* (β-1,4 GlcNAc) under uninduced and induced (+MMC) conditions. Single-lysogenic SH1000 and SH1000 *sarA* (*sarA::ermC* deletion), containing the replication-deficient Φ13K-*rep* mutant, were grown to exponential growth phase, followed by prophage induction with subinhibitory mitomycin C (MMC), and incubation for 60 min. RNA was isolated, *tarM* and *tarS* transcripts were quantified by quantitative reverse transcription polymerase chain reaction (qRT-PCR), and normalized to *gyr* expression. (D) Phage adsorption of Φ13K-*int* and Φ11 to SH1000 (wild type) and SH1000 *agr* (*agr::tetM* deletion). (E) Phage adsorption of Φ11 to SH1000, SH1000 *sarA*, and SH1000 *sarA psarA* in the presence of AgrA, inducing peptide, AIP-I. A total of 100 nM AIP-I was added to the precultures. Data shown are mean ± SD (n = 3). Statistical significance was determined by a two-way ANOVA test (\*\**P* value < 0.001, \*\**P* value < 0.01, \**P* value < 0.05, ns > 0.05).

We next analyzed phage excision of  $\Phi$ 11E (erythromycin resistant derivative of  $\Phi$ 11) lysogen generated in strain SH1000 and its *sarA* mutant. No significant difference in phage excision/replication between wild type and *sarA* mutant was detectable under uninduced conditions (Fig. 3B). After MMC induction,  $\Phi$ 11 copies were increased in the *sarA* mutant in comparison to the wild type, which sharply contrasts the results obtained for  $\Phi$ 13K (Fig. 3A, 3B). The data underline that SarA differentially impacts the life cycle of the analyzed phages.

To dissect whether SarA impacts phage excision, replication, or assembly of  $\Phi$ 13, we quantified phage excision in replication-deficient phage lysogens ( $\Phi$ 13K-*rep*) (12).  $\Phi$ 13K-*rep* can still be excised from the chromosome but is unable to replicate or produce intact phage particles. The number of excised phage copies was comparable to the number of restored *h1b* copies in the bacterial population (Fig. 3C, 3D). No significant SarA-dependent differences were found in phage excision or *h1b* reconstitution. Thus, processes following phage excision are likely to be controlled by SarA.

We next analyzed a phage mutant (-*TSS23*) that can excise and replicate but cannot assemble due to mutations in the main promoter (p23) controlling the expression of structural genes. Consequently, induction of this phage does not result in plaque formation. A significant difference in the replication of phage  $\Phi$ 13K-*TSS23* was observed between the wild type and *sarA* mutant, comparable to the difference detected for the wild type  $\Phi$ 13K (Fig. 3E). These results indicate that SarA affects a step between excision of the prophage and assembly of intact phage particles, which accounts for the significant reduction in the number of wild type  $\Phi$ 13K phage copies released in the *sarA* mutant (Fig. 3A).

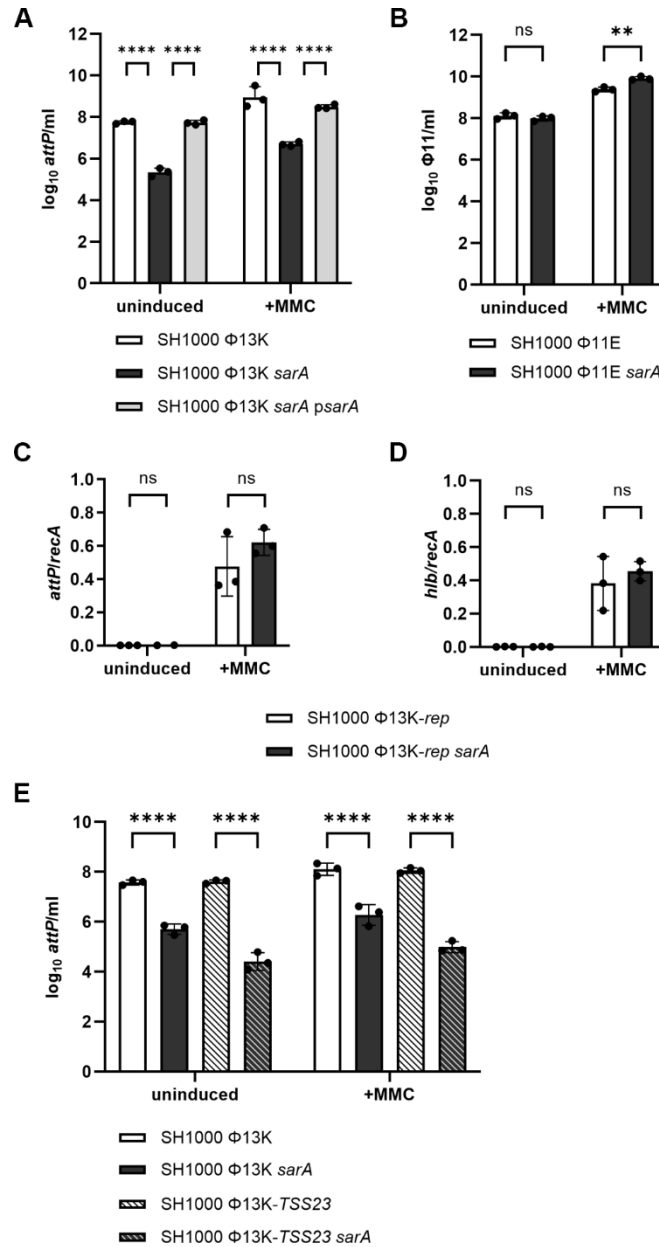


**FIG 3** SarA supports Φ13K phage replication. Phage replication in single-lysogenic SH1000 (wild type), SH1000 *sarA* (*sarA::ermC* deletion), and SH1000 *sarA psarA* (*sarA* complementation) under uninduced and induced (+MMC) conditions. (A) Single-lysogenic Φ13K strains were induced with subinhibitory MMC in exponential growth phase and incubated for 60 min. Phage numbers were determined by qPCR (*attP*). (B) Single-lysogenic Φ11 strains were grown to the exponential growth phase, induced with subinhibitory MMC, and incubated for 60 min. Phage numbers were determined by qPCR on the phage genome. (C, D) Intracellular phage excision and replication. Replication-deficient (*-rep*) Φ13K-*rep* single-lysogenic strains were induced with subinhibitory concentrations of MMC and incubated for 60 min. Intracellular phage replication was enumerated as the ratio of excised, circularized phage genomes (*attP*) per copy of bacterial chromosome (*recA*). Phage excision was quantified by qPCR on reconstituted *hlyB* genes per bacterial chromosome (*recA*). (E) Single-lysogenic Φ13K or Φ13K-*TSS23* (non-infectious phage mutant) strains were grown to exponential growth phase, induced with subinhibitory MMC, and incubated for 60 min. Phage numbers were determined by qPCR on the phage genome. Data shown are mean ± SD (n = 3). Statistical significance was determined by two-way ANOVA tests on log<sub>10</sub>-transformed data (\*\*\*\*P value < 0.0001, \*\*P value < 0.01, ns > 0.05).

**SarA does not impact supercoiling or protease-dependent phage decay**

Overexpression of proteases is a main feature of *sarA* mutant strains (27) and *S. aureus* phages were shown to be protease sensitive (28). We confirmed that the *sarA* mutant has significantly higher proteolytic activity than the wild type (Suppl. Fig. S3). We speculated that phages might be readily degraded in the supernatant of *sarA* mutant strains, which would explain the decrease in phage infectivity (Fig. 3A). However,  $\Phi$ 13 particles after incubation in culture supernatants from wild type or the *sarA* mutant were equally stable (Suppl. Fig. S3). Next, we speculated that SarA might function as a structural DNA-binding protein that modifies supercoiling and thereby may impact phage gene transcription or replication. However, supercoiling of a small plasmid that acts as a monitor for the global level of supercoiling in the cell, was not found to differ between wild type and *sarA* mutant (Suppl. Fig. S4).

**SarA inhibits promoter activities of the phage switch region and the SOS gene *umuC***

To clarify how SarA promotes  $\Phi$ 13 replication, we analyzed whether phage gene expression is affected in a *sarA*-dependent manner. First, we used promoter fusion constructs of the lytic switch region of  $\Phi$ 13. *Cl* and *mor* promoters containing *Cl* binding sites were fused to *yfp* and *cfp*, respectively (*Pcl-yfp* and *Pmor-cfp*). Promoter activities were analyzed in  $\Phi$ 13K-*rep* lysogens of SH1000 and its *sarA* mutant. Under uninduced conditions promoter activities were low and no significant difference between wild type and *sarA* mutants was observed. However, after MMC treatment, the activities of both phage promoters were significantly increased in the *sarA* mutants (Fig. 4A, 4B). This indicates that RecA-dependent *Cl* cleavage or RecA activity might be repressed by SarA. If RecA activity is hampered, the LexA-dependent SOS response should also be altered in the *sarA* mutant. Accordingly, the activity of the *umuC* promoter, a prototypic LexA target gene in *S. aureus*, was also significantly increased in the *sarA* mutant after MMC induction, indicating enhanced SOS-response activation (Fig. 4C). The increased *umuC* expression in the *sarA* mutant after MMC treatment was confirmed by RT-qPCR (Suppl. Fig. S5).

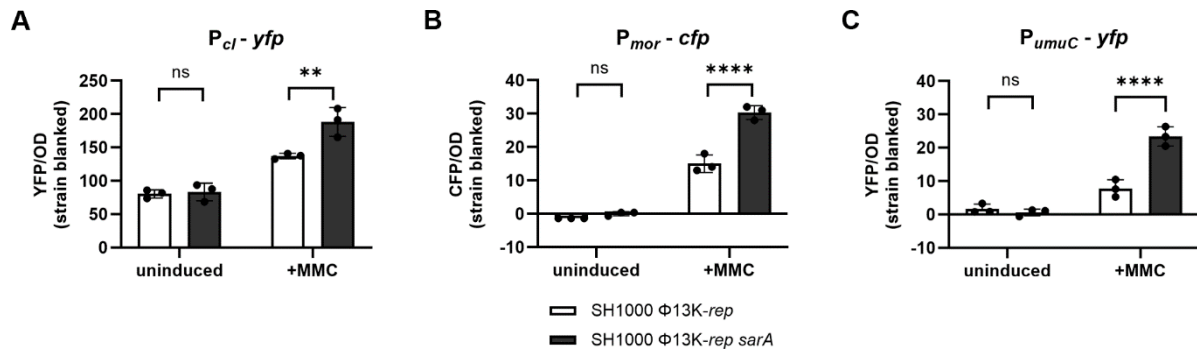


**FIG 4** DNA-damage response activation in the *sarA* mutant background. Promoter activity of  $P_{cl}$ ,  $P_{mor}$ , and  $P_{umuC}$  in single-lysogenic SH1000  $\Phi$ 13K and SH1000  $\Phi$ 13K *sarA* (*sarA::ermC* deletion) under uninduced and induced (+MMC) conditions. (A–C) Reporter plasmid ( $P_{cl}$ : pCG748,  $P_{mor}$ : pCG789,  $P_{umuC}$ : pCG762) containing strains were grown to the exponential growth phase, induced with subinhibitory MMC, and incubated for 60 min. Bacterial cultures were harvested to an OD<sub>600</sub> of 2 and resuspended in phosphate-buffered saline (PBS). Optical density and fluorescence were measured. Arbitrary units of fluorescence (yellow: YFP, blue: CFP) are shown, normalized to OD<sub>600</sub>; strain-specific background fluorescence was subtracted. Data shown are mean  $\pm$  SD (n = 3). Statistical significance was determined by two-way ANOVA tests (\*\*\*\**P* value < 0.0001, \*\**P* value < 0.01, ns > 0.05).

The results indicate that SarA dampens the SOS response and the lytic phage life cycle. This would be consistent with an increase in phage mobilization in *sarA* mutants as observed for  $\Phi$ 11 (Fig. 3B). However, the finding is counterintuitive to the observation that replication of  $\Phi$ 13 is decreased in the *sarA* mutant (Fig. 3A). Only for the replication-deficient phage  $\Phi$ 13K-*rep* a slight increase of phage induction was detectable in the *sarA* mutant (Fig. 3C).

#### SarA does not control gene expression of $\Phi$ 13K

To account for the SarA-dependent promotion of  $\Phi$ 13K replication, we speculated that SarA might control the expression of phage genes. Therefore, we analyzed phage gene expression by RT-qPCR under induced and uninduced conditions. We selected a set of genes from different modules of  $\Phi$ 13K and initiated by different transcriptional start sites (12) (Fig. 5A). Expression of genes was significantly lower in the *sarA* mutant. However, this might be simply due to reduced phage genome copy numbers as phage replication is decreased in the *sarA* mutant. Thus, we also analyzed gene expression in the replication-deficient  $\Phi$ 13K-*rep* lysogens. In these lysogens, no SarA-dependent effects on phage gene expression were detectable (Fig. 5B - 5F). Thus, SarA does not impact phage gene expression. Instead, it is more likely to impact  $\Phi$ 13K phage propagation by interfering with DNA-dependent processes, such as initiation or elongation of replication.

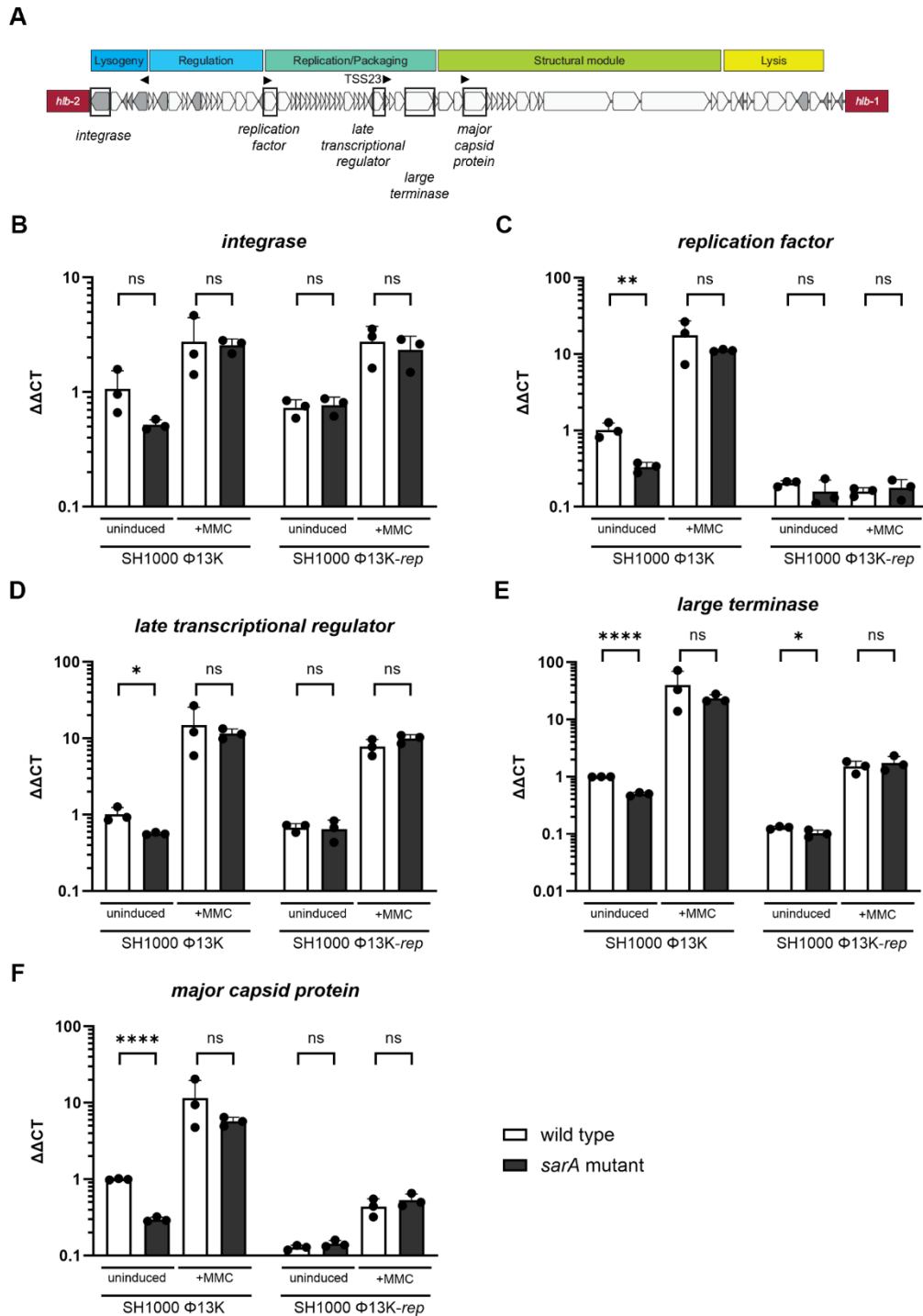


**FIG 5** SarA does not control phage gene expression of  $\Phi$ 13K. Gene expression analysis of phage genes under uninduced and induced (+MMC) conditions. (A) Schematic depiction of gene organization in the  $\Phi$ 13K genome. Transcriptional start sites are displayed as arrowheads. (B–F) Single-lysogenic SH1000 and SH1000 *sarA* (*sarA::ermC* deletion) containing wild-type or replication-deficient  $\Phi$ 13K ( $\Phi$ 13K-*rep*) were grown to exponential growth phase, induced with subinhibitory MMC, and incubated for 60 min. RNA was isolated, and *integrase*, *replication factor*, *late transcriptional regulator*, *large terminase*, and *major capsid protein* transcripts were quantified by RT-qPCR and normalized to *gyrB* expression by the  $\Delta\Delta C_t$  method. Data shown are mean  $\pm$  SD ( $n = 3$ ). Statistical significance was determined by unpaired t-tests comparing wild-type and *sarA* mutant (\*\*\*\* $P$  value  $< 0.0001$ , \* $P$  value  $< 0.05$ , ns  $> 0.05$ ).

## Discussion

Temperate phages such as Sa3int phages fulfill beneficial functions for their bacterial hosts, but they also pose a threat for the host bacterium once mobilized. Thus, balancing mechanisms are necessary for the co-existence of phages with their hosts, as well as for phage-dependent bacterial adaptation to specific niches. Such mechanisms are not well understood, and putative bacterial factors that coordinate these interactions have not yet been described for highly prevalent Sa3int phages. We show that SarA promotes the propagation of two prototypic phages of *S. aureus*,  $\Phi 11$  and  $\Phi 13$ , although via different mechanisms (Fig.6).

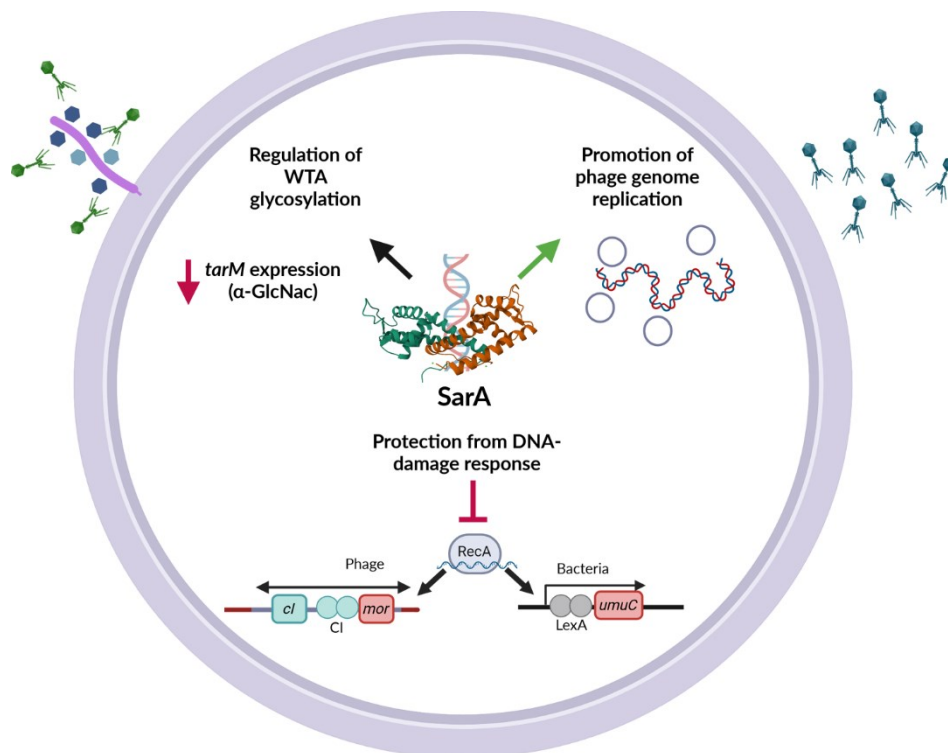


**FIG 6** Multiple effects of the bacterial DNA-binding protein SarA on the life cycle of *S. aureus* phages. SarA promotes phage infection and replication on various levels. Repression of glycosyltransferase TarM affects the glycosylation pattern of WTA and thereby facilitates binding of  $\Phi 11$ . SarA protects the phages and bacteria from DNA-damage response leading to a lower genetic switch- and SOS-response activation. Additionally, the phage replication of  $\Phi 13$  is promoted by SarA, resulting in higher numbers of phages. Crystal structure of SarA downloaded from RCSB Protein Data Bank (Entry ID:2FRH). Image created with BioRender.com.

### SarA promotes $\Phi 11$ phage adsorption through tarM inhibition.

Phage adsorption depends on the tight interaction of phage receptor-binding proteins (RBPs) and WTA. RBPs of *S. aureus* phages can be grouped into 8 distinct clusters (24).  $\Phi 11$  contains two RBPs and requires WTA glycosylation for binding. Binding of  $\Phi 11$  was significantly decreased in the *sarA* mutant. We propose that the SarA-mediated promotion of  $\Phi 11$  binding is due to SarA/Agr-dependent inhibition of *tarM* expression. This is supported by the following findings. *SarA* and *agr* mutants show similar inhibition of  $\Phi 11$  binding and the *sarA* mutant could be complemented by addition of AIP-I, indicating that SarA may at least in part function

via Agr activation (25). Recently, it was shown that Agr quorum-sensing induction reduces TarM-mediated  $\alpha$ -GlcNAc glycosylation of WTA and that  $\alpha$ -GlcNAc glycosylated WTA can hinder infection of some phages (26). In a transposon screen using glycosylation-specific antibodies, *sarA* and *agr* mutants were identified as exhibiting higher levels of  $\alpha$ -GlcNAc glycosylation (29). Reduced TarM-dependent  $\alpha$ -GlcNAc glycosylation leads to glycoswitching, favoring  $\beta$ -GlcNAc glycosylation via TarS. Moreover, the inhibition of *tarM* expression via the two-component system *arIRS* also promotes the infection of glycosylation-dependent phages. Our data indicate that the *sarA* mutant exhibits a phenotype similar to the *arIRS* mutant, resulting in the expression of *tarM*, which in turn hinders  $\Phi$ 11 adsorption. Additionally to successful adsorption the efficient cleavage of peptidoglycan (PG) might play a role in phage genome injection and subsequent replication. However, there is little evidence for the role of hydrolases on *S. aureus* phage infection. Indeed, the putative hydrolase of  $\Phi$ 11 was shown to be dispensable for successful phage infection (30). For  $\Phi$ 13 no gene similar to the already identified PG hydrolases (31) could be identified, thus a potential effect of SarA on cell wall molecules through PG cleavage is not likely. In contrast to the RBP from  $\Phi$ 11, the RBP of  $\Phi$ 13 was shown to bind WTA independent of its glycosylation status (24). This finding is consistent with our results that phage adsorption is SarA- and glycosylation-independent. Surprisingly, mutation of *agr* but not *sarA* resulted in decreased adsorption of  $\Phi$ 13. Agr was shown to increase WTA surface expression through activation of *tarH* and the chain-length through *tarK* (32). One can speculate that such Agr effects on WTA are promoting  $\Phi$ 13K-*int* phage adsorption and that Agr regulation of *tarH* and/or *tarK* only requires basal Agr activity as present in the *sarA* mutant.

### **SarA dampens the SOS response and phage repressor gene expression**

In the search for additional SarA-dependent factors controlling phage propagation, we found that SarA dampens the expression of phage repressor gene *cl* and its antirepressor *mor* as well as the LexA target gene *umuC*. Cl and LexA are both repressors that are activated through autocleavage upon DNA damage-induced RecA activation. SarA effects were only detectable after MMC treatment, indicating that SarA restricts either MMC-induced DNA damage or the consequent RecA activation. A DNA-safeguarding role for SarA is supported by the finding that SarA protects *S. aureus* from the DNA-damaging antibiotic ciprofloxacin (33). Consistent with the hypothesis that SarA antagonizes DNA-damage, we found an increase in intracellular  $\Phi$ 11 copy numbers after MMC induction in *sarA* mutants (Fig. 3B). A slight increase in phage induction was also observed for the replication-deficient  $\Phi$ 13K-*rep* phage (Fig. 3C). However, for the wild type  $\Phi$ 13K, reduced phage copy numbers were detected in the *sarA* mutants, indicating that SarA-dependent promotion of replication of this phage is controlled by other, more dominant mechanisms.

**SarA promotes phage replication of  $\Phi$ 13K**

The main effect of SarA on the  $\Phi$ 13 life cycle is likely due to its promotion of phage replication. In *sarA* mutants, phage propagation after infection is delayed and phage release from lysogenic bacteria is inhibited. This could not be linked to differences in phage adsorption, susceptibility to proteases, phage assembly, phage excision or differences in RecA activity. For the  $\Phi$ 13K-*rep* mutant, no SarA-dependent effects on phage induction were detectable and we could not detect significant differences in phage mRNA levels for the non-replicative phage. Thus, SarA impact on phage replication is likely not caused by its function as classical transcriptional factor or as modulator of transcript stability as previously proposed (19, 34, 35). We conclude that SarA is more likely to increase phage copy numbers by directly interfering with phage replication. Secondary effects on SarA-dependent changes in physiology might have contributed to better replication conditions in SarA-expressing strains. However, there is little evidence that SarA impacts bacterial growth as wild type and *sarA* mutants do not differ in their growth rate (e.g. see Fig. 1B, 1D, 1F). Moreover, we would expect this to be a more general feature also affecting replication of  $\Phi$ 11 after induction of prophages, for which we found no evidence.

SarA was suggested to be a histone-like protein that may alter DNA topology (21, 22). This was supported by the observation that SarA is present at intracellular concentrations far exceeding any classical transcription factor and its concentration remains essentially unchanged during different growth phases (21). One may speculate that SarA binding to extrachromosomal phage DNA somehow differs from binding to chromosomal DNA. SarA binding properties are also dependent on the phage analyzed since we have no evidence that  $\Phi$ 11 replication is influenced by SarA. Interestingly, ChIP-Seq indicate that SarA tends to cluster in certain regions of the chromosome (20). A pathogenic island appeared as a privileged SarA binding zone, supporting that SarA binding is dependent on certain features of DNA topology. However, SarA does not seem to alter DNA supercoiling. It was previously shown, that when expressed in *E. coli*, SarA specifically recognizes the *att* site of phage  $\lambda$  (21). Thus, the detailed mechanisms by which the interaction between SarA and the phage impacts phage replication remain to be elucidated. SarA may specifically interfere with the origin of replication, thereby promoting replication initiation and/or elongation. However, the *ori* for  $\Phi$ 13 replication has yet to be defined, hampering a closer molecular follow-up of this hypothesis. We initiated this study with the hypothesis that SarA might function as XS factor (18). Currently known XS proteins are small proteins that fall into four classes (H-NS, MvaT, Rok and Lsr2). They have been shown to follow a common mode of action by binding to AT-rich DNA, forming an oligomeric nucleoprotein complex and are likely targeted by posttranslational modification enzymes. These are all features shared with SarA, which is modified via cysteine-phosphorylation (36). However, the known XS factors are described to promote the lysogenic

state of phages. SarA instead promotes phage replication, thus functioning as a phage replication factor rather than a silencing factor.

## **Conclusion**

The life cycle of temperate phages must be tightly controlled. Here we got first insights into the specific host-phage interaction for two prototypic temperate *S. aureus* phages. The DNA binding protein SarA interferes with phage propagation at several levels. SarA promotes  $\Phi$ 11 propagation via altering of WTA glycosylation. However, for  $\Phi$ 13, SarA mainly promotes phage replication. This indicates that SarA is not only a transcriptional factor but also functions as a DNA structural protein. Such a function could also explain the DNA protective role of SarA. Future studies will help clarify the exact molecular mechanisms underlying the observed effects of SarA on temperate phage replication. SarA is an important modulator of the phage life cycle which on the one side protects the bacteria from phage induction upon DNA damage but can promote phage propagation via alteration of the phage receptor or interference with phage replication.

## **Material and Methods**

### **Growth conditions**

Strains and phages used in this work are listed in Table S1 and S2. If not stated differently, strains were grown in Tryptic Soy Broth (TSB) (Oxoid) at 37°C and 200 rpm. For strains carrying resistance genes, antibiotics (erythromycin (erm) 10  $\mu\text{g ml}^{-1}$ , tetracyclin (tet) 3  $\mu\text{g ml}^{-1}$ , kanamycin (kan) 50  $\mu\text{g ml}^{-1}$ , chloramphenicol (cm) 10  $\mu\text{g ml}^{-1}$ ) were used in precultures and for selection.

### **Generation of strains and mutants**

Oligonucleotides used for cloning and generation of strains are listed in Table S3.

### **Generation of *sarA* and *agr* mutants**

In order to generate *sarA* and *agr* mutants, phage lysates from ALC1342 and RN6911 were generated and recipient strains were transduced. Correct mutations were confirmed by PCR spanning the mutation site.

### **Generation of *sarA*-complemented strains**

The *sarA* locus (*sarAP1-P3*, *sarA*) was cloned into the integration plasmid pLL39 by amplification with primers pCG921gibfor/rev and following Gibson Assembly into the BamHI digested backbone plasmid. The resulting plasmid pCG921 was integrated into the *geh* site of CYL316 by electroporation (37),(38). Subsequently the *sarA* plasmid was introduced into *sarA* mutants by  $\Phi$ 11 transduction.

**Generation of single-lysogenic SH1000  $\Phi$ 11E**

Phage lysate of  $\Phi$ 11 containing an *erm* cassette was generated by induction of single-lysogenic 8325-4  $\Phi$ 11E. Bacteria in early exponential phase were incubated with phages at MOI of 1 for 4 h. Serial dilutions of the culture in phosphate buffered saline (PBS) were spotted onto agar plates containing *erm* (10  $\mu$ g ml<sup>-1</sup>). Single-lysogens were sub-cultivated for 5 days and stable phage integration was confirmed by PCR.

**Promoter fusion constructs for fluorescence measurements**

Promoter regions of genes of interest (*P*<sub>gene</sub>) were cloned in front of a strong ribosomal binding site (RBS) and genes encoding for fluorescent proteins (*gpVenus*, *gpCerulean*) by Gibson Assembly. For *P*<sub>cl-*yfp*</sub> (pCG748), 130 bps upstream of the putative RBS were amplified with primer *pcl-yfp-gibfor/pcl-yfp-gibrev* and cloned into reporter plasmid pCG725 (*P*<sub>cap-*yfp*</sub>) digested with *Sall* and *SphI* to replace *P*<sub>cap</sub> (32). For *P*<sub>mor-*cfp*</sub> (pCG789), the backbone reporter plasmid pCG733 (*P*<sub>cap-*cfp*</sub>) was digested with *SphI* and *EcoRI*, 133 bp upstream of the RBS of *mor* were amplified by PCR with primer *pCG789-gibfor/pCG789-gibrev* and cloned into the backbone vector. For *P*<sub>umuC-*yfp*</sub> (pCG762), the promoter region, consisting of 130 bp upstream of the RBS of *umuC*, was amplified using primers *pumuCYFP-gibfor/pumuCYFP-gibrev*. The resulting plasmids were verified by PCR and sequencing and introduced into RN4220 for transduction or electroporated directly into the final strains.

**Non-infectious phage mutant ( $\Phi$ 13K-TSS23)**

Substitution of TATA-Box within the promoter region upstream of transcriptional start site 23 (TSS23) in the phage genome was performed to generate a non-infectious phage mutant (12). The resulting phage can still replicate and lyse the bacteria, but can no longer assemble intact phage particles. The promoter region upstream of TSS23 was amplified using primer *pCG925-gibfor/pCG925-gibrev* and cloned into the *Bam*HI digested pIMAY-Z vector in *E. coli* DC10B. The plasmid was used as a template for site-directed mutagenesis (SDM) with primer *pCG910SDMfor/pCG910SDMrev* according to the manufacturer's instructions (Q5 Site-Directed Mutagenesis Kit, New England Biolabs). To confirm the substitution within the TATA-box of the promoter, the plasmid pCG925 was sequenced and subsequently transformed into the desired *S. aureus* strains by electroporation. Genomic pIMAY-Z mutagenesis within the phage genome was performed as described before and final mutants confirmed by PCR and sequencing (39).

**Generation and propagation of phage lysates**

Phage lysates were obtained by induction of single-lysogenic strains by addition of subinhibitory mitomycin C (MMC) (300 ng ml<sup>-1</sup>) and subsequent sterile filtration (0.45  $\mu$ m) of the supernatant. To propagate phages and achieve higher titers, phages were used to infect

propagation strains at a multiplicity of infection (MOI) of 1 and incubated for 4 to 6 h until lysis of bacteria was visible. Phages were harvested by centrifugation, followed by sterile filtration (0.45  $\mu\text{m}$ ) of the supernatant. Phage titers were determined by plaque assays.

### **Plaque assay**

Phage titers were determined by the agar overlay method. Indicator strains were grown to OD<sub>600</sub> of 0.1, 250  $\mu\text{l}$  bacterial culture were mixed with 10 ml phage top agar (Casaminoacids 3 g l<sup>-1</sup>, Yeast Extract 3 g l<sup>-1</sup>, NaCl 5.9 g l<sup>-1</sup>, Agar 7.5 g l<sup>-1</sup>) and poured onto NB2 agar plates supplemented with CaCl<sub>2</sub>. Serial dilution of sterile filtered (0.45  $\mu\text{m}$ ) phages in phage buffer (Tris 50 mM, CaCl<sub>2</sub> 4 mM, MgSO<sub>4</sub> 1mM, NaCl 5.9 g l<sup>-1</sup>, gelatine 1 g l<sup>-1</sup>) were spotted onto a bacterial lawn and incubated overnight at 37°C. Phage titers were quantified as plaque-forming units (PFU) per ml.

### **Infection assay**

Bacterial cultures of phage-free strains were grown to exponential phase, 1x10<sup>6</sup> bacteria were infected with phages at an MOI of 1 in a 24-well plate and incubated at 37°C and 130 rpm. At timepoints 0 h, 1 h, 3 h, and 6 h, bacterial and phage numbers were determined. For bacterial quantification, colony-forming units (CFU) were enumerated by spotting serial dilutions onto TSA plates and overnight incubation at 37°C. Extracellular phage titers were quantified by quantitative PCR (qPCR) on the circularized phage genome in sterile filtrated (0.45  $\mu\text{m}$ ) culture supernatants.

### **Adsorption assay**

Bacteria were grown to an OD<sub>600</sub> of 1 to reach exponential growth phase. For induction of AgrA, 100 nM AIP-I (autoinducing peptide I) were added to the culture (26). 1x10<sup>8</sup> bacteria were infected with 1x10<sup>6</sup> phages in TSB supplemented with CaCl<sub>2</sub> and incubated for 10 min at room temperature without shaking. Cultures were pelleted by centrifugation, and supernatants, containing unbound phages, were sterile filtrated and further analyzed by qPCR and plaque assay. For calculating the percentage of bound phages, a control condition without bacteria was included to determine phage titer after incubation (100% unbound phages).

### **Prophage induction and replication**

Phage induction and the resulting phage progeny replication were analyzed as described before (12). Briefly, single-lysogens were grown to exponential phase and induced with subinhibitory concentration of MMC (300 ng ml<sup>-1</sup>). To quantify spontaneous induction and following replication, cultures were incubated untreated. One hour post-induction, cell supernatants were harvested and sterile filtrated (0.45  $\mu\text{m}$ ), pellets were resuspended in TE buffer and stored for further analysis by qPCR.

**Quantitative PCR (qPCR) for phage genome quantification**

To quantify phage genomes within phage lysates, samples were treated with Proteinase K (AppliChem) for 1 h at 55°C, followed by inactivation for 10 min at 95°C. For quantification of phage genomes within the bacterial pellet, bacteria were lysed using a high-speed homogenizer (2x 20 s, 6500 rpm) and zirconia/silica beads (0.1 mm diameter). Lysed pellets were boiled for 10 min. Lysates and lysed pellets were diluted 1:10 in nuclease-free water for qPCR. qPCR was performed with QuantiFAST SYBR Green PCR Kit (Qiagen). For excised or extracellular phage genome quantification, primers spanning the reconstituted *attP* site were used. To quantify the excision of phage genomes from the bacterial genome, qPCR on reconstituted *h1b* was performed. Additionally, *recA* was quantified for normalization to the number of bacterial genomes for intracellular phage replication analysis.

Oligonucleotides used for qPCR are listed in Table S3.

**RNA isolation, RT-qPCR**

For RNA isolation, bacteria were harvested and resuspended in 1 ml TRIzol (Thermo Fisher Scientific). Cells were lysed using a high-speed homogenizer (6500 rpm) and zirconia/silica beads (0.1 mm diameter). RNA was isolated as recommended by the TRIzol manufacturer. 5 µg of isolated RNA were DNase-treated (Roche) and subsequently diluted 1:10 in nuclease-free water for RT-qPCR.

To determine gene expression of target genes, RT-qPCR was performed with QuantiFast SYBR Green RT-PCR Kit (Qiagen) using the Quantstudio3 system (Applied Biosystems) with the recommended settings. Relative expression was calculated using the  $\Delta\Delta CT$  method with *gyrB* as the housekeeping gene for normalization. Untreated wild type bacteria were used as control condition.

Oligonucleotides used for RT-qPCR are listed in Table S3.

**Promoter activity measurement**

Bacteria from an overnight culture were inoculated to an initial OD<sub>600</sub> of 0.05 and grown to OD<sub>600</sub> of 0.7. Subsequently, cultures were induced by addition of subinhibitory MMC (300 ng ml<sup>-1</sup>). One hour post-induction, cells were adjusted to OD<sub>600</sub> of 2 in PBS and 200 µl were transferred to a 96-well plate. Optical density (absorbance: 600 nm) and fluorescence (yellow, gpVenus: excitation 500 nm, emission 545 nm; blue, gpCerulean: excitation 434 nm, emission 485 nm) were measured using a Tecan Spark plate reader. Control bacteria without the plasmids were included for each strain to correct for strain-background fluorescence (strain blanked). Resulting values were normalized to OD<sub>600</sub>.

### **Proteolysis assay**

Skim milk agar plate assays were performed as described before (40). In brief, overnight cultures were grown, diluted to OD<sub>600</sub> of 1 in TSB and 25 µl of bacterial suspension were filled into wells (5 mm diameter) cut in 2% skim milk agar plates. Proteolysis was quantified by measurement of clear areas surrounding the bacteria, after 48 h of incubation at 37°C.

### **Influence of supernatant/ proteases on phage titers**

Cultures were grown to OD<sub>600</sub> of 0.5 and supernatants of 1x10<sup>8</sup> bacteria were collected by centrifugation, followed by sterile filtration (0.45 µm). 1x10<sup>8</sup> phages were incubated in culture supernatants, titers of phage lysates were determined by plaque assay after 3 h of incubation at 37°C and 130 rpm. RN4220 and LS1 were used as indicator strains for Φ11 and Φ13 respectively. Phages were additionally incubated in fresh TSB as control.

### **Supercoiling assay**

Assessment of DNA supercoiling status of individual strains was performed by chloroquine gel electrophoresis essentially as described before (41). Strains were initially transformed by electroporation with the small staphylococcal plasmid pC194 and selected on chloramphenicol (10 µg ml<sup>-1</sup>). 10 ml overnight cultures of respective transformants were used for plasmid purification using the GeneJet Plasmid Miniprep Kit (Thermo Fisher Scientific), including a 30 min preincubation step with lysostaphin (50 µg ml<sup>-1</sup>) in resuspension buffer at 37°C. Plasmid preparations were run on a 1% agarose (2xTBE) gel containing 2.5 µg ml<sup>-1</sup> chloroquine (10 V, 16 h), which was subsequently washed twice with water for 30 min and stained with SYBR Safe for 30 min before visualization.

### **Statistics**

Statistical analyses were performed using GraphPad Prism 10.3.1 software. Information on the tests performed for each dataset was added to figure captions; means ± SD are indicated in graphs. Differences with p < 0.05 were considered significant. All data represent values from independent biological replicates; statistical analysis was performed with at least 3 biological replicates (n = 3).

**Funding:** CW and RD were supported by the Deutsche Forschungsgemeinschaft program SPP2330 (grant numbers 464612409 to C. Wo.) and infrastructural funding Cluster of Excellence EXC 2124 Controlling Microbes to Fight Infections (grant number 390838134). HI/MSB were supported by the Novo Nordisk Foundation, NNF22OC0077593 and the Research council for independent research, FTP, 2035-00110B

**Acknowledgements:** We thank Libera Lo Presti for scientific discussions and editing of the manuscript. We thank José Penades for providing Φ11E.

## References

1. Turner NA, Sharma-Kuinkel BK, Maskarinec SA, Eichenberger EM, Shah PP, Carugati M, Holland TL, Fowler VG, Jr. 2019. Methicillin-resistant *Staphylococcus aureus*: an overview of basic and clinical research. *Nat Rev Microbiol* 17:203-218.
2. Matuszewska M, Murray GGR, Harrison EM, Holmes MA, Weinert LA. 2020. The Evolutionary Genomics of Host Specificity in *Staphylococcus aureus*. *Trends Microbiol* 28:465-477.
3. Haag AF, Fitzgerald JR, Penades JR. 2019. *Staphylococcus aureus* in Animals. *Microbiol Spectr* 7.
4. Ingmer H, Gerlach D, Wolz C. 2019. Temperate Phages of *Staphylococcus aureus*. *Microbiol Spectr* 7.
5. Xia G, Wolz C. 2014. Phages of *Staphylococcus aureus* and their impact on host evolution. *Infect Genet Evol* 21:593-601.
6. Rohmer C, Wolz C. 2021. The Role of hlb-Converting Bacteriophages in *Staphylococcus aureus* Host Adaptation. *Microb Physiol* 31:109-122.
7. Chaguza C, Smith JT, Bruce SA, Gibson R, Martin IW, Andam CP. 2022. Prophage-encoded immune evasion factors are critical for *Staphylococcus aureus* host infection, switching, and adaptation. *Cell Genom* 2.
8. Nepal R, Houtak G, Bouras G, Feizi S, Shaghayegh G, Shearwin K, Ramezanpour M, Psaltis AJ, Wormald PJ, Vreugde S. 2025. A  $\phi$ Sa3int (NM3) Prophage Domestication in *Staphylococcus aureus* Leads to Increased Virulence Through Human Immune Evasion. *MedComm* (2020) 6:e70313.
9. Goerke C, Wirtz C, Fluckiger U, Wolz C. 2006. Extensive phage dynamics in *Staphylococcus aureus* contributes to adaptation to the human host during infection. *Mol Microbiol* 61:1673-85.
10. Poupel O, Kenanian G, Touqui L, Abrial C, Msadek T, Dubrac S. 2025. Timely excision of prophage  $\Phi$ 13 is essential for the *Staphylococcus aureus* infectious process. *Infect Immun* doi:10.1128/iai.00314-25:e0031425.
11. Goerke C, Pantucek R, Holtfreter S, Schulte B, Zink M, Grumann D, Broker BM, Doskar J, Wolz C. 2009. Diversity of prophages in dominant *Staphylococcus aureus* clonal lineages. *J Bacteriol* 191:3462-8.
12. Rohmer C, Dobritz R, Tuncbilek-Dere D, Lehmann E, Gerlach D, George SE, Bae T, Nieselt K, Wolz C. 2022. Influence of *Staphylococcus aureus* Strain Background on Sa3int Phage Life Cycle Switches. *Viruses* 14.
13. Brady A, Felipe-Ruiz A, Gallego Del Sol F, Marina A, Quiles-Puchalt N, Penades JR. 2021. Molecular Basis of Lysis-Lysogeny Decisions in Gram-Positive Phages. *Annu Rev Microbiol* 75:563-581.
14. Kristensen CS, Varming AK, Leinweber HAK, Hammer K, Lo Leggio L, Ingmer H, Kilstrup M. 2021. Characterization of the genetic switch from phage  $\phi$ 13 important for *Staphylococcus aureus* colonization in humans. *Microbiologyopen* 10:e1245.
15. Rasmussen KK, Palencia A, Varming AK, El-Wali H, Boeri Erba E, Blackledge M, Hammer K, Herrmann T, Kilstrup M, Lo Leggio L, Jensen MR. 2020. Revealing the mechanism of repressor inactivation during switching of a temperate bacteriophage. *Proc Natl Acad Sci U S A* 117:20576-20585.
16. Pedersen M, Hammer K. 2008. The role of MOR and the CI operator sites on the genetic switch of the temperate bacteriophage TP901-1. *J Mol Biol* 384:577-89.
17. Feiner R, Argov T, Rabinovich L, Sigal N, Borovok I, Herskovits AA. 2015. A new perspective on lysogeny: prophages as active regulatory switches of bacteria. *Nat Rev Microbiol* 13:641-50.
18. Pfeifer E, Hunnefeld M, Popa O, Frunzke J. 2019. Impact of Xenogeneic Silencing on Phage-Host Interactions. *J Mol Biol* 431:4670-4683.
19. Cheung AL, Nishina KA, Trotonda MP, Tamber S. 2008. The SarA protein family of *Staphylococcus aureus*. *Int J Biochem Cell Biol* 40:355-61.

20. Oriol C, Cengher L, Manna AC, Mauro T, Pinel-Marie ML, Felden B, Cheung A, Rouillon A. 2021. Expanding the *Staphylococcus aureus* SarA Regulon to Small RNAs. *mSystems* 6:e0071321.
21. Fujimoto DF, Higginbotham RH, Sterba KM, Maleki SJ, Segall AM, Smeltzer MS, Hurlburt BK. 2009. *Staphylococcus aureus* SarA is a regulatory protein responsive to redox and pH that can support bacteriophage lambda integrase-mediated excision/recombination. *Mol Microbiol* 74:1445-58.
22. Schumacher MA, Hurlburt BK, Brennan RG. 2001. Crystal structures of SarA, a pleiotropic regulator of virulence genes in *S. aureus*. *Nature* 409:215-9.
23. Lehmann E, van Dalen R, Gritsch L, Slavetinsky C, Korn N, Rohmer C, Krause D, Peschel A, Weidenmaier C, Wolz C. 2024. The Capsular Polysaccharide Obstructs Wall Teichoic Acid Functions in *Staphylococcus aureus*. *J Infect Dis* 230:1253-1261.
24. Krusche J, Beck C, Lehmann E, Gerlach D, Daiber E, Mayer C, Muller J, Onallah H, Wurstle S, Wolz C, Peschel A. 2025. Characterization and host range prediction of *Staphylococcus aureus* phages through receptor-binding protein analysis. *Cell Rep* 44:115369.
25. Heinrichs JH, Bayer MG, Cheung AL. 1996. Characterization of the *sar* locus and its interaction with *agr* in *Staphylococcus aureus*. *J Bacteriol* 178:418-23.
26. Yang J, Bowring JZ, Krusche J, Lehmann E, Bejder BS, Silva SF, Bojer MS, Grunert T, Peschel A, Ingmer H. 2023. Cross-species communication via *agr* controls phage susceptibility in *Staphylococcus aureus*. *Cell Rep* 42:113154.
27. Campbell MJ, Beenken KE, Ramirez AM, Smeltzer MS. 2024. Increased production of aureolysin and staphopain A is a primary determinant of the reduced virulence of *Staphylococcus aureus sarA* mutants in osteomyelitis. *mBio* 15:e0338323.
28. Resch A, Fehrenbacher B, Eisele K, Schaller M, Gotz F. 2005. Phage release from biofilm and planktonic *Staphylococcus aureus* cells. *FEMS Microbiol Lett* 252:89-96.
29. Kuijk MM, Tusveld E, Lehmann E, van Dalen R, Lasa I, Ingmer H, Pannekoek Y, van Sorge NM. 2025. The two-component system ArIRS is essential for wall teichoic acid glycoswitching in *Staphylococcus aureus*. *mBio* 16:e0266824.
30. Rodríguez-Rubio L, Quiles-Puchalt N, Martínez B, Rodríguez A, Penadés JR, García P. 2013. The peptidoglycan hydrolase of *Staphylococcus aureus* bacteriophage 11 plays a structural role in the viral particle. *Appl Environ Microbiol* 79:6187-90.
31. Rodríguez L, Martínez B, Zhou Y, Rodríguez A, Donovan DM, García P. 2011. Lytic activity of the virion-associated peptidoglycan hydrolase HydH5 of *Staphylococcus aureus* bacteriophage vB\_SauS-philPLA88. *BMC Microbiol* 11:138.
32. Keinhorster D, Salzer A, Duque-Jaramillo A, George SE, Marincola G, Lee JC, Weidenmaier C, Wolz C. 2019. Revisiting the regulation of the capsular polysaccharide biosynthesis gene cluster in *Staphylococcus aureus*. *Mol Microbiol* 112:1083-1099.
33. Lamichhane-Khadka R, Cantore SA, Riordan JT, Delgado A, Norman AE, Duenas S, Zaman S, Horan S, Wilkinson BJ, Gustafson JE. 2009. *sarA* inactivation reduces vancomycin-intermediate and ciprofloxacin resistance expression by *Staphylococcus aureus*. *Int J Antimicrob Agents* 34:136-41.
34. Morrison JM, Anderson KL, Beenken KE, Smeltzer MS, Dunman PM. 2012. The staphylococcal accessory regulator, SarA, is an RNA-binding protein that modulates the mRNA turnover properties of late-exponential and stationary phase *Staphylococcus aureus* cells. *Front Cell Infect Microbiol* 2:26.
35. Chu LC, Arede P, Li W, Urdaneta EC, Ivanova I, McKellar SW, Wills JC, Frohlich T, von Kriegsheim A, Beckmann BM, Granneman S. 2022. The RNA-bound proteome of MRSA reveals post-transcriptional roles for helix-turn-helix DNA-binding and Rossmann-fold proteins. *Nat Commun* 13:2883.
36. Sun F, Ding Y, Ji Q, Liang Z, Deng X, Wong CC, Yi C, Zhang L, Xie S, Alvarez S, Hicks LM, Luo C, Jiang H, Lan L, He C. 2012. Protein cysteine phosphorylation of SarA/MgrA family transcriptional regulators mediates bacterial virulence and antibiotic resistance. *Proc Natl Acad Sci USA* 109:15461-6.
37. Luong TT, Lee CY. 2007. Improved single-copy integration vectors for *Staphylococcus aureus*. *J Microbiol Methods* 70:186-90.

38. Lee CY, Buranen SL, Ye ZH. 1991. Construction of single-copy integration vectors for *Staphylococcus aureus*. *Gene* 103:101-5.
39. Monk IR, Tree JJ, Howden BP, Stinear TP, Foster TJ. 2015. Complete Bypass of Restriction Systems for Major *Staphylococcus aureus* Lineages. *mBio* 6:e00308-15.
40. Miedzobrodzki J, Kaszycki P, Bialecka A, Kasprowicz A. 2002. Proteolytic activity of *Staphylococcus aureus* strains isolated from the colonized skin of patients with acute-phase atopic dermatitis. *Eur J Clin Microbiol Infect Dis* 21:269-76.
41. Sharkey LKR, Guerillot R, Walsh CJ, Turner AM, Lee JYH, Neville SL, Klatt S, Baines SL, Pidot SJ, Rossello FJ, Seemann T, McWilliam HEG, Cho E, Carter GP, Howden BP, McDevitt CA, Hachani A, Stinear TP, Monk IR. 2023. The two-component system WalkR provides an essential link between cell wall homeostasis and DNA replication in *Staphylococcus aureus*. *mBio* 14:e0226223.

## Supplementary Information

Table S1: Strains

Strain	Description	Reference/ Origin
<b><i>Escherichia coli</i></b>		
DC10B		(1)
<b><i>Staphylococcus aureus</i></b>		
8325-4 (RN0450)	NCTC8325 cured of $\Phi$ 11, $\Phi$ 12 and $\Phi$ 13	(2)
8325-4 $\Phi$ 13K	Single-lysogen, <i>kan<sup>R</sup></i>	(3)
SH1000	<i>rsbU</i> repaired derivative of 8325-4	(4) Susanne Engelmann, TU Braunschweig, Germany
RN6390 <i>sarA</i> (ALC1342)	<i>sarA::ermC</i> , <i>sarA</i> nt 586 to 1107 replaced by <i>ermC</i> gene,	(5)
SH1000 <i>sarA</i>	<i>sarA::ermC</i> , via transduction	This study
SH1000 <i>sarA psarA</i>	<i>sarA::ermC</i> , complemented with integrative vector carrying <i>sarA</i> locus ( <i>psarA</i> )	This study
SH1000 $\Phi$ 13K	Single-lysogen, <i>kan<sup>R</sup></i>	(3)
SH1000 $\Phi$ 13K <i>sarA</i>	<i>sarA::ermC</i> , single-lysogen, <i>kan<sup>R</sup></i>	This study
SH1000 $\Phi$ 13K <i>sarA psarA</i>	<i>sarA::ermC</i> , single-lysogen, complemented with <i>psarA</i> , <i>kan<sup>R</sup></i>	This study
SH1000 $\Phi$ 13K- <i>rep</i>	Single-lysogen, carrying replication deficient phage mutant (3), <i>kan<sup>R</sup></i>	This study
SH1000 $\Phi$ 13K- <i>rep sarA</i>	<i>sarA::ermC</i> , single-lysogen, carrying replication deficient phage mutant, <i>kan<sup>R</sup></i>	This study
SH1000 $\Phi$ 11E	Single-lysogen, <i>erm<sup>R</sup></i>	This study
SH1000 $\Phi$ 11E <i>sarA</i>	<i>sarA::kan</i> , <i>erm<sup>R</sup></i>	This study
Newman-c	Phage-cured	(6)
Newman-c <i>sarA</i>	<i>sarA::ermC</i>	This study
Newman-c <i>sarA psarA</i>	<i>sarA::ermC</i> , complemented with integrative vector carrying <i>sarA</i> locus ( <i>psarA</i> )	This study
RN6911	<i>agr::tetM</i>	(7)
SH1000 <i>agr</i>	<i>agr::tetM</i> , via transduction	This study
SH1000 $\Phi$ 13K <i>agr</i>	<i>agr::tetM</i> , <i>kan<sup>R</sup></i>	This study
SH1000 $\Phi$ 13K-TSS23	Non-infectious phage mutant	This study
SH1000 $\Phi$ 13K-TSS23 <i>sarA</i>	Non-infectious phage mutant, <i>sarA::ermC</i>	This study
8325-4 $\Phi$ 11E	Single-lysogen, <i>erm<sup>R</sup></i>	(8) Hanne Ingmer, Copenhagen, Denmark
LS1		(9) Löffler, Münster, Germany
RN4220	restriction deficient derivate of 8325-4, rK-mK+	(10)
CYL316	RN4220 (pYL112 $\Delta$ 19), L54 int gene	(11)

**Table S2:** Phages

Phage Lysates	Resistance cassette	Propagation/ Indicator strain	Reference
Φ13K	<i>kan<sup>R</sup></i>	LS1	
Φ13K- <i>int</i>	<i>kan<sup>R</sup></i>	LS1	(12)
Φ11		RN4220	
Φ11E	<i>erm<sup>R</sup></i>	RN4220	(8)

**Table S3:** Oligonucleotides

Oligonucleotide	Sequence	Used for
SarA DIGfor	CAATGATTGCTTTGAGTTGT	Control PCR <i>sarA</i>
SarA DIGrev	CGTTTATTTACTCGACTCAA	Control PCR <i>sarA</i>
Sa5intfor	AAAGATGCCAAACTAGCTG	Control PCR Φ11
Sa5intrev	CTTGTGGTTTTGTTCTGG	Control PCR Φ11
pCG921gibfor	tcgagctcggtagccgggTAACTTTT AGCTTATCATTTTAACTTGT	Cloning pCG921
pCG921gibrev	tgcaggtcgactctagagTATGTGA TATATAAACCTAGGGCA	Cloning pCG921
pLL39newfor	GTAATGGGCCCAATCACTAGTG	Control PCR pCG921
pLL39rev2016	ACGCCAGAAGATACAAAGCA	Control PCR pCG921
pCG921insidecontrolfor	GGGCAAATGTATCGAGCAAGA	Control PCR pCG921
Scv2.1	TGTGCCATGATAACAGCACG	Control PCR pCG921
Scv4	ACCCAGTTTGTAATTCCAGGAG	Control PCR pCG921
Scv8	GCACATAATTGCTCACAGCCA	Control PCR pCG921
Scv1	GCAACACCACATAATGGTTCAC	Control PCR pCG921
pcllyfpbibfor	GCTGGCGGCCGCTGCATGCAAG TTCACGTATCATGAACT	Cloning pCG748
pcllyfpbibrev	CATAAATAATCATCCTCCTAAGGT TTGATAACTTCATAATAAAGCTTGT	Cloning pCG748
pCG789gibfor	gagctggcggccgctgcatgTTTTGTATTGAC TTGATTCAAAACAAGGT	Cloning pCG789
pCG789gibrev	cataaataatcatcctcctaagCAAGTTCACG TATCATGAACT	Cloning pCG789
pumuCYFPgibfor	CGGCCGCTGCATGGCATGCCCAA ACCTCCTAATCATTA	Cloning pCG762
pumuCYFPgibrev	AAATAATCATCCTCCTAAGGTCGA CTACTTGAATCTTATT	Cloning pCG762
pcllyfpcontrolrev	TGACAAGTGTGGCCATGGA	Control PCR
pcllyfpoutsidecontrolfor	GGACAGGTATCCGGTAAGCG	Control PCR
pcapmutseqfor	TTTGTGATGCTCGTCAGGGG	Control PCR
pCG925gibfor	aattctgcagcccgggCTATGACTATT GTATTTGCTATATTGCT	Cloning pCG925
pCG925gibrev	gccgctctagaactagtgGCACATCACTC	Cloning pCG925

Results Part III

	CTTGTCGAC	
pCG910SDMfor	cggccGCTGTGTAGCAAAACATTTA TATTC	Cloning pCG925
pCG910SDMrev	cggcgAAAAACAATATGTAGCATCA AAATTAG	Cloning pCG925
pCG925outsidecontrolfor	GCGGAGGTAAGTGAGTGA	Cloning pCG925
pCG925outsidecontrolrev	GGATGACCACATCGCTTCA	Cloning pCG925
pCG849i1gibfor	tcgataagcttgatcgTAAACAAAAA CGCCTACAAGTGT	Cloning pCG849
pCG849i1gibrev	TTAACTTTATACAAAATTGGCAAA AAATAATAAGGT	Cloning pCG849
pCG849i2gibfor	TGCCAATTTTGTATAAAGTTAATT ATAAAGCCGAAACCT	Cloning pCG849
pCG849i2gibrev	GATCCCCCGGGCTGCAGGGTTC TTACCATTTTCTCTATTTTTGT	Cloning pCG849
pIMAYcontrolfor	CCAGCCCCCTCACTACAT	Control PCR pCG849
pIMAYcontrolrev	ATCACCCGACGCACTTTG	Control PCR pCG849
pCG849outsidectlfor	CAACTGGTGCTGGCATAGGA	Control PCR <i>int</i>
pCG849outsidectlrev	TCGATCATGTCCAGCACCAC	Control PCR <i>int</i>
pCG844insidecontrolfor	TTTTGGCTTGTACCGTTCAC	Control PCR <i>int</i>
circlefor	TTTTATTTTATATGGGGTATTATTGA	qPCR ( $\Phi$ 13 <i>attP</i> )
circlorev	GTGTATTCTCATTTGTTAGAAGAAAA	qPCR ( $\Phi$ 13 <i>attP</i> )
Sa5intStafor	ACAAACGAAAAATGAAGCGT	qPCR ( $\Phi$ 11)
Sa5intStarev	AGTCTAGTTAGCTGACGAGA	qPCR ( $\Phi$ 11)
recAF1	GCTCAAGCATTAGGCGTAGAT	qPCR ( <i>recA</i> )
recA661	ATTTAATGCACGTCCACCTGG	qPCR ( <i>recA</i> )
h1b258	ATTAGTTGGTGCACCTACTG	qPCR ( <i>h1b</i> )
h1b675	GCTATCATTATCGAATCCAC	qPCR ( <i>h1b</i> )
tarMqPCRfor	CAAGGTAAAATGGATCGAAGAAC	RT-qPCR ( <i>tarM</i> )
tarMqPCRrev	GTAGGCAATATATGTACCAGTC	RT-qPCR ( <i>tarM</i> )
tarSqPCRfor	TAGTGCGTATGTTTCACCTG	RT-qPCR ( <i>tarS</i> )
tarSqPCRrev	AAGTCTCCTAGAGCATTAATCC	RT-qPCR ( <i>tarS</i> )
umuCqPCRfor	TCTAAGATTGCATTGCGTTA	RT-qPCR ( <i>umuC</i> )
umuCqPCRrev	CATATTAGAACCAATGCCCA	RT-qPCR ( <i>umuC</i> )
SAOUHSC02196for2	CACGAATCAAACGGCATT	RT-qPCR ( <i>terminase</i> )
SAOHHS02196rev2	ACAACAATCGAATCAATGGC	RT-qPCR ( <i>terminase</i> )
SAOUHSC_02200qPCRfor	GGCACGACTAGCAATAAA	RT-qPCR ( <i>ltr</i> )
SAOUHSC_02200qPCRrev	GTCTCTGCCTATATCAAGAAT	RT-qPCR ( <i>ltr</i> )
SAOUHSC_02191for	TTTGCATCTTCGATTGCTTC	RT-qPCR ( <i>mcp</i> )
SAOUHSC_02191DIGrev	TACGACAATCAGAAGTTGCA	RT-qPCR ( <i>mcp</i> )
Gyr574	AGTCTTGACAAATGCGTTTACA	RT-qPCR ( <i>gyr</i> )
Gyr297	TTAGTGTGGGAAATTGTGATAAT	RT-qPCR ( <i>gyr</i> )
SAOUHSC02234DIGfor	TAATACGACTCACTATAGGGAGAT GCAAATTGTACTGAGTGC	RT-qPCR ( <i>mor</i> )
SAOUHSC02234DIGrev	ATGTGTTACGACTACTCACG	RT-qPCR ( <i>mor</i> )
clqPCRfor	AGAACGTCAAGATGAAACGA	RT-qPCR ( <i>cl</i> )
clqPCRrev	AATTCTTCTCCTATGCCAGC	RT-qPCR ( <i>cl</i> )

**Table S4:** Plasmids

<b>Plasmid</b>	<b>Description</b>	<b>Resistance cassette</b>	<b>Reference/ Origin</b>
pLL39	Integrative vector, integrates into <i>geh</i>	<i>tet</i>	(13)
pIMAY-Z	Mutagenesis vector	<i>cm</i>	(14)
pIMAY	Mutagenesis vector	<i>cm</i>	(1)
pCG921	Complementation vector <i>psarA</i> , pLL39 containing <i>sarA</i> locus	<i>tet</i>	This study
pCG725	$P_{cap}$ - <i>yfp</i>	<i>cm</i>	(15)
pCG733	$P_{cap}$ - <i>cfp</i>	<i>cm</i>	(15)
pCG762	Promoter construct $P_{umuC}$ - <i>yfp</i>	<i>cm</i>	This study
pCG748	Promoter construct $P_{ci}$ - <i>yfp</i>	<i>cm</i>	This study
pCG789	Promoter construct $P_{mor}$ - <i>yfp</i>	<i>cm</i>	This study
pCG925	Mutagenesis vector for p23 TATA Box mutation (pIMAY-Z), non-infectious phage mutant	<i>cm</i>	This study
pCG849	Mutagenesis vector for <i>int</i> deletion (pIMAY)	<i>cm</i>	This study
pCG32	<i>Int</i> complementation	<i>cm</i>	(16)

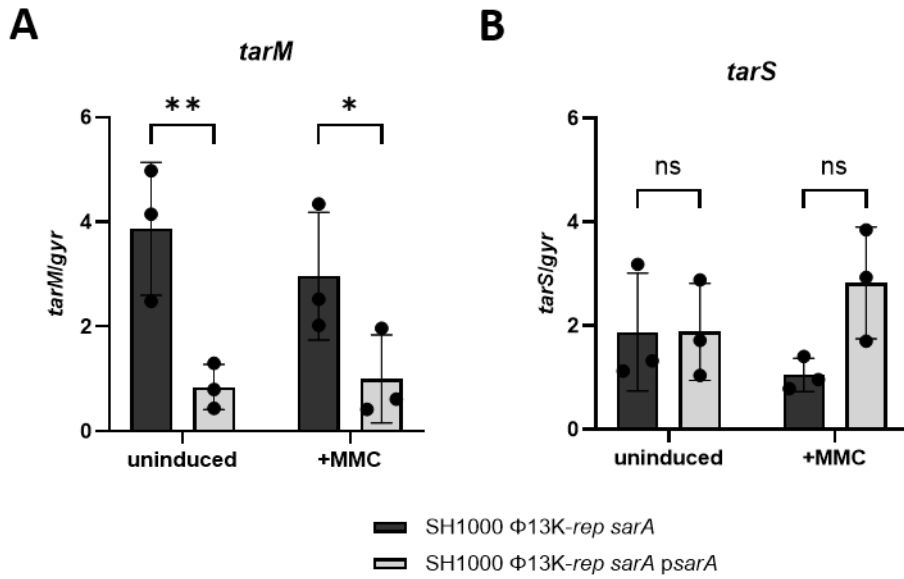


**Figure S1: *tarM* and *tarS* expression in *sarA*-complemented background.** Gene expression analysis of *tarM* ( $\alpha$ -1,4 GlcNAc) and *tarS* ( $\beta$ -1,4 GlcNAc) under uninduced and induced (+MMC) conditions. Single-lysogenic SH1000 *sarA* (*sarA::ermC* deletion) and SH1000 *sarA psarA* (*sarA* complementation), containing the replication-deficient  $\Phi$ 13K-*rep* mutant, were grown to exponential growth phase, followed by prophage induction with subinhibitory mitomycin C (MMC), and incubation for 60 min. RNA was isolated, *tarM* and *tarS* transcripts were quantified by qRT-PCR and normalized to *gyr* expression.

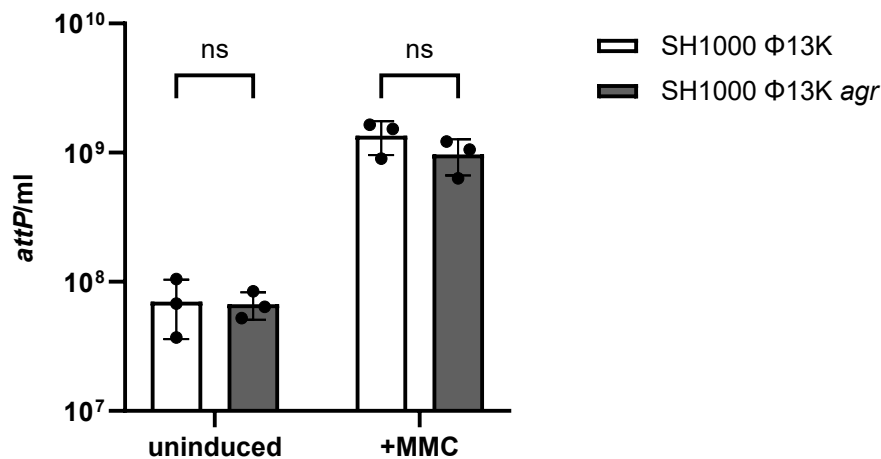


**Figure S2:  $\Phi$ 13K phage replication is not *agr* dependent.** Phage replication in SH1000  $\Phi$ 13K and SH1000  $\Phi$ 13K *agr* (*agr::tetM* deletion) under uninduced and induced (+MMC) conditions. Single-lysogenic strains were induced with subinhibitory mitomycin C (MMC) in exponential growth phase and incubated for further 60 min. Phage lysates were harvested by centrifugation and following sterile filtration of the supernatant. Phage numbers were determined by qPCR on the circularization site of the phage genome (*attP*) and presented per ml. Data shown are mean  $\pm$  SD ( $n = 3$ ). Statistical analysis was determined by 2way ANOVA test (ns > 0.05).

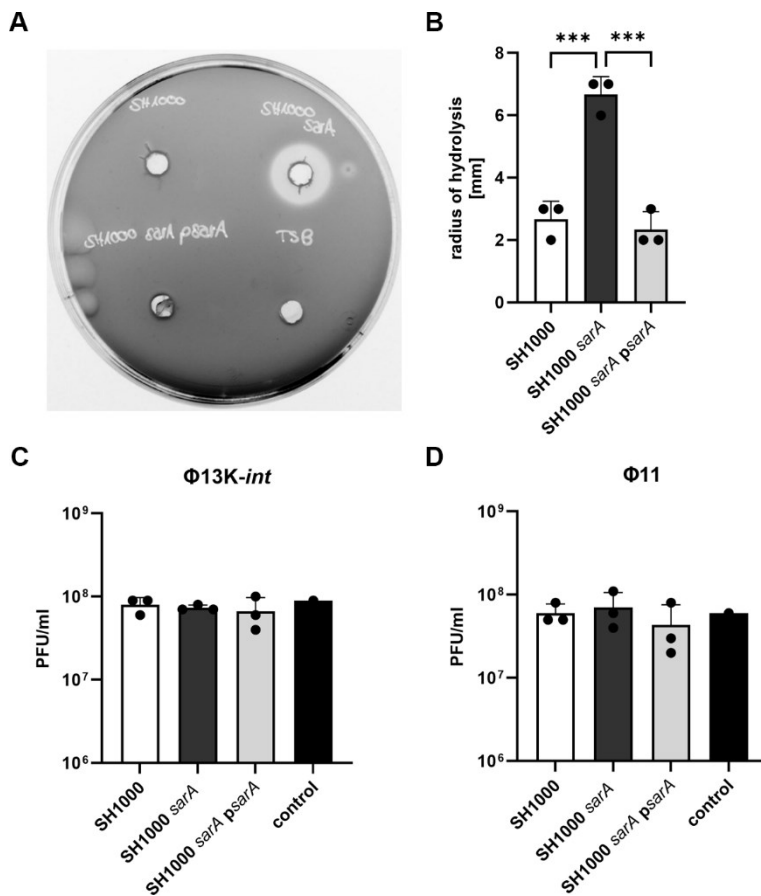


**Figure S3: Protease-dependent phage decay is not *sarA* dependent.** (A,B) Proteolysis activity of SH1000 (wild type), SH1000 *sarA* (*sarA::ermC* deletion) and SH1000 *sarA psarA* (*sarA* complemented). Overnight cultures were diluted to OD<sub>600</sub> of 1 and 25  $\mu$ l of bacterial suspensions were filled into wells cut into skim milk agar plates. (A) Pictures were taken after 24 h of incubation at 37°C showing proteolysis haloes. (B) Proteolysis radii were measured after 48 h of incubation at 37°C. Data shown are mean  $\pm$  SD (n = 3). Statistical significance was determined by ordinary one-way ANOVA. (C,D) Phage numbers after incubation in spent media of SH1000, SH1000 *sarA* and SH1000 *sarA psarA* 1x10<sup>8</sup> phages of (C)  $\Phi$ 13K-*int* or (D)  $\Phi$ 11 were incubated for 3 h in the supernatant of 1x10<sup>8</sup> bacteria, grown to OD<sub>600</sub> = 0.5. Titers of phage lysates were determined by plaque assay on bacterial lawn of LS1 ( $\Phi$ 13K-*int*) or RN4220 ( $\Phi$ 11) as indicator strains. Phages incubated in fresh TSB were included as control. Data shown are mean  $\pm$  SD (n = 3). Statistical significance was determined by ordinary one-way ANOVA (ns > 0.05).

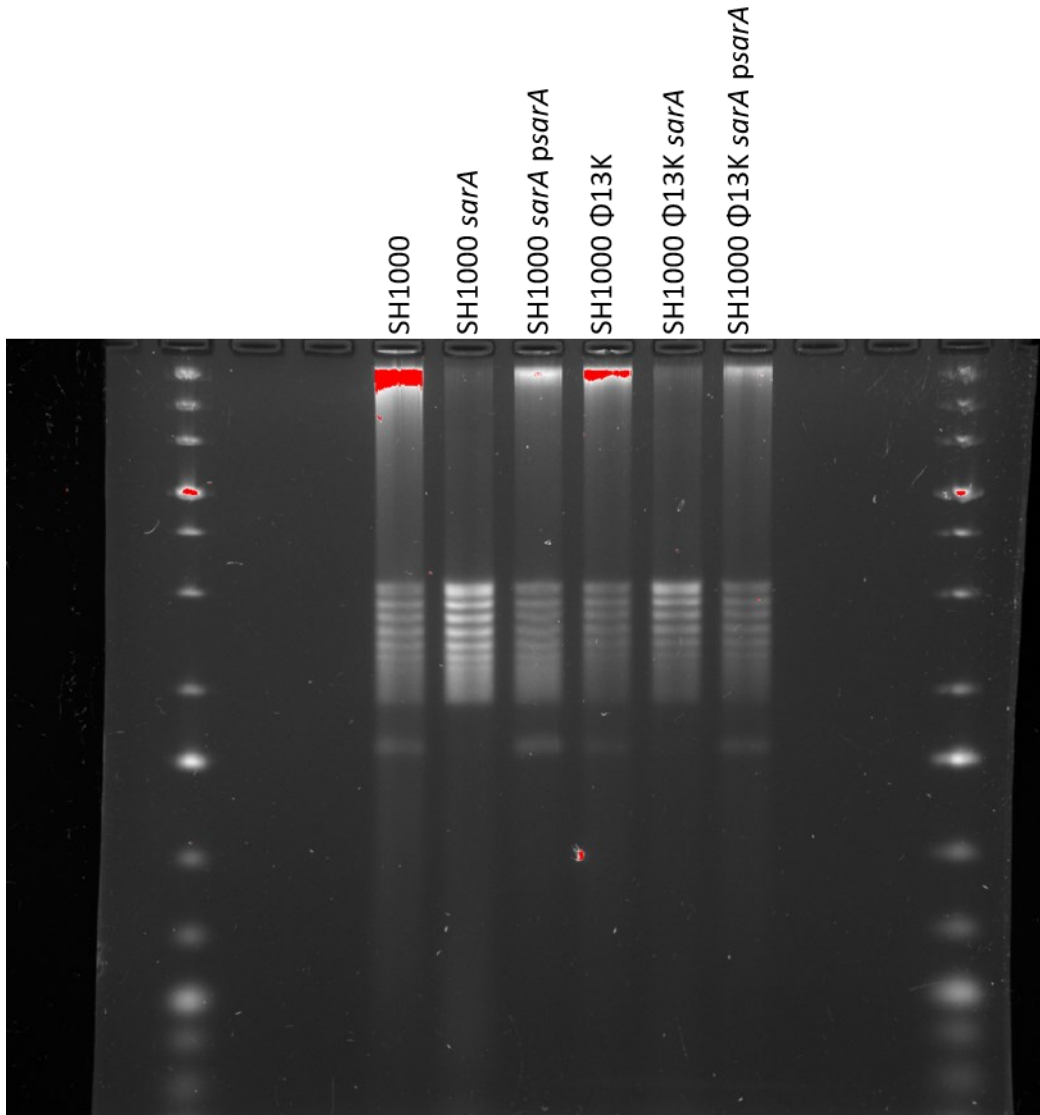


**Figure S4: No apparent effect of *sarA* on DNA supercoiling.** Plasmid (pC194) preparations from SH1000, *sarA* derivatives, and  $\Phi$ 13K lysogens were separated by chloroquine agarose gel electrophoresis. GeneRuler 1 kb Plus DNA Ladder (Thermo Scientific) was used in first and last lane.

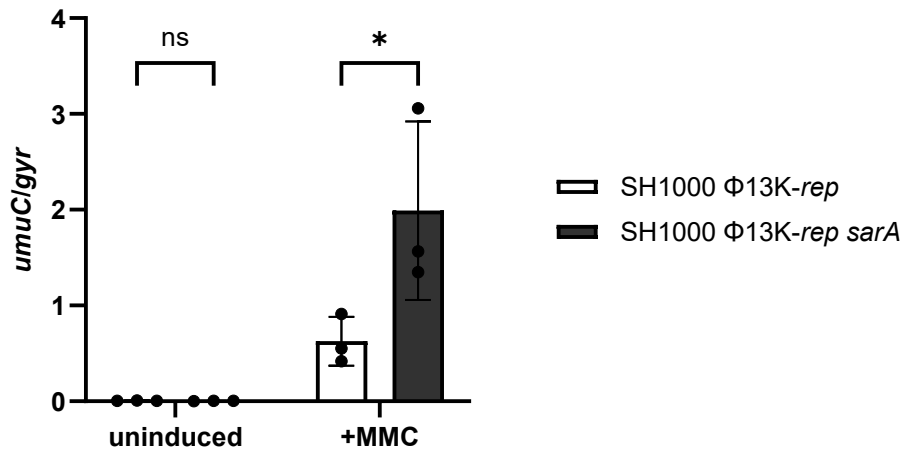


**Figure S5: Higher SOS-response activation in *sarA* deleted background, determined by *umuC* gene expression.** Gene expression analysis of *umuC* under uninduced and induced (+MMC) conditions. Single-lysogenic SH1000 and SH1000 *sarA* (*sarA::ermC* deletion), containing replication deficient phage mutant (*rep*), were grown to exponential growth phase, induced with subinhibitory mitomycin C (MMC) and incubated for 60 min. RNA was isolated, *umuC* transcripts were measured by qRT-PCR and normalized to *gyr*. Data shown are mean  $\pm$  SD (n = 3). Statistical analysis was determined by 2way ANOVA test (\*p-value < 0.05, ns > 0.05).

**References (Supplementary Information)**

1. Monk IR, Shah IM, Xu M, Tan MW, Foster TJ. 2012. Transforming the untransformable: application of direct transformation to manipulate genetically *Staphylococcus aureus* and *Staphylococcus epidermidis*. *mBio* 3:e00277-11.
2. Novick R. 1967. Properties of a cryptic high-frequency transducing phage in *Staphylococcus aureus*. *Virology* 33:155-66.
3. Rohmer C, Dobritz R, Tuncbilek-Dere D, Lehmann E, Gerlach D, George SE, Bae T, Nieselt K, Wolz C. 2022. Influence of *Staphylococcus aureus* Strain Background on Sa3int Phage Life Cycle Switches. *Viruses* 14:2471.
4. Horsburgh MJ, Aish JL, White IJ, Shaw L, Lithgow JK, Foster SJ. 2002. sigmaB modulates virulence determinant expression and stress resistance: characterization of a functional rsbU strain derived from *Staphylococcus aureus* 8325-4. *J Bacteriol* 184:5457-67.
5. Cheung AL, Schmidt K, Bateman B, Manna AC. 2001. SarS, a SarA homolog repressible by agr, is an activator of protein A synthesis in *Staphylococcus aureus*. *Infect Immun* 69:2448-55.
6. Bae T, Baba T, Hiramatsu K, Schneewind O. 2006. Prophages of *Staphylococcus aureus* Newman and their contribution to virulence. *Mol Microbiol* 62:1035-47.
7. Novick RP, Ross HF, Projan SJ, Kornblum J, Kreiswirth B, Moghazeh S. 1993. Synthesis of staphylococcal virulence factors is controlled by a regulatory RNA molecule. *Embo j* 12:3967-75.
8. Quiles-Puchalt N, Martínez-Rubio R, Ram G, Lasa I, Penadés JR. 2014. Unravelling bacteriophage  $\phi$ 11 requirements for packaging and transfer of mobile genetic elements in *Staphylococcus aureus*. *Mol Microbiol* 91:423-37.
9. Bremell T, Abdelnour A, Tarkowski A. 1992. Histopathological and serological progression of experimental *Staphylococcus aureus* arthritis. *Infect Immun* 60:2976-85.
10. Kreiswirth BN, Lofdahl S, Betley MJ, O'Reilly M, Schlievert PM, Bergdoll MS, Novick RP. 1983. The toxic shock syndrome exotoxin structural gene is not detectably transmitted by a prophage. *Nature* 305:709-12.
11. Lee CY, Buranen SL, Ye ZH. 1991. Construction of single-copy integration vectors for *Staphylococcus aureus*. *Gene* 103:101-5.
12. Lehmann E, van Dalen R, Gritsch L, Slavetinsky C, Korn N, Rohmer C, Krause D, Peschel A, Weidenmaier C, Wolz C. 2024. The Capsular Polysaccharide Obstructs Wall Teichoic Acid Functions in *Staphylococcus aureus*. *J Infect Dis* 230:1253-1261.
13. Luong TT, Lee CY. 2007. Improved single-copy integration vectors for *Staphylococcus aureus*. *J Microbiol Methods* 70:186-90.
14. Monk IR, Tree JJ, Howden BP, Stinear TP, Foster TJ. 2015. Complete Bypass of Restriction Systems for Major *Staphylococcus aureus* Lineages. *mBio* 6:e00308-15.
15. Keinhörster D, Salzer A, Duque-Jaramillo A, George SE, Marincola G, Lee JC, Weidenmaier C, Wolz C. 2019. Revisiting the regulation of the capsular polysaccharide biosynthesis gene cluster in *Staphylococcus aureus*. *Mol Microbiol* 112:1083-1099.
16. Mainiero M, Goerke C, Geiger T, Gonser C, Herbert S, Wolz C. 2010. Differential target gene activation by the *Staphylococcus aureus* two-component system saeRS. *J Bacteriol* 192:613-23.

## General Discussion

Parts of this discussion have been published in the following articles. The submitted manuscript has been uploaded to the preprint server bioRxiv and might differ from the final published article. Publications can be accessed under the following links:

**'Influence of *Staphylococcus aureus* strain background on Sa3int phage life cycle switches'**, research article, <https://doi.org/10.3390/v14112471>

**'The phage  $\Phi$ 13-encoded transcriptional regulator Ltr controls phage assembly in *Staphylococcus aureus*'**, submitted manuscript, <https://doi.org/10.1101/2025.11.28.691083>

**'Multiple effects of the bacterial DNA-binding protein SarA on the life cycle of *Staphylococcus aureus* phages'**, research article, <https://doi.org/10.1128/jb.00279-25>

## Phage Replication as Driver of Strain-Specific Sa3int Transfer Frequencies

Sa3int phages, which integrate into the *hlyB* gene, represent the most prevalent group of temperate phages in *Staphylococcus aureus* [4, 91]. These phages function as regulatory switches, as their integration disrupts *hlyB* expression while enabling their host to produce phage-encoded highly human-specific virulence factors encoded on the immune evasion cluster. Excision of the prophage from the bacterial genome restores *hlyB* expression [82]. Through this reversible modulation, Sa3int phages play a central role in the adaptation of *S. aureus* to the human host [73]. The emergence of HlyB-positive and HlyB-negative subpopulations during infection highlights the importance of dynamic Sa3int phage integration and excision [64, 89]. Thus, *S. aureus* requires tight regulation of Sa3int phage life cycles to ensure a beneficial phage-host co-existence. However, the molecular processes modulating the cross-talk between phages and their host remain poorly understood.

In Part I of this thesis, we investigated Sa3int phage dynamics in different *S. aureus* strain backgrounds, to get further insights into host-dependent regulatory mechanisms affecting phage replication. We observed clear strain-specific differences in  $\Phi$ 13 and  $\Phi$ N315 transfer, which we discovered to be dependent on the recipient strain.

To identify the factors influencing transfer frequencies, we analyzed the different steps of the phage life cycle. No significant strain-dependent differences were detected in phage adsorption, prophage integration, or prophage excision. However, phage replication was significantly increased in strains exhibiting high transfer frequencies, suggesting that efficient replication is the critical step for strain-specific variations. Such host-dependent effects on phage dynamics have been reported previously. For instance, the PVL-encoding phage

Sa2mw displays strain-specific differences in induction and replication patterns, and also Stab20 infection efficiency varies across different strain backgrounds [70, 92].

To explore the molecular processes resulting in the transfer-frequency differences, we performed comparative RNA-seq analysis of  $\Phi$ 13 gene transcription in a high- and a low-transfer strain. We observed significant transcriptional differences upon induction of the lytic life cycle.

$\Phi$ 13, originally isolated from *S. aureus* NCTC8325, serves as representative of the Sa3int group and was extensively studied. Recent work has characterized its genetic switch region, which comprises *cl*, encoding for the repressor of lytic genes, and *mor* (modulator of repression) [93]. Unlike Cro in  $\lambda$ -like switch systems, Mor acts through protein-protein interactions with CI rather than transcriptional regulation [94]. However, genes within the genetic switch region, controlling the transition from lysogenic to lytic life cycle, were not differentially expressed. This finding indicates that the activation of the lytic life cycle is strictly RecA-dependent and does not require additional host-specific factors. Supporting this hypothesis, promoter activity of the genetic switch has been previously analyzed in *B. subtilis*, confirming that no *S. aureus*-specific factors are required for lytic activation of  $\Phi$ 13 [93].

Moreover, our transcriptional analysis revealed that genes within the regulatory module of  $\Phi$ 13, as well as a cluster of late genes required for phage assembly were expressed at higher levels in the high-transfer strain. These findings support the hypothesis that enhanced phage replication and not the life cycle switch causes host-dependent differences in  $\Phi$ 13 transfer frequencies. The regulation of late genes, and the mechanisms of their strain-dependent expression, were investigated in Part II of this thesis.

### **Ltr Mediates the Activation of Late Gene Expression in $\Phi$ 13**

Within the differentially expressed late gene modules, several transcriptional start sites (TSSs) were predicted, indicating the presence of multiple promoters that are individually regulated during the lytic life cycle. Among these, the TSS23 was of particular interest due to its localization upstream of late phage genes that were strongly upregulated in the high-transfer strain. Thus, characterizing the regulatory processes of TSS23 could improve our understanding of late gene activation in  $\Phi$ 13 and the host-dependent mechanisms involved in this process. Therefore, further analysis of the TSS23 region was performed in Part II of this work.

We identified the promoter region upstream of TSS23 and analyzed the activity of the corresponding  $P_{23}$  promoter. As phage gene regulation is known to be under tight temporal control to ensure efficient phage genome replication before particle assembly and host cell lysis, it is notable that the identified  $P_{23}$  promoter region separates early lytic genes from late

lytic genes. We identified a conserved -10 TATA-box motif within the  $P_{23}$  promoter, whereas no conserved -35 consensus element was found. A similar promoter architecture has been described for the late genes of *S. aureus* phage K, in which early genes contain both -10 and -35 elements but late genes lack a -35 motif, indicating distinct regulatory processes for early and late gene transcription [95].

In several phages infecting Gram-negative and Gram-positive bacteria, multiple conserved strategies for late gene activation have been described. For example, in model phage  $\lambda$ , the Q anti-termination protein converts the RNA polymerase into a termination-resistant form, whereas *E. coli* phage T7 encodes its own specific RNA polymerase to initiate late transcription [57, 58]. In *S. aureus* phage  $\Phi 11$ , RinA has been demonstrated to serve as an activator of late gene expression [59]. Four additional families of late transcriptional regulators (Ltrs) have since been described in phages infecting Gram-positive bacteria, despite minimal or no sequence homology [60]. These Ltrs share their genomic position upstream of late genes and their essential function in activating late gene transcription.

Through sequence analysis, we identified SAOUHSC\_02200 as  $\Phi 13$ -encoded Ltr, exhibiting 100% homology to the Ltr IV family regulator of staphylococcal phage PVL (hypothetical protein PVL\_60). Previous work has shown ~70% similarity between  $\Phi 13$  and phage PVL [56]. Our work emphasized that the conserved regions between these phages are primarily present in regulatory regions, suggesting shared regulatory strategies.

To confirm the essential role of Ltr in the  $\Phi 13$  lytic cycle, we generated an *ltr*-deficient phage mutant. No mature phage particles were produced by this mutant. However, phage genome replication was unaffected, as demonstrated under uninduced conditions, where phage genomes are released through phage-independent bacterial lysis. A similar phenotype has been reported for phage  $\Phi 10403S$  infecting *Listeria monocytogenes*, where host-dependent repression of the late regulator LlgA blocks late gene transcription, while phage genome excision and replication proceeds. In  $\Phi 10403S$ , genome replication is thought to facilitate reintegration at later infection stages. The excision of  $\Phi 10403S$  from the bacterial chromosome restores *comK* expression, which is required for phagosomal escape of *L. monocytogenes*, representing a regulatory switch similar to Sa3int phages. Post-transcriptional inhibition of LlgA by host factors induces a pseudo-lysogenic state in response to environmental changes [96]. One could hypothesize that host-dependent modulation of *ltr* expression in  $\Phi 13$  could induce a similar state, consistent with previous reports of active lysogeny in Sa3int phages [88, 97].

In accordance with descriptions of late transcriptional regulators, the expression of late genes downstream of  $P_{23}$  was significantly reduced in the *ltr*-deficient background, confirming that Ltr is required for activation of structural, lysis, and virulence-associated late transcription. However, the TSS analysis in Part I also revealed additional TSSs downstream of TSS23,

suggesting more complex regulatory processes. Some of these TSSs were unique to a specific strain background, indicating host-dependent regulation of late gene transcription. Supporting this, Northern blot analysis detected shorter transcripts from co-transcription of the genes encoding the large terminase subunit (*terL*) and the major capsid protein (*mcp*). Co-transcription of lysis genes (*amidase*, *holin*) with immune evasion cluster genes has previously been described, further suggesting the involvement of additional regulators [85, 98].

Nevertheless, our findings identified the phage-encoded Ltr as key regulator of late gene transcription in the Sa3int phage  $\Phi$ 13, while also highlighting the complexity of the regulation of late lytic genes.

### **Host Factors Influence Phage Dynamics**

Virulence genes and late phage genes are often located in close proximity, and have been shown to be co-transcribed and upregulated following prophage induction. This has been demonstrated in *S. aureus* for enterotoxin A, PVL, and staphylokinase [70, 85, 98]. Host regulators such as SigB and Agr are involved in controlling the transcription of phage-encoded virulence genes [99]. However, their influence on other phage genes and on the phage life cycle remains largely uninvestigated.

### **SigB-Dependent Regulation of Late Gene Expression**

Strain-specific differences between SH1000 and its SigB-deficient derivative 8325-4 in  $P_{23}$  activity and *ltr* expression suggested a potential role of SigB in late gene regulation. Indeed, 8325-4 displayed the lowest  $P_{23}$  activity and *ltr* expression. Since SigB was proposed to be important for the fine-tuning of virulence in response to environmental changes [39], regulation of Sa3int phages that act as regulatory switches for virulence factors does not seem unlikely. Deletion of the SigB operon ( $\Delta mazEFrsbUVWsigB$ ) in single-lysogenic strains resulted in significantly decreased phage production and reduced  $P_{23}$  activity following lytic induction.

Involvement of sigma factors and RNA polymerases (RNAPs) in temporal phage gene regulation enabling preferential transcription of phage over host genes has been described in several phage-host interactions. For example, the RpoC RNA polymerase of USA300 MRSA specifically recognizes late promoters in phage K, and mutations in this RNAP confer phage resistance [95]. In phage T4, AsiA binds the *E. coli*  $\sigma$ 70 factor, preventing interactions with the host promoter regions [100]. Further, the anti-sigma factor of *S. aureus* phage G1 interacts with SigA to redirect the RNAP activity towards phage transcription [101]. These findings in other phages support a possible role for SigB in enhancing  $P_{23}$  activity and late gene expression, including phage-encoded virulence genes. Notably, SigB transcription is upregulated following *S. aureus* infection with kayvirus or lysogenization with  $\Phi$ 11 or  $\Phi$ 80 $\alpha$ ,

further suggesting a connection between phage activity and SigB signaling [102, 103]. This aspect requires further investigation in future studies.

Although *ltr* expression has been described to depend on the activation of the early lytic genes [60], there is evidence for post-transcriptional regulations of late transcriptional regulators. In *L. monocytogenes*, repression of the  $\Phi$ 10403S late regulator LlgA in the intracellular niche occurs post-transcriptionally through host factors [96]. In *Lactococcus lactis* phage TP901-1, late promoter activation is delayed in comparison to the expression of the late regulator Alt, indicating additional regulatory layers [104]. The timing of *ltr* expression, which peaks in late-exponential to early-stationary phase, correlates with the observed  $P_{23}$  activation, but also with the phase of SigB activation [38, 105]. Thus, a growth phase-dependent regulation of Ltr activity mediated by SigB could serve as a sensing mechanism of bacterial density and growth phase. Similar strategies have been described for other phages, to modulate phage dynamics in highly dense bacterial host environments. For instance, SPbeta phages produce a secreted signal peptide to guide lysis-lysogeny decisions during *Bacillus subtilis* infection [106]. In *Clostridium difficile*, phage  $\Phi$ CDHM1 encodes *agr*-like quorum-sensing homologs that could interfere with or use the quorum sensing system to enable phage replication [107].

Despite the observed SigB-dependent effects on *ltr*-expression and  $P_{23}$  activity, no SigB consensus sequences were identified within the corresponding promoter regions. SigB is known to regulate some target genes indirectly through downstream effectors. SpoVG has been proposed as mediator of SigB-dependent transcription for genes lacking consensus motifs. Similar to the deletion of the *sigB* operon, the deletion of *spoVG* resulted in significantly decreased phage production and  $P_{23}$  activity. SpoVG functions as a transcriptional regulator and modulates primarily virulence factors [39, 43], partly through the repression of the Agr quorum-sensing system [108]. However, phage replication in an *agr*-deleted background was unaffected (Results Part III), indicating that the decreased replication we observed in the *spoVG* mutant is not Agr-dependent.

Moreover, *spoVG* expression is repressed by the phage-encoded small RNA SprX that exhibits decreasing transcription in the stationary phase [109]. In  $\Phi$ 13, *sprX* is located within the immune evasion cluster downstream of *sak*, which is repressed by SigB [39]. Activation of SigB in late-exponential growth could therefore repress *sprX* transcription, which subsequently leads to derepression of *spoVG*, and enhance late phage gene expression. The location of *sprX* at the distal end of the lytic phage modules could provide a feedback to inhibit SpoVG activity and stop late transcription and the lytic cycle.

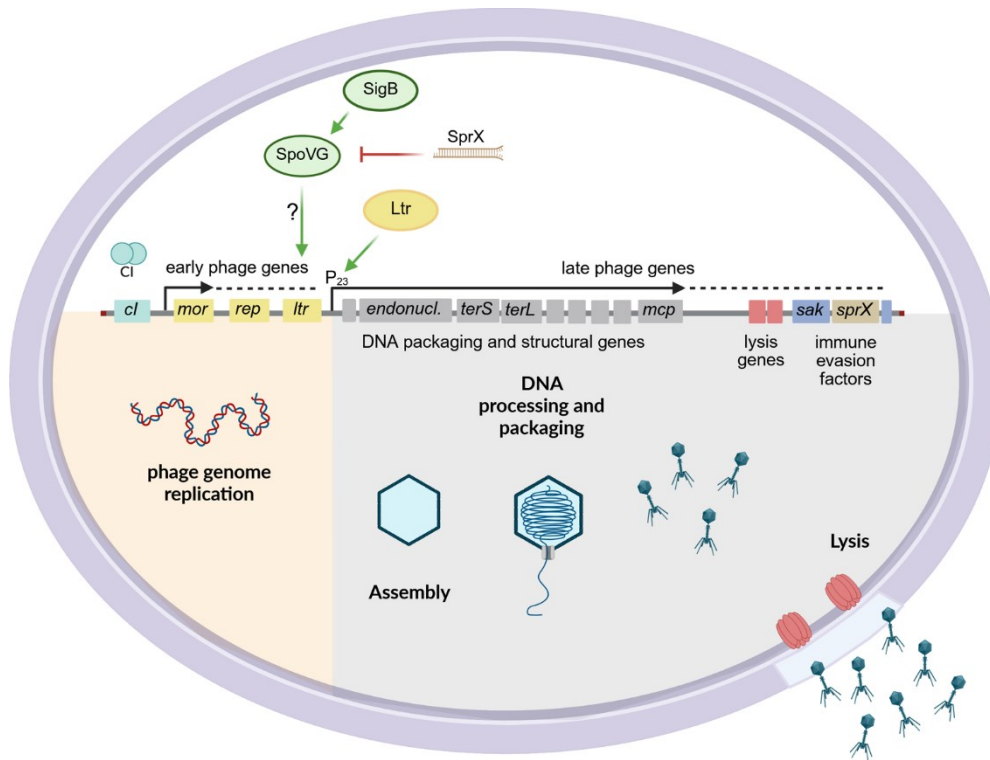


**Figure 3. Temporal control of phage gene expression within the bacterial host.** Genetic organization of the bacteriophage  $\Phi 13$ . Release of CI from the *mor* promoter results in derepression of the lytic cycle and expression of early lytic genes, including the replication factor (*rep*) and late transcriptional regulator (*ltr*). Subsequently, late expression of DNA-packaging (*endonuclease*, *terS*, *terL*) and structural genes (e.g. *mcp*) leads to DNA-processing, capsid assembly and DNA-packaging. The products of lysis genes enable host cell lysis, releasing mature phage particles, while immune evasion factors (e.g. *sak*) aid in escaping the host immune system. These late phage genes are transcribed from the  $P_{23}$  promoter, which is activated by the Ltr transcriptional regulator encoded by *ltr*. Ltr expression and  $P_{23}$  activity are regulated in a SigB and SpoVG-dependent manner. Small RNA SprX provides a feedback for post-transcriptional SpoVG repression. <https://doi.org/10.1101/2025.11.28.691083>

### Impact of the Global Regulator SarA on Multiple Stages of the Phage Life Cycle

In addition to investigating SigB, we analyzed the impact of the global regulator SarA on the phage life cycle, as both factors play central roles in *S. aureus* virulence regulation. Different mechanisms by which SarA influences the phage life cycle were demonstrated in Results Part III.

We observed that SarA promotes propagation of the phages  $\Phi 11$  and  $\Phi 13$ , following infection of phage-free *S. aureus* strains. To define the underlying mechanisms, we analyzed the individual steps of the phage life cycle. Analysis of phage adsorption revealed significantly reduced adsorption for  $\Phi 11$  in a *sarA*-deleted background, whereas  $\Phi 13$  adsorption was unaffected. Deletion of SarA led to increased expression of *tarM*, a gene repressed by the Agr system. Increased *tarM* expression has been shown to enhance  $\alpha$ -GlcNAc glycosylation of wall teichoic acid (WTA), the surface receptor for *S. aureus* phages [92]. Recently, receptor-binding proteins (RBPs) have been identified in *S. aureus* phages that recognize WTA as

receptor, but differ in their preferences for WTA glycosylation patterns and backbone structures [110]. Consistent with this, altered WTA glycosylation has been shown to modulate the phage-susceptibility of the host [111, 112]. The reduced  $\Phi 11$  adsorption in the *sarA* mutant was completely restored by addition of Agr-inducing peptide AIP-I, demonstrating that the SarA-dependent effect on  $\Phi 11$  adsorption is mediated through Agr activation and subsequent WTA glycosylation.

The RBP of  $\Phi 13$  does not bind to WTA glycosylations but to the ribitol-phosphate (Rbo-P) backbone [110]. Therefore, changes in WTA glycosylation would not be expected to impair  $\Phi 13$  binding, consistent with our observations. Nonetheless, adsorption was reduced in the *agr*-deleted strain. This could be explained by the global effects of Agr on WTA biosynthesis. *Agr* mutants produce reduced amounts of WTA [113] and display shorter WTA chain length [114]. Basal Agr activity might therefore be sufficient to maintain WTA properties that allow  $\Phi 13$  binding, without full SarA-dependent activation of the Agr system. Overall, our findings and previous studies suggest that the Agr quorum-sensing system modulates WTA amount, length and glycosylation patterns in response to growth phase and thereby change phage-susceptibility of the bacterial host.

Further, we found that SarA dampens the SOS response in *S. aureus* upon addition of mitomycin C, which is consistent with the protective effect that has been described against the DNA-damaging antibiotic ciprofloxacin [115]. SarA not only functions as a transcriptional regulator but also as a histone-like architectural protein that may alter DNA topology. The high copy number of SarA with 50000 copies per cell exceeds the abundance of classical transcription factors, supporting the hypothesis for additional structural roles [29]. The reduced SOS response activation in the presence of SarA could therefore result from SarA-mediated DNA stabilization or shielding.

Lastly, we identified the phage genome replication as a major target of SarA during the  $\Phi 13$  lytic cycle. Following induction, phage genome copy numbers were significantly reduced in the *sarA*-mutated strain. Moreover, expression of all analyzed phage genes was significantly decreased in the absence of SarA. Importantly, this reduction was not observed in a replication-deficient phage mutant, indicating that SarA affects the phage genome replication and not the transcription of the genes. Efficient phage genome replication after induction has been associated with increased expression of phage-encoded virulence factors, through the multi copy effect [70, 85, 98]. Thus, SarA may promote virulence indirectly by facilitating phage genome replication, potentially as a DNA-structural component.

Further, SarA binds preferentially to AT-rich sequences and modulates DNA structure to control transcription [30]. Xenogeneic silencing (XS) proteins, which target foreign DNA and aid in maintaining prophage lysogeny, also recognize AT-rich regions [116]. While XS factors

repress phage lytic activation, our findings indicate positive effects of SarA on different stages of the lytic life cycle.

Additional findings indicate a role of SarA in phage-host interactions. SarA has been shown to replace the excisionase of phage  $\lambda$ , aiding in recombination by interacting with the phage attachment site *attL* to form an alternative intasome [29]. Moreover, the late transcriptional regulator RinA of  $\Phi$ 11 binds to the *sarA* promoter, repressing its expression. *RinA* mutants display reduced virulence in *Galleria mellonella* larvae and mice infection models, potentially due to altered SarA activity [105]. Together, these findings support the hypothesis that SarA is involved in phage life cycle regulation and modulation of virulence.

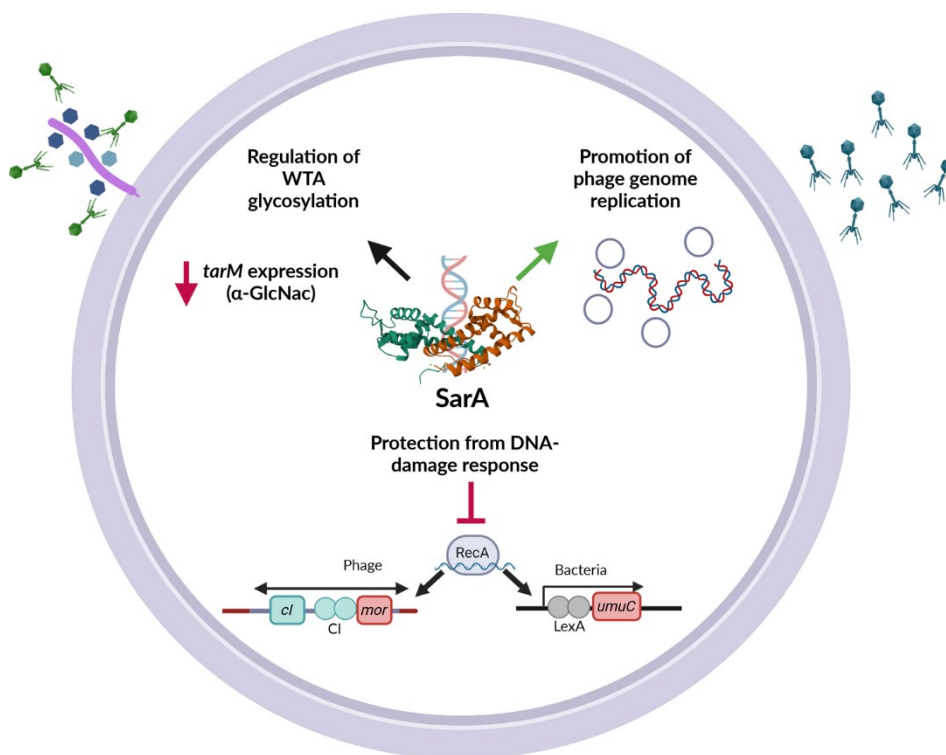


**Figure 4. Multiple effects of the bacterial DNA-binding protein SarA on the life cycle of *S. aureus* phages.** SarA promotes phage infection and replication on various levels. Repression of glycosyltransferase TarM affects the glycosylation pattern of WTA and thereby facilitates binding of  $\Phi$ 11. SarA protects the phages and bacteria from DNA-damage response leading to a lower genetic switch- and SOS-response activation. Additionally, the phage replication of  $\Phi$ 13 is promoted by SarA, resulting in higher numbers of phages. Crystal structure of SarA downloaded from RCSB Protein Data Bank (Entry ID:2FRH). <https://doi.org/10.1128/jb.00279-25>

## **Conclusion**

Our findings demonstrate that phage gene expression and replication are controlled by a regulatory network of phage-encoded regulators and host factors associated with virulence regulation. Strain-specific differences in phage dynamics are influenced by global *S. aureus* regulators SigB and SarA, which modulate late gene expression, phage adsorption, the DNA-damage response, and phage genome replication. These interactions support the hypothesis that phages are included into the host regulatory mechanisms, influencing virulence and adaptability to certain environmental conditions. Overall, this work highlights the importance of investigating the molecular cross-talk between phages and their hosts to improve our understanding of bacterial adaptation and virulence during infection.

1. Wertheim, H.F., et al., *The role of nasal carriage in Staphylococcus aureus infections*. Lancet Infect Dis, 2005. **5**(12): p. 751-62.
2. Lowy, F.D., *Staphylococcus aureus infections*. N Engl J Med, 1998. **339**(8): p. 520-32.
3. Feil, E.J., et al., *How clonal is Staphylococcus aureus?* J Bacteriol, 2003. **185**(11): p. 3307-16.
4. Goerke, C., et al., *Diversity of prophages in dominant Staphylococcus aureus clonal lineages*. J Bacteriol, 2009. **191**(11): p. 3462-8.
5. McCarthy, A.J., A.A. Witney, and J.A. Lindsay, *Staphylococcus aureus temperate bacteriophage: carriage and horizontal gene transfer is lineage associated*. Front Cell Infect Microbiol, 2012. **2**: p. 6.
6. Waldron, D.E. and J.A. Lindsay, *Sau1: a novel lineage-specific type I restriction-modification system that blocks horizontal gene transfer into Staphylococcus aureus and between S. aureus isolates of different lineages*. J Bacteriol, 2006. **188**(15): p. 5578-85.
7. Katayama, Y., T. Ito, and K. Hiramatsu, *A new class of genetic element, staphylococcus cassette chromosome mec, encodes methicillin resistance in Staphylococcus aureus*. Antimicrob Agents Chemother, 2000. **44**(6): p. 1549-55.
8. Shorr, A.F., *Epidemiology of staphylococcal resistance*. Clin Infect Dis, 2007. **45 Suppl 3**: p. S171-6.
9. Otto, M., *MRSA virulence and spread*. Cell Microbiol, 2012. **14**(10): p. 1513-21.
10. Thurlow, L.R., G.S. Joshi, and A.R. Richardson, *Virulence strategies of the dominant USA300 lineage of community-associated methicillin-resistant Staphylococcus aureus (CA-MRSA)*. FEMS Immunol Med Microbiol, 2012. **65**(1): p. 5-22.
11. Otto, M., *Staphylococcus aureus toxins*. Curr Opin Microbiol, 2014. **17**: p. 32-7.
12. Berube, B.J. and J. Bubeck Wardenburg, *Staphylococcus aureus  $\alpha$ -toxin: nearly a century of intrigue*. Toxins (Basel), 2013. **5**(6): p. 1140-66.
13. Wang, R., et al., *Identification of novel cytolytic peptides as key virulence determinants for community-associated MRSA*. Nat Med, 2007. **13**(12): p. 1510-4.
14. Löffler, B., et al., *Staphylococcus aureus panton-valentine leukocidin is a very potent cytotoxic factor for human neutrophils*. PLoS Pathog, 2010. **6**(1): p. e1000715.
15. Kreger, A.S., et al., *Purification and properties of staphylococcal delta hemolysin*. Infect Immun, 1971. **3**(3): p. 449-65.
16. McCormick, J.K., J.M. Yarwood, and P.M. Schlievert, *Toxic shock syndrome and bacterial superantigens: an update*. Annu Rev Microbiol, 2001. **55**: p. 77-104.
17. Thomer, L., O. Schneewind, and D. Missiakas, *Multiple ligands of von Willebrand factor-binding protein (vWbp) promote Staphylococcus aureus clot formation in human plasma*. J Biol Chem, 2013. **288**(39): p. 28283-92.
18. Malachowa, N. and F.R. DeLeo, *Mobile genetic elements of Staphylococcus aureus*. Cell Mol Life Sci, 2010. **67**(18): p. 3057-71.

19. Villanueva, M., et al., *Sensory deprivation in Staphylococcus aureus*. Nat Commun, 2018. **9**(1): p. 523.
20. Novick, R.P. and E. Geisinger, *Quorum sensing in staphylococci*. Annu Rev Genet, 2008. **42**: p. 541-64.
21. Dunman, P.M., et al., *Transcription profiling-based identification of Staphylococcus aureus genes regulated by the agr and/or sarA loci*. J Bacteriol, 2001. **183**(24): p. 7341-53.
22. Jenul, C. and A.R. Horswill, *Regulation of Staphylococcus aureus Virulence*. Microbiol Spectr, 2019. **7**(2).
23. Ibarra, J.A., et al., *Global analysis of transcriptional regulators in Staphylococcus aureus*. BMC Genomics, 2013. **14**: p. 126.
24. Heinrichs, J.H., M.G. Bayer, and A.L. Cheung, *Characterization of the sar locus and its interaction with agr in Staphylococcus aureus*. J Bacteriol, 1996. **178**(2): p. 418-23.
25. Liu, Y., et al., *Structural and function analyses of the global regulatory protein SarA from Staphylococcus aureus*. Proc Natl Acad Sci U S A, 2006. **103**(7): p. 2392-7.
26. Cheung, A.L., et al., *The SarA protein family of Staphylococcus aureus*. Int J Biochem Cell Biol, 2008. **40**(3): p. 355-61.
27. Didier, J.P., A.J. Cozzone, and B. Duclos, *Phosphorylation of the virulence regulator SarA modulates its ability to bind DNA in Staphylococcus aureus*. FEMS Microbiol Lett, 2010. **306**(1): p. 30-6.
28. Morrison, J.M., et al., *The staphylococcal accessory regulator, SarA, is an RNA-binding protein that modulates the mRNA turnover properties of late-exponential and stationary phase Staphylococcus aureus cells*. Front Cell Infect Microbiol, 2012. **2**: p. 26.
29. Fujimoto, D.F., et al., *Staphylococcus aureus SarA is a regulatory protein responsive to redox and pH that can support bacteriophage lambda integrase-mediated excision/recombination*. Mol Microbiol, 2009. **74**(6): p. 1445-58.
30. Schumacher, M.A., B.K. Hurlburt, and R.G. Brennan, *Crystal structures of SarA, a pleiotropic regulator of virulence genes in S. aureus*. Nature, 2001. **409**(6817): p. 215-9.
31. Chien, Y. and A.L. Cheung, *Molecular interactions between two global regulators, sar and agr, in Staphylococcus aureus*. J Biol Chem, 1998. **273**(5): p. 2645-52.
32. Chien, Y., et al., *SarA, a global regulator of virulence determinants in Staphylococcus aureus, binds to a conserved motif essential for sar-dependent gene regulation*. J Biol Chem, 1999. **274**(52): p. 37169-76.
33. Oriol, C., et al., *Expanding the Staphylococcus aureus SarA Regulon to Small RNAs*. mSystems, 2021. **6**(5): p. e0071321.
34. Kullik, I.I. and P. Giachino, *The alternative sigma factor sigmaB in Staphylococcus aureus: regulation of the sigB operon in response to growth phase and heat shock*. Arch Microbiol, 1997. **167**(2-3): p. 151-9.

35. Kang, C.M., et al., *Homologous pairs of regulatory proteins control activity of Bacillus subtilis transcription factor sigma(b) in response to environmental stress*. J Bacteriol, 1996. **178**(13): p. 3846-53.
36. Pane-Farre, J., et al., *Role of RsbU in controlling SigB activity in Staphylococcus aureus following alkaline stress*. J Bacteriol, 2009. **191**(8): p. 2561-73.
37. Pane-Farre, J., et al., *The sigmaB regulon in Staphylococcus aureus and its regulation*. Int J Med Microbiol, 2006. **296**(4-5): p. 237-58.
38. Senn, M.M., et al., *Molecular analysis and organization of the sigmaB operon in Staphylococcus aureus*. J Bacteriol, 2005. **187**(23): p. 8006-19.
39. Bischoff, M., et al., *Microarray-based analysis of the Staphylococcus aureus sigmaB regulon*. J Bacteriol, 2004. **186**(13): p. 4085-99.
40. Bischoff, M., J.M. Entenza, and P. Giachino, *Influence of a functional sigB operon on the global regulators sar and agr in Staphylococcus aureus*. J Bacteriol, 2001. **183**(17): p. 5171-9.
41. Homerova, D., et al., *Optimization of a two-plasmid system for the identification of promoters recognized by RNA polymerase containing Staphylococcus aureus alternative sigma factor sigmaB*. FEMS Microbiol Lett, 2004. **232**(2): p. 173-9.
42. Meier, S., et al., *sigmaB and the sigmaB-dependent arlRS and yabJ-spoVG loci affect capsule formation in Staphylococcus aureus*. Infect Immun, 2007. **75**(9): p. 4562-71.
43. Schulthess, B., et al., *The sigmaB-dependent yabJ-spoVG operon is involved in the regulation of extracellular nuclease, lipase, and protease expression in Staphylococcus aureus*. J Bacteriol, 2011. **193**(18): p. 4954-62.
44. Gerlach, D., et al., *Methicillin-resistant Staphylococcus aureus alters cell wall glycosylation to evade immunity*. Nature, 2018. **563**(7733): p. 705-709.
45. Weidenmaier, C. and A. Peschel, *Teichoic acids and related cell-wall glycopolymers in Gram-positive physiology and host interactions*. Nat Rev Microbiol, 2008. **6**(4): p. 276-87.
46. Xia, G., et al., *Wall teichoic Acid-dependent adsorption of staphylococcal siphovirus and myovirus*. J Bacteriol, 2011. **193**(15): p. 4006-9.
47. Xia, G., et al., *Glycosylation of wall teichoic acid in Staphylococcus aureus by TarM*. J Biol Chem, 2010. **285**(18): p. 13405-15.
48. van Dalen, R., A. Peschel, and N.M. van Sorge, *Wall Teichoic Acid in Staphylococcus aureus Host Interaction*. Trends Microbiol, 2020. **28**(12): p. 985-998.
49. Gerlach, D., et al., *Horizontal transfer and phylogenetic distribution of the immune evasion factor tarP*. Front Microbiol, 2022. **13**: p. 951333.
50. Argov, T., et al., *Temperate bacteriophages as regulators of host behavior*. Curr Opin Microbiol, 2017. **38**: p. 81-87.
51. Maslowska, K.H., K. Makiela-Dzbenska, and I.J. Fijalkowska, *The SOS system: A complex and tightly regulated response to DNA damage*. Environ Mol Mutagen, 2019. **60**(4): p. 368-384.

52. Brent, R. and M. Ptashne, *Mechanism of action of the *lexA* gene product*. Proc Natl Acad Sci U S A, 1981. **78**(7): p. 4204-8.
53. Little, J.W., *Mechanism of specific LexA cleavage: autodigestion and the role of RecA coprotease*. Biochimie, 1991. **73**(4): p. 411-21.
54. Oppenheim, A.B., et al., *Switches in bacteriophage lambda development*. Annu Rev Genet, 2005. **39**: p. 409-29.
55. Weigel, C. and H. Seitz, *Bacteriophage replication modules*. FEMS Microbiol Rev, 2006. **30**(3): p. 321-81.
56. landolo, J.J., et al., *Comparative analysis of the genomes of the temperate bacteriophages phi 11, phi 12 and phi 13 of Staphylococcus aureus 8325*. Gene, 2002. **289**(1-2): p. 109-18.
57. Friedman, D.I. and D.L. Court, *Transcription antitermination: the lambda paradigm updated*. Mol Microbiol, 1995. **18**(2): p. 191-200.
58. Summers, W.C. and R.B. Siegel, *Transcription of late phage RNA by T7 RNA polymerase*. Nature, 1970. **228**(5277): p. 1160-2.
59. Ferrer, M.D., et al., *RinA controls phage-mediated packaging and transfer of virulence genes in Gram-positive bacteria*. Nucleic Acids Res, 2011. **39**(14): p. 5866-78.
60. Quiles-Puchalt, N., et al., *A super-family of transcriptional activators regulates bacteriophage packaging and lysis in Gram-positive bacteria*. Nucleic Acids Res, 2013. **41**(15): p. 7260-75.
61. Feiss, M. and V.B. Rao, *The bacteriophage DNA packaging machine*. Adv Exp Med Biol, 2012. **726**: p. 489-509.
62. Young, R. and U. Bläsi, *Holins: form and function in bacteriophage lysis*. FEMS Microbiol Rev, 1995. **17**(1-2): p. 191-205.
63. Fischetti, V.A., *Bacteriophage endolysins: a novel anti-infective to control Gram-positive pathogens*. Int J Med Microbiol, 2010. **300**(6): p. 357-62.
64. Goerke, C., et al., *Extensive phage dynamics in Staphylococcus aureus contributes to adaptation to the human host during infection*. Mol Microbiol, 2006. **61**(6): p. 1673-85.
65. Ackermann, H.W., *Tailed bacteriophages: the order caudovirales*. Adv Virus Res, 1998. **51**: p. 135-201.
66. Deghorain, M. and L. Van Melderren, *The Staphylococci phages family: an overview*. Viruses, 2012. **4**(12): p. 3316-35.
67. Brüssow, H. and F. Desiere, *Comparative phage genomics and the evolution of Siphoviridae: insights from dairy phages*. Mol Microbiol, 2001. **39**(2): p. 213-22.
68. Kwan, T., et al., *The complete genomes and proteomes of 27 Staphylococcus aureus bacteriophages*. Proc Natl Acad Sci U S A, 2005. **102**(14): p. 5174-9.
69. Růžičková, V., et al., *Major clonal lineages in impetigo Staphylococcus aureus strains isolated in Czech and Slovak maternity hospitals*. Int J Med Microbiol, 2012. **302**(6): p. 237-41.

70. Wirtz, C., et al., *Transcription of the phage-encoded Panton-Valentine leukocidin of Staphylococcus aureus is dependent on the phage life-cycle and on the host background*. Microbiology (Reading), 2009. **155**(Pt 11): p. 3491-3499.
71. Shallcross, L.J., et al., *The role of the Panton-Valentine leukocidin toxin in staphylococcal disease: a systematic review and meta-analysis*. Lancet Infect Dis, 2013. **13**(1): p. 43-54.
72. Doery, H.M., et al., *A phospholipase in staphylococcal toxin which hydrolyses sphingomyelin*. Nature, 1963. **198**: p. 1091-2.
73. Rohmer, C. and C. Wolz, *The Role of hlb-Converting Bacteriophages in Staphylococcus aureus Host Adaption*. Microb Physiol, 2021. **31**(2): p. 109-122.
74. Rooijackers, S.H., et al., *Anti-opsonic properties of staphylokinase*. Microbes Infect, 2005. **7**(3): p. 476-84.
75. de Haas, C.J., et al., *Chemotaxis inhibitory protein of Staphylococcus aureus, a bacterial antiinflammatory agent*. J Exp Med, 2004. **199**(5): p. 687-95.
76. Postma, B., et al., *Chemotaxis inhibitory protein of Staphylococcus aureus binds specifically to the C5a and formylated peptide receptor*. J Immunol, 2004. **172**(11): p. 6994-7001.
77. Rooijackers, S.H., et al., *Structural and functional implications of the alternative complement pathway C3 convertase stabilized by a staphylococcal inhibitor*. Nat Immunol, 2009. **10**(7): p. 721-7.
78. Rooijackers, S.H., et al., *Immune evasion by a staphylococcal complement inhibitor that acts on C3 convertases*. Nat Immunol, 2005. **6**(9): p. 920-7.
79. Betley, M.J. and J.J. Mekalanos, *Staphylococcal enterotoxin A is encoded by phage*. Science, 1985. **229**(4709): p. 185-7.
80. O'Brien, G.J., et al., *Staphylococcus aureus enterotoxins induce IL-8 secretion by human nasal epithelial cells*. Respir Res, 2006. **7**(1): p. 115.
81. Pinel-Marie, M.L., R. Brielle, and B. Felden, *Dual toxic-peptide-coding Staphylococcus aureus RNA under antisense regulation targets host cells and bacterial rivals unequally*. Cell Rep, 2014. **7**(2): p. 424-435.
82. Salgado-Pabón, W., et al., *Staphylococcus aureus  $\beta$ -toxin production is common in strains with the  $\beta$ -toxin gene inactivated by bacteriophage*. J Infect Dis, 2014. **210**(5): p. 784-92.
83. Katayama, Y., et al., *Beta-hemolysin promotes skin colonization by Staphylococcus aureus*. J Bacteriol, 2013. **195**(6): p. 1194-203.
84. Gulbins, E., et al., *Ceramide, membrane rafts and infections*. J Mol Med (Berl), 2004. **82**(6): p. 357-63.
85. Goerke, C., J. Köller, and C. Wolz, *Ciprofloxacin and trimethoprim cause phage induction and virulence modulation in Staphylococcus aureus*. Antimicrob Agents Chemother, 2006. **50**(1): p. 171-7.

86. Hedström, S.A. and T. Malmqvist, *Sphingomyelinase activity of Staphylococcus aureus strains from recurrent furunculosis and other infections*. Acta Pathol Microbiol Immunol Scand B, 1982. **90**(3): p. 217-20.
87. van Wamel, W.J., et al., *The innate immune modulators staphylococcal complement inhibitor and chemotaxis inhibitory protein of Staphylococcus aureus are located on beta-hemolysin-converting bacteriophages*. J Bacteriol, 2006. **188**(4): p. 1310-5.
88. Tran, P.M., et al., *φSa3mw Prophage as a Molecular Regulatory Switch of Staphylococcus aureus β-Toxin Production*. J Bacteriol, 2019. **201**(14).
89. Poupel, O., et al., *Timely excision of prophage Φ13 is essential for the Staphylococcus aureus infectious process*. Infect Immun, 2025: p. e0031425.
90. Nepal, R., et al., *A φSa3int (NM3) Prophage Domestication in Staphylococcus aureus Leads to Increased Virulence Through Human Immune Evasion*. MedComm (2020), 2025. **6**(8): p. e70313.
91. Verkaik, N.J., et al., *Immune evasion cluster-positive bacteriophages are highly prevalent among human Staphylococcus aureus strains, but they are not essential in the first stages of nasal colonization*. Clin Microbiol Infect, 2011. **17**(3): p. 343-8.
92. Yang, J., et al., *Cross-species communication via agr controls phage susceptibility in Staphylococcus aureus*. Cell Rep, 2023. **42**(9): p. 113154.
93. Kristensen, C.S., et al., *Characterization of the genetic switch from phage 13 important for Staphylococcus aureus colonization in humans*. Microbiologyopen, 2021. **10**(5): p. e1245.
94. Pedersen, M. and K. Hammer, *The role of MOR and the CI operator sites on the genetic switch of the temperate bacteriophage TP901-1*. J Mol Biol, 2008. **384**(3): p. 577-89.
95. Kongari, R., et al., *The Transcriptional Program of Staphylococcus aureus Phage K Is Affected by a Host rpoC Mutation That Confers Phage K Resistance*. Viruses, 2024. **16**(11).
96. Pasechnek, A., et al., *Active Lysogeny in Listeria Monocytogenes Is a Bacteria-Phage Adaptive Response in the Mammalian Environment*. Cell Rep, 2020. **32**(4): p. 107956.
97. Huang, W., et al., *Glucose-induced active lysogeny of prophage ΦSa3XN promotes Staphylococcus aureus virulence*. Virol J, 2025. **22**(1): p. 371.
98. Sumbly, P. and M.K. Waldor, *Transcription of the toxin genes present within the Staphylococcal phage phiSa3ms is intimately linked with the phage's life cycle*. J Bacteriol, 2003. **185**(23): p. 6841-51.
99. Xia, G. and C. Wolz, *Phages of Staphylococcus aureus and their impact on host evolution*. Infect Genet Evol, 2014. **21**: p. 593-601.
100. Hinton, D.M., *Transcriptional control in the prereplicative phase of T4 development*. Virol J, 2010. **7**: p. 289.
101. Dehbi, M., et al., *Inhibition of transcription in Staphylococcus aureus by a primary sigma factor-binding polypeptide from phage G1*. J Bacteriol, 2009. **191**(12): p. 3763-71.

102. Finstrlová, A., et al., *Global Transcriptomic Analysis of Bacteriophage-Host Interactions between a Kayvirus Therapeutic Phage and Staphylococcus aureus*. *Microbiol Spectr*, 2022. **10**(3): p. e0012322.
103. Fernández, L., et al., *Lysogenization of Staphylococcus aureus RN450 by phages  $\phi$ 11 and  $\phi$ 80 $\alpha$  leads to the activation of the SigB regulon*. *Sci Rep*, 2018. **8**(1): p. 12662.
104. Brøndsted, L., M. Pedersen, and K. Hammer, *An activator of transcription regulates phage TP901-1 late gene expression*. *Appl Environ Microbiol*, 2001. **67**(12): p. 5626-33.
105. Jiang, M., et al., *Phage transcription activator RinA regulates Staphylococcus aureus virulence by governing sarA expression*. *Genes Genomics*, 2023. **45**(2): p. 191-202.
106. Erez, Z., et al., *Communication between viruses guides lysis-lysogeny decisions*. *Nature*, 2017. **541**(7638): p. 488-493.
107. Hargreaves, K.R., A.M. Kropinski, and M.R. Clokie, *What does the talking?: quorum sensing signalling genes discovered in a bacteriophage genome*. *PLoS One*, 2014. **9**(1): p. e85131.
108. Ma, K., et al., *The global regulator SpoVG modulates Staphylococcus aureus virulence through Agr-dependent pathways*. *Virulence*, 2025. **16**(1): p. 2561827.
109. Eyraud, A., et al., *A small RNA controls a protein regulator involved in antibiotic resistance in Staphylococcus aureus*. *Nucleic Acids Res*, 2014. **42**(8): p. 4892-905.
110. Krusche, J., et al., *Characterization and host range prediction of Staphylococcus aureus phages through receptor-binding protein analysis*. *Cell Rep*, 2025. **44**(3): p. 115369.
111. Li, X., et al., *An accessory wall teichoic acid glycosyltransferase protects Staphylococcus aureus from the lytic activity of Podoviridae*. *Sci Rep*, 2015. **5**: p. 17219.
112. Beck, C., et al., *Wall teichoic acid substitution with glucose governs phage susceptibility of Staphylococcus epidermidis*. *mBio*, 2024. **15**(4): p. e0199023.
113. Wanner, S., et al., *Wall teichoic acids mediate increased virulence in Staphylococcus aureus*. *Nat Microbiol*, 2017. **2**: p. 16257.
114. Meredith, T.C., J.G. Swoboda, and S. Walker, *Late-stage polyribitol phosphate wall teichoic acid biosynthesis in Staphylococcus aureus*. *J Bacteriol*, 2008. **190**(8): p. 3046-56.
115. Lamichhane-Khadka, R., et al., *sarA inactivation reduces vancomycin-intermediate and ciprofloxacin resistance expression by Staphylococcus aureus*. *Int J Antimicrob Agents*, 2009. **34**(2): p. 136-41.
116. Pfeifer, E., et al., *Impact of Xenogeneic Silencing on Phage-Host Interactions*. *J Mol Biol*, 2019. **431**(23): p. 4670-4683.

## **Danksagung**

An erster Stelle möchte ich mich bei meiner Betreuerin, Prof. Dr. Christiane Wolz, bedanken. Danke für die Möglichkeit, meine Doktorarbeit in dieser tollen Arbeitsgruppe durchführen zu können. Vielen Dank für all die wertvollen Tipps und die Unterstützung während der vergangenen vier Jahre sowie für die Freiheit, eigene Ideen umsetzen zu können, und für die Chance, Konferenzen im In- und Ausland besuchen zu dürfen.

Außerdem möchte ich Prof. Dr. Andreas Peschel herzlich für die Erstellung des Zweitgutachtens danken. Zudem einen großen Dank für inspirierende Fragen und Diskussionen zu Phagen im Rahmen des Seminars und der TAC-Meetings.

Von Herzen danken möchte ich der gesamten AG Wolz mit allen aktuellen und ehemaligen Mitgliedern. Ich danke euch für all die schönen Momente im Büro, im Labor, aber auch abseits der Arbeit. Parvati, Janina, Andrea und Esther: Ihr seid in den letzten Jahren zu engen Freundinnen geworden und habt diese Zeit unvergesslich gemacht. Naty, Vitty und Ellen: Danke für eure Unterstützung im Labor und darüber hinaus, wenn es einmal schwierig wurde. Ihr seid wunderbare Menschen. Naisa: Danke für alles, vor allem für das letzte Jahr, in dem wir so viele gemeinsame Höhen und Tiefen erlebt haben. An unsere gemeinsamen Erlebnisse, insbesondere Mailand, werde ich immer gerne zurückdenken.

Auch möchte ich mich bei meinen Studierenden bedanken, die mich immer tatkräftig im Labor unterstützt haben und mir die Rolle als Betreuerin sehr leicht gemacht haben.

Ein weiterer großer Dank geht an Carina, die mich während meiner Bachelorarbeit begleitet und meine Begeisterung für Phagen geweckt hat. Ich bin froh, dass ich deine Arbeit an diesem Projekt fortführen durfte, und du weiterhin ein Teil davon warst.

Danke auch an die gesamte AG Peschel. Besonderer Dank gilt Janes und Chris für die hilfreichen Diskussionen über Phagen sowie für die tolle Zeit in Portugal und auf anderen Phagen-Konferenzen.

Großer Dank geht zudem an meine Familie und meine Freunde, die mich stets unterstützen und mir geholfen haben, Stress und Sorgen zu vergessen.

Zuletzt möchte ich mich herzlich bei meinem Partner Joël bedanken. Du bist mein größter Cheerleader und Motivator. Ohne deine Unterstützung wäre all dies nicht möglich gewesen. Danke, dass du immer an meiner Seite bist und an mich glaubst.

## **Eidesstattliche Erklärung**

Ich erkläre hiermit, dass ich die zur Promotion eingereichte Arbeit mit dem Titel

**„Molecular cross-talk between Sa3int phages and their *Staphylococcus aureus* host“**

selbständig verfasst, nur die angegebenen Quellen und Hilfsmittel benutzt und wörtlich oder inhaltlich übernommene Stellen als solche gekennzeichnet habe. Ich erkläre, dass die Richtlinien zur Sicherung guter wissenschaftlicher Praxis der Universität Tübingen beachtet wurden. Ich versichere an Eides statt, dass diese Angaben wahr sind und dass ich nichts verschwiegen habe. Meine eigenen Beiträge zu Gemeinschaftsarbeiten habe ich im Abschnitt „List of publications and personal contributions“ dargestellt.

Tübingen, den

---

Ronja Dobritz